POLITECNICO DI MILANO
DIPARTIMENTO DI INGEGNERIA IDRAULICA, AMBIENTALE,
INFRASTRUTTURE VIARIE E RILEVAMENTO

DOCTORAL PROGRAMME IN ENVIRONMENTAL AND
INFRASTRUCTURE ENGINEERING

EFFECTS OF ARSENIC PARTITIONING AND DYNAMICS ON THE ASSESSMENT OF GROUNDWATER BACKGROUND LEVELS

Doctoral Dissertation of:
Antonio Molinari
Matricola: 753327

Supervisor
Prof. Alberto Guadagnini

Tutor:
Prof. Alberto Guadagnini

The Chair of the Doctoral Program:
Prof. Fernando Sansò

2013 – XXV CYCLE

This dissertation is dedicated to my family

and to all the people who believed in my skills

ABSTRACT

The research investigates the effect of arsenic (As) partitioning and dynamics on the assessment of the Natural Background Level (NBL) of this metalloid in selected target aquifers of the Emilia-Romagna Region, Italy.

The application of global statistical methodologies highlighted that the analyzed groundwater bodies are characterized by distinct responses (in space and time) in terms of estimated NBLs. Estimated NBLs of target chemical species were found to (*a*) increase with the average depth of the investigated water bodies and (*b*) display different temporal dynamics within the observation time frame. Background concentrations are the result of several factors, including physical and chemical processes taking place in the natural environments which are typically not captured by global statistical methods. Experimental activities have been performed to improve the understanding of mechanisms influencing As NBLs. Experimental characterizations focus on (*i*) arsenic fractioning within different solid matrices, and (*ii*) the effects of redox changes on arsenic mobility. A distinct correlation between temporal dynamics of aerobic/anaerobic conditions and As release was evidenced. The largest As release were observed from vegetal matter. The latter releases As faster and with larger amounts than the other tested solid matrices. This suggested that the high hot-spot As concentrations detected within Emilia-Romagna aquifers could be consistent with the localized occurrence of vegetal matter which releases arsenic as a consequence of redox changes. Geochemical modeling of experimental results evidenced that (*a*) organic matter strongly affect pH and redox conditions, thus influencing As speciation and mobility, (*b*) large dissolved As concentrations should be expected when the low crystallinity phases are subject to dissolution, (*c*) iron minerals appear to govern As dynamics for short time scales while Mn phases can contribute significantly to As release over long time scales of water/solid matrix interaction.

It is concluded that estimates of NBLs of chemical species such as arsenic need to be performed by considering real field conditions to assure consistency with the hydro-geochemical behavior of the tested aquifer.

Keywords: arsenic; natural background level; controlled redox conditions; natural aquifer matrices; sequential extractions; geochemical modeling.

RIASSUNTO

Il lavoro di ricerca è focalizzato sullo studio degli effetti del partizionamento e delle dinamiche di arsenico (As) sul livello di fondo naturale (NBL) di questo metalloide in corpi acquiferi della Regione Emilia-Romagna, Italia.

L'applicazione di metodologie statistiche globali per la stima di NBL ha evidenziato il diverso comportamento (nello spazio e nel tempo) dei corpi idrici sotterranei analizzati, in termini di NBL stimate. Quest'ultime sono risultate (*a*) in aumento con la profondità media dei corpi idrici indagati e (*b*) caratterizzate da diverse dinamiche temporali nel periodo di monitoraggio analizzato. Le concentrazioni di fondo naturale sono il risultato di diversi fattori che includono gli specifici processi fisici e chimici che si svolgono negli ambienti naturali e che, in genere, non sono incorporati in metodi statistici globali. Diverse attività sperimentali sono state eseguite per migliorare la comprensione dei meccanismi che influenzano il NBL dell'As. Le caratterizzazioni sperimentali hanno riguardato (*i*) il frazionamento dell'arsenico all'interno di diverse matrici solide e (*ii*) gli effetti dei cambiamenti redox sulla mobilità dell'arsenico. Una netta correlazione tra le dinamiche temporali delle condizioni aerobiche/anaerobiche ed il rilascio di As è stata evidenziata. Le più elevate concentrazioni di As sono state osservate nella sostanza vegetale associata alla matrice solida del sistema, che rilascia l'arsenico più velocemente e in quantità maggiori rispetto alle altre matrici solide esaminate. Questo ha suggerito che le elevate concentrazioni di As riscontrate negli acquiferi dell'Emilia-Romagna potrebbero essere coerenti con la presenza localizzata di sostanza vegetale che rilascia il metalloide a seguito delle dinamiche temporali delle condizioni redox. La modellazione geochimica dei risultati sperimentali ha evidenziato che (*a*) la sostanza organica influenza significativamente le condizioni redox e di pH, influenzando la speciazione e la mobilità dell'As, (*b*) elevate concentrazioni di As in acqua sono da aspettarsi quando le fasi a bassa cristallinità sono soggette a dissoluzione, (*c*) i minerali ferrosi sembrano governare le dinamiche di As per brevi tempi scala, mentre le fasi di Mn sembrano contribuire in modo significativo al rilascio dell'As su lunghi tempi scala d'interazione acqua/matrice solida.

Si è concluso che le stime di valori di NBL di specie chimiche come l'arsenico devono essere effettuate tenendo conto delle reali condizioni di campo per garantire la consistenza delle stime con il comportamento idro-geo-chimico dell'acquifero in esame.

Parole chiave: arsenico; livello di fondo naturale; condizioni redox controllate; matrici naturali; estrazioni sequenziali; modellazione geochimica.

EFFECTS OF ARSENIC PARTITIONING AND DYNAMICS ON THE ASSESSMENT OF GROUNDWATER BACKGROUND LEVELS

CONTENTS

INTRODUCTION

The overall pressure load acting on the soil-water environment has dramatically increased during the last decades due to the effect of anthropogenic activities. Changes in land use, including urbanization, mining, and the disposal of liquid and solid wastes, has caused an increase of the number of locations where concentrations of one or more chemical species exceeding drinking water regulation thresholds are detected. At the same time, chemical compounds might be associated with naturally large concentrations for reasons which are only marginally related (or might even be unrelated) to human activities. These large concentrations might be linked to specific local hydrogeochemical processes taking place in the context of water-rock interactions because of the particular geological composition of the host porous matrix. The application of remediation techniques to restore these waters to a chemical state which can be considered as good according to current regulations might not be possible under these conditions. These actions can also be economically ineffective because it is unrealistic to set clean-up goals that are below a threshold which can be considered as natural background level (NBL).

In this context, NBL represents "*the concentration of a substance or the value of an indicator in a body of groundwater corresponding to no, or only very minor, anthropogenic alterations to undisturbed conditions*" (GroundWater Daughter Directive 2006/118/EC, article 2.5). The evaluation of background concentrations is required by the EU Water Framework Directive (WFD 2000/60/EC), according to which each Member State should identify significant and sustained upward trends of chemical species that could compromise the achievement of good chemical status of a target water body.

A proper estimation of the NBL of a target compound is useful to (*a*) define threshold values which are consistent with specific natural features of water bodies; (*b*) distinguish effective anthropogenic contamination from cases where natural conditions occur; and (*c*) define the correct chemical status of groundwater bodies.

The most reliable approach for the estimation of the NBL of given inorganic compounds within a target groundwater body should probably be based on the analysis of samples collected from locations in the geologic formation where water quality has not been altered by anthropogenic activities. Unfortunately, it is difficult to find pristine portions of aquifers in populated areas. Other approaches should therefore be applied. These include, e.g., methodologies based on (*i*) statistical analysis of available data, (*ii*)

experimental characterization of soil and water samples, and/or (*iii*) geochemical modeling of processes occurring in the systems.

Evaluation of concentration levels which can be considered as consistent with actual natural processes taking place in a specific system and with observed space-time dynamics is also critical in the framework of quality management of groundwater bodies within which relatively large natural concentrations of target species are detected. This task can be accomplished through theoretical and/or experimental approaches. For example, statistical analyses could be employed to model observed frequencies of concentrations detected at several monitoring wells. With reference to experimental analyses, batch/incubations or column tests can be performed to characterize the behavior of target solid matrices under specific redox and flux conditions consistent with natural environments investigated. These types of experimental results can then be interpreted through mathematical modeling of geochemical processes, *e.g.*, dissolution/precipitation or other types of heterogeneous and homogeneous reactions, to provide improved understanding and predictive capabilities of the key processes which can contribute to define the NBL of a target species for a given water body.

Arsenic is arguably one of the most dangerous species which can be observed in groundwater systems when occurs with concentrations above regulation limits. It is a ubiquitous element which can be found in the atmosphere, soils and rocks, natural waters and organisms. Most environmental problems related to arsenic are the result of its mobilization under natural conditions. The main natural sources of arsenic in terrestrial and aquatic environments are the weathering of arsenic minerals, volcanic activities and the occurrence of strong reducing conditions which can promote arsenic release to groundwater. Arsenic is commonly used for many industrial and agricultural applications. Therefore, large concentrations of this metalloid can be found in groundwater as a result of anthropogenic activities.

In the presence of large arsenic concentrations it is important to distinguish between effective anthropogenic contamination and scenarios under which arsenic dissolution in water is triggered by specific natural conditions. In this framework, the abundant and high quality data-set available from ARPA (Regional Agency for Environmental Protection) Emilia-Romagna has highlighted the occurrence of large hot-spot of arsenic concentrations in groundwater bodies located in Emilia-Romagna Region, Italy. Previous studies hypothesized that these large concentrations could be associated with natural release processes from geomaterials filling the Po Basin, consistent with the large arsenic

concentrations detected in the host porous matrix. A key aim of this research work is the investigation of the effect of arsenic partitioning and dynamics on the groundwater background level of this metalloid in selected target aquifers of the Emilia-Romagna Region, Italy.

The first Chapter of the dissertation reports the key chemical characteristics of arsenic and illustrates its geochemical behavior in soil-groundwater environments worldwide and in Italy. This literature survey is followed by Chapter 2, which reports the application of global statistical methodologies to estimate NBLs of target chemical species and assess the environmental quality status of given groundwater bodies. Variability of NBL values across various groundwater bodies located at different representative depths and temporal dynamics of NBLs are also explored in Chapter 2.

Background concentrations are the result of several factors, including physical and chemical processes taking place in the natural environment which are typically not captured by global statistical methods. A set of experimental activities have then been performed to improve our understanding of mechanisms influencing arsenic NBLs. These activities include batch tests and selective sequential extractions which have been designed and performed employing samples which are representative of the natural host matrix occurring in the deep groundwater systems investigated. Chapter 3 reports the results of these experimental characterizations and focuses on (*a*) the effects of redox changes on arsenic mobility, and (*b*) arsenic fractioning within different solid matrices. Batch tests are useful to understand the overall arsenic dynamics in the presence of different redox conditions. However, they did not allow to exhaustively evaluate the role of the main solid phases on redox and pH variations, which are key to trigger arsenic release, and the contribution of different solid phases on the detected arsenic concentrations. These aspects are explored in Chapter 4, which is keyed to the development and application of a geochemical modeling framework conducive to the interpretation of the experimental results obtained from the batch tests on the basis of the results of sequential extractions. The results of this activity lead to define a conceptual model of the system which is consistent with physico-chemical processes that could took place in the experimental microcosm which was set-up to reproduce natural environmental conditions. Chapter 5 reports the conclusions stemming from this research, highlighting practical implications in the framework of groundwater management and preservation strategies.

CHAPTER 1

Geochemical behavior of Arsenic in the soil-groundwater environments

1.1. Key chemical characteristics of Arsenic

Arsenic (As) (atomic number: 33, atomic weight: 74.9216, density, at 293 K: 5.776 g/cm^3) is a metalloid belonging to group V of the periodic table of elements and is classified as a heavy metal due to its (a) high atomic weight, (b) high density and (c) basically null biodegradability. The latter leads to bioaccumulation in living organisms (Wackett et al., 2004). Arsenic is the twentieth most abundant element in the Earth's crust with detected concentration levels greater than those of Hg, Cd, Au, Ag, Sb, and Se (Bhumbla and Keefer, 1994) naturally occurring in four oxidation states: -3 (arsine), 0 (elemental), +3 (arsenite) and +5 (arsenate). In natural systems, and in particular in aqueous environments, arsenic mostly exists either in inorganic forms, as oxyanions of arsenite, As(III), in anaerobic conditions, or as arsenate, As(V), in oxidized environments (Adriano, 2001; WHO, 2008).

1.2. Arsenic sources in the environment

Arsenic is a ubiquitous element which can be found in the atmosphere, soils and rocks, natural waters and organisms. Most environmental problems related to arsenic are the result of As mobilization under natural conditions. Anthropogenic activities which can contribute to As-related environmental problems include mining, combustion of fossil fuels, the use of arsenical pesticides, herbicides and crop desiccants, and the use of As as an additive to livestock feed (Smedley and Kinniburgh, 2002).

It has been shown that groundwater is significantly exposed to As contamination, with high hot-spot concentrations (Smedley and Kinniburgh, 2002). In 1993 the WHO reduced from 50 to 10 μg/L the limit value of As in drinking waters (WHO, 1993). This limit is also valid for US, Japan and Europe.

1.2.1 Arsenic distribution in groundwater worldwide and Italy

Arsenic concentration within aquifers worldwide has been found to exceed 50 µg/L. This causes a significant threat to groundwater quality and poses a notable element of risk for human beings and ecosystems. The most critical occurrences of arsenic-affected aquifers around the world (Fig. 1.1) are in Argentina, Bangladesh, Chile, China, Hungary, India (West Bengal), Mexico, Romania, Taiwan, Vietnam and south-west USA. Moreover, arsenic springs associated with geothermal waters have been reported in Japan, New Zealand, Kamchatka, Iceland, France, Dominica and the USA. Alongside these "natural" contaminations there are zones where the high As concentrations are related to mining operations like Alaska, Canada, Mexico, Ghana, Zimbabwe, South Africa, Greece, England and Thailand (Bundschuh et al., 2004; Harvey et al., 2002; Smedley and Kinniburgh, 2002).

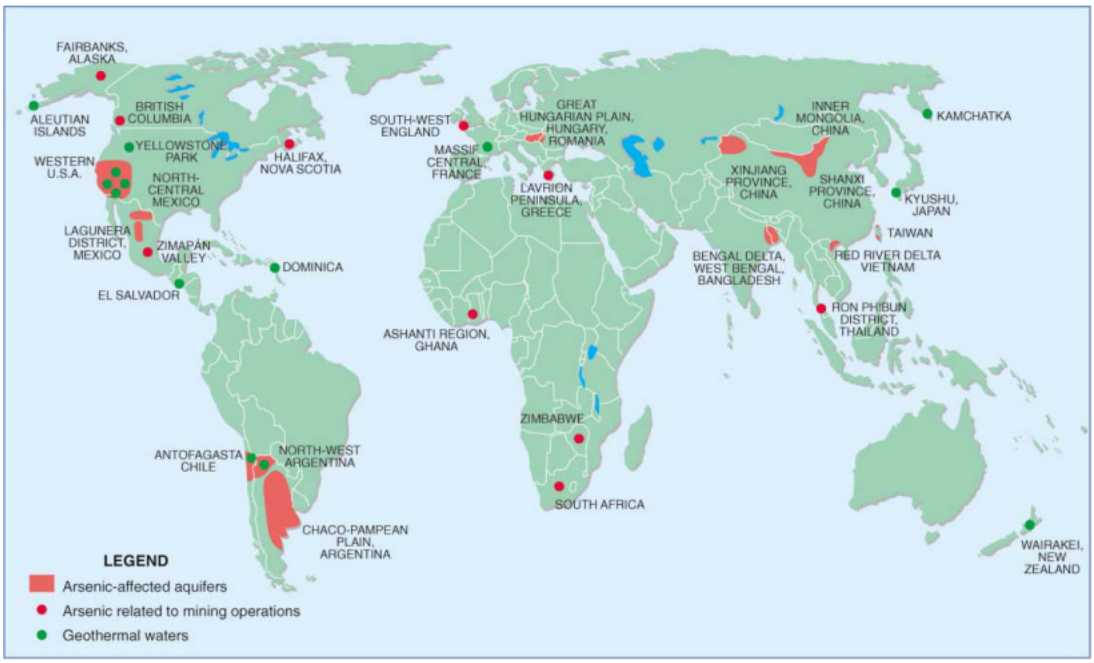

Fig. 1.1 – Arsenic-affected aquifers, water and environmental problems related to mining and geothermal sources around the world. Blue areas are lakes. (Smedley and Kinniburgh, 2002).

High natural As concentrations in soils are common in volcanic matrixes. For example, Baiocchi et al. (2011) report a map of volcanic aquifers in Central and Southern Italy where As concentrations frequently exceed 50 µg/L. Alongside these naturally or anthopogenically influenced polluted areas, As in aquifers can be related to industrial or agronomical applications.

Significant As concentrations have been recorded at a number of locations in Italy, including Sardinia (Frau et al., 2008), the Brenta Plain in Northeastern Italy (Ungaro et al., 2007), southern Tuscany (Baroni et al, 2004), the Ischia Island (Daniele, 2004) and Central Italy (Preziosi et al., 2009).

1.2.2 Natural Arsenic Sources

The main natural source of arsenic in terrestrial and aquatic environment under both oxic and anoxic conditions is the weathering of As minerals and volcanic activity (Rhine et al., 2006). Arsenic in the subsurface is commonly found at trace levels in bearing minerals such as arsenopyrite (FeAsS), realgar (AsS), orpiment (As_2S_3), scorodite ($FeAsO_4 \cdot 2H_2O$) (Dove and Rimstidt, 1985; Newman et al., 1998; Smedley and Kinniburgh, 2002; Bissen and Frimmel, 2003) or adsorbed to the surface of Fe(III) oxides/hydroxides whose more important forms are hydroxide ($Fe(OH)_3$), goethite (α-FeOOH), akaganeite (β-FeOOH), lepidocrocite (γ-FeOOH) and haematite (Fe_2O_3) (Bissen and Frimmel, 2003). Discharge of geothermal waters can cause high concentrations of As in surface streams. Evaporation can also contribute to high natural arsenic concentrations because As is not incorporated in most evaporite minerals (Welch and Lico, 1998).

A possible natural source of dissolved As occurrence in groundwater is the occurrence of strongly reducing conditions within alluvial and deltaic sediments with rapid burial of large amounts of sediment together with high organic matter content. Dissolved arsenic can also be found in volcanogenic areas or in arid or semi-arid areas that represent two possible natural sources of As occurrence in groundwater. Aquifers which are composed of flooded sediments could represent sources of high dissolved arsenic (> 50 µg/L) (Smedley and Kinniburgh, 2002; Nordstrom, 2002).

1.2.3 Anthropogenic Arsenic Sources

Anthropogenic activities such as smelter slag, coal combustion, run-off from mine tailings, hide tanning waste, pigment production for paints and dyes, and the application of As based pesticides are key causes of As contamination (Oremland and Stolz, 2003). Fly ash from thermal power plants may contribute to As contamination of the soil. An additional anthropogenic source of As release is represented by the use of arsenic in coloring agents such as Scheele's green ($CuHAsO_3$) or Paris green ($Cu(AsO_2)_2$

$Cu(C_2H_3O_2)_2$) (Azcue and Nriagu, 1994). Arsenic contamination of the environment can also occur through the use of arsenical fungicides, herbicides, and insecticides in the agriculture and wood industry (Bissen and Frimmel, 2003). The most common wood preservatives used in the industry are chromated copper arsenate (CCA) and ammonical copper arsenate (ACA) in conjunction with 99% of the arsenical wood preservatives (Perker, 1981). Currently, As is being used in the production of glass and semiconductor industry (Azcue and Nriagu, 1994).

Excessive exploitation of aquifers due to pumping activities in the context of, e.g., irrigation and industrial activities, could result in lowering of water table level in free aquifers. Thus could promote pyrite oxidation in unconfined aquifers where pyrite occurs. High As concentrations have been found in regions where such fluctuations of water table oscillation have been evidenced (Schreiber et al., 2000).

1.3. Arsenic in waters

1.3.1 Speciation

Arsenic speciation in aquatic systems is mainly controlled by redox potential (Eh or ORP-Oxidation Reduction Potential) and pH. These two factors typically govern the four oxidation states of As. The predominant soluble forms are As(III) and As(V), where As(III) is more toxic and mobile than As(V) and it is more difficult to remove from water (Clifford, 1990; Smedley and Kinniburgh, 2002; Rhine et al., 2006). The high mobility of As(III) is due to its neutral charge at most pH ranges in natural water. Binding of As(V) to minerals occurs in the presence of a wide pH range, whereas, As(III) may bind to certain compounds such as iron oxy-hydroxides and metal sulfides within a very narrow pH range (Belzile and Tessier, 1990; Welch et al., 2000). Although As(III) and As(V) have been simultaneously detected in both oxic and anoxic conditions, As(III) is the dominant form in anoxic environments, whereas As(V) is mostly prevalent in aerobic environments (Smedley and Kinniburgh 2002; Oremland and Stolz 2003; Lievremont et al., 2003).

Apart from the main inorganic forms of As, methylated forms have also been detected in natural environments. These methylated compounds are produced as a result of biomethylation by certain groups of microorganisms (Stolz et al., 2006). Methylated As compounds which are formed during biomethylation chain reactions are monomethylarsonic acid (MMA(V)), monomethyarsonous acid (MMA(III)),

dimethylarsinic acid (DMA(V)), dimethylarsinous acid (DMA(III)), trimethylarsine oxide (TMA (V)), and trimethylarsine (TMA(III)) respectively (Dombrowski et al., 2005).

1.3.2 Mechanisms of arsenic mobility in groundwater

Several factors influence the mobility of arsenic in groundwater. One of the most important is sorption onto minerals and soil particles. Several studies (e.g., Anderson et al., 1976; Sadiq, 1997; Smith et al., 1998; Stollenwerk, 2003; Sracek et al., 2004) show that As could adsorb on clay, oxides of Al(III), Fe(III), Mn(III/IV), calcium carbonates and organic matter (e.g., humic substances). Adsorption capacities are different between minerals. For instance halloysite and chlorite were found to adsorb As to a much greater extent than kaolinite, illite and montmorillonite (Lin and Puls, 2000). This behavior was attributed to the larger surface area of disordered halloysite and to the presence of Fe species in chlorite. Amongst the different phases, there is a general consensus that iron oxides/hydroxides are probably the most important adsorbents for arsenic in sandy aquifers in the presence of both acidic and alkaline soils because of their large abundance and strong binding affinity with As (Sadiq, 1997; Manning et al., 1998; Smedley and Kinniburgh, 2002; Dixit and Hering, 2003). For these reasons, the reductive dissolution of Fe oxides, promoted by burial, flooding, transport of organic material or other reducing agents and/or conditions into soil, is considered one of the main possible mechanisms of As release in groundwater (e.g., Matisoff et al., 1982; Korte, 1991; Korte and Fernando, 1991; Stumm and Sulzberger, 1992; Nickson et al., 2000; Anawar, 2003).

Arsenic adsorption can also be affected by the presence of competing ions and in particular of phosphate. The latter has a geochemical behavior which is similar to that of arsenate and can compete for sorption sites with As (Hingston et al., 1971; Livesey and Huang, 1981; Manning and Goldberg, 1996). Adsorption capacity of soil particles depends on different physico-chemical factors such as hydratation, pH and crystallinity (Sadiq, 1997). Amongst these, pH is one of the key parameters governing arsenic mobility because the occurrence of the two inorganic arsenic forms (As(III) and As(V)) strongly depend on pH. As(V) is preferentially sorbed on hydrous oxides for pH values ranging from 4 to 7 whereas As(III) is preferentially sorbed for pH values raging from 7 to 10 (Pierce and Moore, 1980; 1982). As a result, it is clear that changes in groundwater pH can promote adsorption or desorption. Referring to iron-oxide surfaces, adsorption appears to be related to the change in iron-oxide net surface charge from positive to negative as pH

increases above the zero-point-of-charge (pH at which the net surface charge is equal to zero) of about 7.7 for goethite (crystalline iron oxide) (Stumm and Morgan, 1996) or 8.0 for ferrihydrite (amorphous iron oxide) (Dzombak and Morel, 1990). Similarly to pH, redox reactions can control aqueous arsenic concentrations by their effects on arsenic speciation, and hence, arsenic adsorption/desorption.

pH and redox conditions, that are also related to aerobic/anaerobic conditions that could occur in underground, strongly influence arsenic mobilization (Smedley and Kinniburgh, 2002). Redox conditions in soil layers tend to vary widely from +500 mV (surface soils) to –300 mV (strongly reducing conditions) (Signes-Pastor et al., 2007). If pH is not in the alkaline range and ORP is high, arsenic mobilization is difficult (Oscarson et al., 1983; Gulens et al., 1979; Masscheleyn et al., 1991). Under neutral and acidic conditions for ORP < +200 mV Fe(III) is reduced to Fe(II) and Mn(III/IV) to Mn(II). As a consequence, arsenic which is bound to Mn and Fe oxides/hydroxides is mobilized. Under alkaline conditions reduction occurs at lower ORP values (Ferguson and Gavis, 1972). Masscheleyn et al., 1991 found that at –200 mV the solubility of As increase by a factor of 13 when compared to the solubility at +500 mV. Carbonell-Barrachina et al., 2000 found that the mobility of arsenic at –250 mV decreases due to the formation of sulfides.

Arsenic mobility is also influenced by the occurrence of natural organic matter (NOM) that interacts strongly with both soluble metals and metal (hydro)oxide surfaces and plays an important role in governing the speciation, solubility, mobility and bioavailability of chemical species such as arsenic (Wang and Mulligan, 2006). Previous studies reported that arsenic speciation and its mobility in water strongly depends on interactions between NOM and arsenic (Kalbitz and Wennrich, 1998; Anawar et al., 2003) also because NOM can catalyze both oxidation and reduction reactions among chemical species (Senesi and Steelink, 1989; Schwarzenbach et al., 1990; Dunnivant et al., 1992; Perlinger et al., 1996). NOM may serve as electron shuttle between kinetically inert redox species or between microorganisms and arsenic species (Scott et al., 1998). The main influencing mechanisms of arsenic mobility include (a) the competition of arsenic and phosphate (PO_4^{3-}) for available adsorption sites that inhibits or enhances the dissolution of arsenic-binding minerals because of the decrease in phosphate adsorption due to the occurrence of organic acid (e.g., citrate and humic acids) (Fontes et al., 1992; Geelhoed et al., 1998; Eick et al., 1999), and (b) the formation of aqueous complexes and/or changes in the redox potential of surfaces site and arsenic redox speciation (Welch and Lico, 1998; Bradley et al., 1998; McArthur et al., 2001 and 2004; Redman et al., 2002). NOM may also constitute a binding

agent, reducing arsenic mobility. Humic acids were found to adsorb arsenic in the range between 100 mmol/kg and 120 mmol/kg by fixing the metalloid during the precipitation under acidic conditions (Thanabalasingam and Pickering, 1986). Moreover, it was found that NOM can reduce Fe(III) and Mn(III or IV) oxides, leading to leaching of sorbed As (Stone et al., 1994; McArthur et al., 2001). Wang and Mulligan (2006) reported a summary of research studies on interactions between NOM and arsenic concluding that most investigations have been performed on purified minerals under laboratory conditions whereas little research has been performed on NOM in relation with arsenic. Redman et al. (2002) concluded that the presence of NOM may explain observed large mobility of As(III) in soils suggesting that NOM may play a greater role in arsenic mobility than previously recognized.

References

Adriano DC. Trace element in terrestrial environments: Biochemistry, Bioavailability, and risks of metals. 2nd ed. New York: Springer; 2001.

Anderson MA, Ferguson JF, Gavis J. Arsenate adsorption on amorphous aluminium hydroxides. J. Colloid Interface Sci. 1976;54:391–399.

Anawar HM, Akaib J, Komakic K, Teraod H, Yoshiokae T, Ishizukaf T, et al. Geochemical occurrence of arsenic in ground water of Bangladesh: sources and mobilization processes. Journal of Geochemical Exploration 2003;77:109–131.

Azcue JM and Nriagu JO. Arsenic: Historical perspectives. In: Nriagu JO editor. Arsenic in the Environment. Part I: Cycling and Characterization. Wiley New York: 1994. p.1-16.

Baiocchi A, Lotti F, Piscopo V. Influence of hydrogeological setting on the arsenic occurrence in groundwater of the volcanic areas of central and southern Italy. AQUA mundi 2011;131 – 142.

Baroni F, Boscagli A, Di Lella LA, Protano G, Riccobono F. Arsenic in soil and vegetation of contaminated areas in southern Tuscany (Italy). Journal of Geochemical Exploration 2004;81:1 –14.

Bhumbla DK and Keefer RF. Arsenic mobilization and bioavailability in soils. In: Niagru JO editor. Arsenic in environment. Part1: Cycling and Characterization. Wiley New York: 1994. p. 51-82.

Bissen M and Frimmel FH. Arsenic – a Review. Part I: Occurrence, Toxicity, Speciation, Mobility. Acta hydrochim. hydrobiol. 2003;31(1):9–18.

Bradley PM, Chapelle FH, Lovley DR. Humic acids as electron acceptors for anaerobic microbial oxidation of vinyl chloride and dichloroethene. Appl Environ Microbiol 1998;64:3102–3105.

Bundschuh J, Farias B, Martin R, Storniolo A, Bhattacharya P, Cortes J, et al. Groundwater arsenic in the Chaco-Pampean Plain, Argentina: case study from Robles country, Santiago del Estero Province. Appl. Geochem 2004;19:231-243.

Carbonell-Barrachina AA, Jugsujinda A, Burlo F, Delaune RD, Patrick WH. Arsenic chemistry in municipal sewage sludge as affected by redox potential and pH. Water Res 2000;34:216–224.

Clifford DA. Ion exchange and Inorganic Adsorption. Water Quality and Treatment. New York: McGraw-Hill Inc; 1990 p. 613-615.

Daniele L. Distribution of arsenic and other minor trace elements in the groundwater of Ischia Island (southern Italy). Environmental Geology 2004;46:96–103.

Dixit S and Hering JG. Comparison of arsenic(V) and arsenic(III) sorption onto iron oxide minerals: implications for arsenic mobility. Environ Sci Technol 2003;37:4182–4189.

Dombrowski PM, Long W, Farley KJ, Mahony JD, Capitani JF, Di Toro DM. Thermodynamic Analysis of Arsenic Methylation. Environ. Sci. Technol. 2005;39:2169-2176.

Dunnivant FM, Schwarzenbach RP, Macalady DL. Reduction of substituted nitrobenzenes in aqueous solutions containing natural organic matter. Environ. Sci. Technol. 1992;26:2133-2141.

Dzombak DA and Morel FMM. Surface Complexation Modelling: Hydrous Ferric Oxide. Toronto: John Wiley & Sons; 1990.

Frau F, Biddau R, Fanfani L. Effect of major anions on arsenate desorption from ferrihydrite-bearing natural samples. Applied Geochemistry 2008;23:1451–1466.

Ferguson JF and Gavis J. A review of the arsenic cycle in natural waters. Water Res. 1972;6:1259–1274.

Fontes MR, Weed SB, Bowen LH. Association of microcrystalline goethite and humic acid in some Oxisols from Bazil. Soil Sci Soc Am J 1992;56:982–990.

Geelhoed JS, Hiemsta T, Riemsdijk WHV. Competitive adsorption between phosphate and citrate on goethite. Environ Sci Technol 1998;32:2119–2123.

Grafe M, Eick MJ, Grossl PR, Saunders AM. Adsorption of arsenate and arsenite on ferrihydrite in the presence and absence of dissolved organic carbon. J. Environ. Qual. 2002;31:1115– 1123.

Gulens J, Champ DR, Jackson RE. Influence of redox environments on the mobility of arsenic in groundwater. In: Jenne EA. Chemical Modelling in Aqueous Systems. Washington D.C: American Chemical Society; 1979. p. 81–95.

Harvey CF, Swartz CH, Badruzzaman AB, Keon-Blute N, Yu W, Ali MA, et al. Arsenic Mobility and Groundwater Extraction in Bangladesh. Science 2002;298:1602-1606.

Hingston FJ, Posner AM, Quirk JP. Competitive adsorption of negatively charged ligands on oxide surfaces: Discuss. Faraday Soc. 1971;52:334–342.

Kalbitz K and Wennrich R. Mobilization of heavy metals and arsenic in polluted wetland soils and its dependence on dissolved organic matter. Sci Total Environ 1998;209:27–39.

Korte N. Naturally occurring arsenic in groundwaters of the midwestern United States. Environ. Geol. Water Sci. 1991;18:137–141.

Korte NE and Fernando Q. A review of arsenic(III) in groundwater. Crit. Rev. Environ. Control 1991; 21:1–39.

Lievremont D, N'negue MA, Behra P, Lett MC. Biological oxidation of arsenite: batch reactor experiments in presence of kutnahorite and chabazite. Chemosphere 2003;51(5):419 - 428.

Lin Z and Puls RW. Adsorption, desorption and oxidation of arsenic affected by clay minerals and aging process. Environ. Geol. 2000;39:753–759.

Livesey NT and Huang PM. Adsorption of arsenate by soils and its relation to selected chemical properties and anions: Soil Science 1981;131:88–94.

Manning BA and Goldberg S. Modeling arsenate competitive adsorption on kaolinite, montmorillonite and illite. Clays and Clay Minerals. 1996;44:609–623.

Manning BA, Fendorf SE, Goldberg S. Surface structures and stability of arsenic(III) on goethite: spectroscopic evidence for innersphere complexes. Environ Sci Technol 1998;32:2383–2388.

Masscheleyn PH, DeLaune RD, Patrick Jr WH. Effect of redox potential and pH on arsenic speciation and solubility in a contaminated soil. Environ. Sci. Technol. 1991;25:1414-1419.

Matisoff G, Khourey CJ, Hall JF, Varnes AW, Strain WH. The nature and source of arsenic in northeastern Ohio groundwater. Ground Water 1982;20:446–456.

McArthur JM, Ravenscroft P, Safiullah S, Thirlwall MF. Arsenic in groundwater: testing pollution mechanisms for sedimentary aquifers in Bangladesh. Water Resour Res 2001;37:109–117.

Nickson RT, McArthur JM, Ravenscroft P, Burgess WG, Ahmed KM. Mechanism of arsenic release to groundwater, Bangladesh and West Bengal. Appl Geochem 2000;15:403–413.

Nordstrom DK. Worldwide Occurrences of Arsenic in Ground Water. Science 2002;296:2143-2145.

Oremland RS and Stolz JF. The Ecology of Arsenic. Science 2003;300(5621):939 - 944.

Oscarson DW, Huang PM, Liaw WK, Hammer UT. Kinetics of oxidation of arsenite by various manganese dioxides. Soil Sci. Soc. Am. J. 1983;47:644–648.

Perlinger J, Angst W, Schwarzenbach RP. Kinetics of reduction of hexachloroethane by juglone in solutions containing hydrogen sulfide. Environ Sci Technol 1996;30:3408–3417.

Perker CL. The Mitre Corporation. USEPA 1981.

Pierce ML and Moore CB. Adsorption of arsenite on amorphous iron hydroxide from dilute aqueous solution. Environ. Sci. Technol 1980;14(2):214–216.

Pierce ML and Moore CB. Adsorption of arsenite and arsenate on amorphous iron hydroxide. Water Res. 1982;16:1247–1253.

Preziosi E, Giuliano G, Vivona R. Natural background level and threshold values derivation for naturally As, V and F rich groundwater bodies: a methodological case study in Central Italy. Environ Earth Sci 2010;61:885–897. doi:10.1007/S12665-009-0404-y.

Razzak A, Jinno K, Hiroshiro Y, Halim MA, Oda K. Mathematical modeling of biologically mediated redox processes of iron and arsenic release in groundwater. Environ Geol 2009;58:459–469.

Redman AD, Macalady D, Ahmann D. Natural organic matter affects arsenic speciation and sorption onto hematite. Environ Sci Technol 2002;36:2889–2896.

Rhine ED, Phelps CD, Young LY. Anaerobic arsenite oxidation by novel denitrifying isolates. Environmental Microbiology 2006;8(5):899-908.

Sadiq M. Arsenic chemistry in soils: an overview of thermodynamic predictions and field observations. Water Air Soil Pollut. 1997;93:117–136.

Schreiber ME, Simo JA, Freiberg PG. Stratigraphic and geochemical controls on naturally occurring arsenic in groundwater, eastern Wisconsin, USA. 2000;8:161-176.

Schwarzenbach RP, Stierli R, Lanz K and Zeyer J. Quinone and Iron Porphyrin Mediated Reduction of Nitroaromatic Compounds in Homogeneous Aqueous Solution. Environ. Sci. Technol 1990;24:1566-1574.

Scott DT, McKnight DM, Harris BEL, Kolesar SE, Loveley DR. Quinone moieties act as electron acceptors in the reduction of humic substances by humic-reducing microorganisms. Environ Sci Technol 1998;32:2984–2989.

Signes-Pastor A, Burlo F, Mitra K, Carbonell-Barrachina. Arsenic biogeochemistry as affected by phosphorus fertilizer addition, redox potential and pH in a west Bengal (India) soil. Geoderma 2007;137:504–510.

Smedley PL and Kinniburgh DG. A review of the source, behaviour and distribution of arsenic in natural waters. Appl. Geochem 2002;17:517–568.

Smith E, Naidu R, Alston AM. Arsenic in the soil environment: a review. Adv. Agron. 1998;64:149–195.

Stollenwerk KG. Geochemical processes controlling transport of arsenic in groundwater: a review of adsorption. In: Welch AH, Stollenwerk KG. Arsenic in Ground Water: Geochemistry and Occurrence. Boston: Kluwer Academic Publishers; 2003. p. 67–100.

Stolz JF, Basu P, Santini JM, Oremland RS. Arsenic and Selenium in Microbial metabolism. Annu. Rev. Microbiol. 2006;60:107-130.

Stone AT, Godtfredsen KL, Deng B. Sources and reactivity of reductants encountered in aquatic environments. In: Bidoglio G and Stumm W. Chemistry of Aquatic Systems: Local and Global Perspectives. ECSC: Ed. Book; 1994. p. 337–374.

Stumm W and Sulzberger B. The cycling of iron in natural environments: considerations based on laboratory studies of heterogeneous redox processes. Geochim. Cosmochim. Acta 1992;56:3233–3257.

Stumm W and Morgan JJ. Aquatic Chemistry. 3rd ed. New York: Wiley; 1996.

Thanabalasingam P and Pickering WF. Arsenic adsorption by humic acids. Environ. Pollut. 1986;12:233–246.

Ungaro F, Ragazzi F, Cappellin R, Giandon P. Arsenic concentration in the soils of the Brenta Plain (Northern Italy): Mapping the probability of exceeding contamination thresholds. Journal of Geochemical Exploration 2008;96:17– 131.

Wackett LP, Dodge AG, Ellis LBM. Microbial genomics and the periodic table. Appl. Environ. Microbiol. 2004;70:647-655.

Wang S and Mulligan CN. Effect of natural organic matter on arsenic release from soils and sediments into groundwater. Environmental Geochemistry and Health. 2006;28:197–214.

Welch AH and Lico MS. Factors controlling As and U in shallow ground water, southern Carson Desert, Nevada. Appl. Geochem. 1998;13:521–539.

WHO. Guidelines for drinking-water quality. Volume 1: Recommendations. 2nd ed. Geneva: WHO; 1993.

WHO. Guidelines for drinking-water quality. Volume1: Recommendations. 3rd ed. Geneva: WHO; 2008.

CHAPTER 2

Natural Background Level of inorganic compounds in groundwater

2.1. Introduction

The evaluation of natural background level of inorganic compounds such as arsenic is required by EU Water Framework Directive (WFD 2000/60/EC, article 17) that stresses the need for Member States to identify significant and sustained upward trends of compounds that can compromise the achieving of good chemical status of groundwater to determine the starting points for reversing these trends. Procedures and criteria to achieve these objectives are presented in the GroundWater Daughter Directive (GWDD 2006/118/EC). In this context, it is relevant to provide estimates of Natural Background Levels (NBLs) and Threshold Values (TVs) of chemical species considered to be of particular interest.

Several definitions of natural background have been proposed (Reimann and Garret, 2005). The GWDD (article 2.5) defines the NBL as "the concentration of a substance or the value of an indicator in a body of groundwater corresponding to no, or only very minor, anthropogenic alterations to undisturbed conditions". The TV is considered as the environmental quality standard of groundwater and is determined on the basis of the NBL. For a given compound, it represents the concentration value which must not be exceeded to protect human health and environment (GWDD 2006/118/EC; European Commission, 2009).

NBLs depend primarily on the petrographical composition of the aquifer (Hinsby et al., 2006). They can be considered as the result of (a) water-rock interactions, (b) chemical and biological processes taking place in variably saturated subsoil, (c) interactions with other water bodies, (d) residence times of solutes within a given host formation, (e) time fluctuations of flow paths, and (f) climate impacts on the soil-aquifer environment. For these reasons, a groundwater body is characterized by its own natural chemical signature, which may display significant space-time heterogeneity (Edmunds et al., 2003; Wendland et al., 2005; Panno et al., 2006; Edmunds and Shand, 2008; European Commission, 2009). Spatial variations of NBL can be large and it might be convenient from a practical standpoint to introduce a range of values rather than a single average (or absolute) value (Edmunds et al., 2003; Reimann and Garret, 2005; Hinsby et al., 2006). In this context, the

GWDD requires setting a unique TV for a given chemical species for which there is the need to discriminate between natural and anthropogenic effects on the concentrations detected in the groundwater.

Edmunds et al. (1997) consider estimating NBLs at a large scale (national/regional level) on the basis of the concept of groundwater residence time. This allows to discriminate among waters of different ages (i.e., palaeowaters, pre-industrial and/or modern waters (Hinsby et al., 2001)) and the NBL is evaluated as the 95th percentile of the concentrations distribution of the chemical species detected.

A variety of methodologies are adopted by different Countries to assess NBLs of compounds in groundwater. For example, NBLs can be estimated upon comparing current chemical status against some defined drinking water standards (Swedish EPA, 2000). The Ireland EPA (Buss et al., 2004) examines the concentration of a chemical species prior to anthropogenic impacts and then calculates an upper and lower concentration limit by extrapolation of the identified natural distribution. A statistical approach is proposed in Germany (Wendland et al., 2005), relying on the separation of natural and anthropogenic contribution in monitored concentration distributions. The South Australia EPA (2008) suggests to evaluate NBL by means of (a) statistical methods, or (b) historic analysis of groundwater or (c) selection of a subset of data that is assumed to be representative of the natural composition of the residing groundwater on the basis of hydrological and geochemical tracers (e.g., tritium). Griffioen et al. (2008) compare three selection approaches (i.e., historic method, tritium method, oxidation capacity method) adopted in The Netherlands to establish NBLs which are calculated as the 90th percentile of the selected concentration data.

In principle, NBL can be viably evaluated (i) from groundwater samples unaffected by human impact, or (ii) with the aid of modern multicomponent reactive transport modeling. Both methods are not immune from drawbacks. On one hand, only samples from deep aquifers can be assumed to be relatively free from anthropogenic influences. On the other hand, even though multicomponent reactive transport modeling is widely used in environmental problems (e.g., Lichtner, 1985; Yeh and Tripathi, 1989; Steefel et al., 2005; Bea et al., 2009; Miller et al., 2010, and references therein), critical outstanding challenges still need to be fully addressed and resolved for their routine use in real aquifer systems (Steefel et al., 2005). With special reference to large scale aquifer systems, these include the need to address the discrepancies observed between reaction rates at the laboratory and

field scales, the problem of bridging across scales, and the conceptual and parametric uncertainty which plagues groundwater flow and transport modeling.

Estimating NBLs relying on global statistical analyses of monitored data is an alternative to these two approaches which can be pursued in practical applications involving large scale aquifer bodies (Edmunds et al., 2003; Wendland et al., 2005; Panno et al., 2006; Edmunds and Shand, 2008; Walter, 2008). At the same time, global statistical analyses can result in merging different populations (stemming, e.g., different redox environments) within a unique data-set. As such, redox conditions should be carefully evaluated before analysis (Hinsby and Condesso de Melo, 2006).

Global statistical approach starts from the idea that the empirical distribution of available resident concentration data can be decomposed into a mixture of contributions of natural and/or anthropogenic origin. Along these lines, a recommendation stemming from the EU research project BRIDGE (2007), Background cRiteria for the IDentification of Groundwater thrEsholds, is that when there is sufficient availability of data (in terms of quality and quantity of information) the Component Separation method (CS) developed by Wendland at al. (2005) should be adopted. On the other hand, a simplified approach based on Pre-Selection (PS) of data points (Hart et al., 2006) might be preferable in cases where hydrochemical characterization of a given water body can be considered of a mediocre level.

Recently, Hinsby et al. (2008) present an application of the Pre-Selection method to 14 European groundwater bodies representative of different aquifer types, climate settings and ecoregions. This work focus on three large-scale water bodies representative of the same aquifer type (i.e., marine deposits) and located within the same ecoregion, i.e., Italy, Mediterranen sea (according to the analysis of Wendland et al. (2008)).

Both the CS and PS methods are here applied to provide estimates of NBLs (and associated TVs) of the target chemical compounds which are adopted in the context of assessing the environmental quality status of these systems. Inorganic compounds considered are ammonium (NH_4), boron (B), and arsenic (As), which are characterized, in the aquifers bodies analyzed, by the occurrence of concentrations larger than reference values provided by Italian regulations.

The areas investigated are associated with an abundant and high quality data-set, thus allowing application and comparison of both methodologies. The specific setting of the investigated water bodies allows investigating possible dependencies of NBLs on representative depths of the target groundwater bodies. An analysis of the dynamics of the

evolution of NBL within the investigated groundwater bodies is then performed upon considering data aggregated according to different temporal observation windows. Up to now, this application represents the first large scale joint application in Italy of both methodologies which addresses the above mentioned temporal and spatial dynamics.

2.2. Materials and methods

2.2.1 Hydrogeological setting of the study area

The three groundwater bodies analyzed are located in Northern Italy, within the Emilia Romagna region (Fig. 2.1a). They are part of the Po Basin fill, which is a syntectonic sedimentary wedge (Ricci Lucchi, 1984) forming the infill of the Pliocene-Pleistocene fore-deep. The sedimentary evolution of the basin is characterized by an overall regressive trend from Pliocene open marine facies to Quaternary marginal marine and alluvial deposits, respectively indicated as cycle *Qm* and *Qc* by Ricci Lucchi et al. (1982). According to recent studies (Regione Emilia Romagna & ENI, 1998) cycle *Qc* is subdivided into two coarse units, respectively denominated Cycle A and Cycle B. The lower portion of these units, whose thickness is about 100-150 m, is formed by clayey deposits. The latter lay on Cycle C, which, in turn, is the upper portion of Cycle *Qm*. The stratigraphic features of cycle *Qc* have been investigated by well correlation. Cycle *Qc* is essentially composed by coarse deposits with subordinate clay, while sand deposits are scarce. The alluvial deposits form large and productive aquifer systems.

Three Plio-Pleistocenic age aquifers of fresh water have been identified: aquifer group A (between 0 m and 150-200 m), aquifer group B (between 150 m and 300-350 m) and aquifer group C (more than 300-350 m deep). They correspond to Cycles A, B and C, respectively, as depicted in Fig. 2.1b). Aquifer group A and B are essentially composed by alluvial deposits. Aquifer group C is composed by sea deposits (Regione Emilia-Romagna & ENI, 1998).

Based on sedimentological and hydrogeological analysis, three main hydrogeological complexes, i.e., Apennines alluvial fans, Apennine alluvial plain and alluvial and deltaic Po plain, are identified. The Apennines alluvial fans complex characterizes the uppermost portion of the Po basin at its southern border (Appennine piedmont area). It is formed by an array of coalescent fans. The mainly coarse deposits are related to the fluvial activity of the Apennine streams. In the proximal regions of the alluvial fans, where recharge boundary conditions can be identified for the plain aquifers,

the ground water is essentially unconfined. Multilayered confined or semiconfined waters can be recognized in the distal portions, due to the occurrence of interbedded fine deposits.

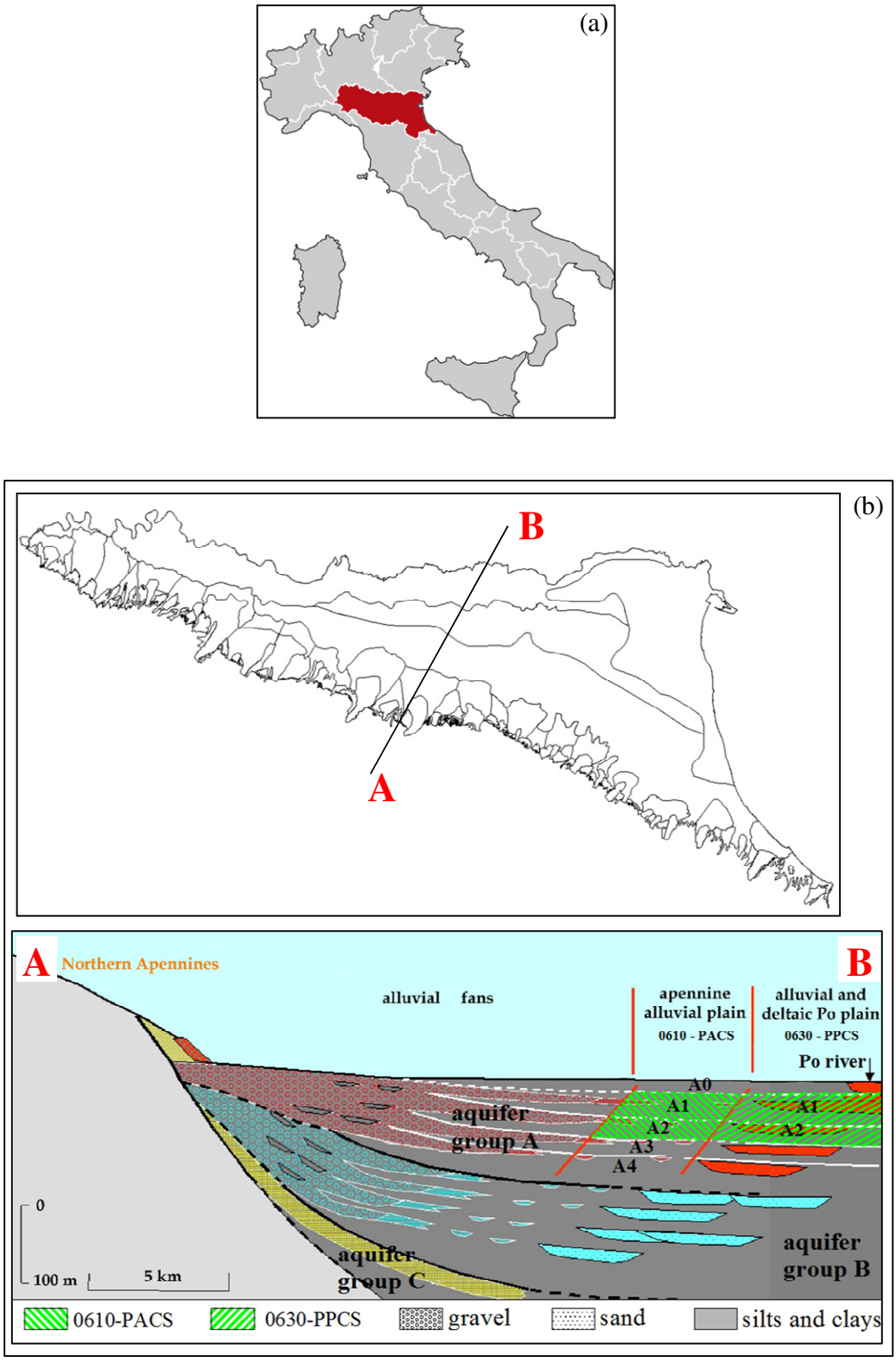

Fig. 2.1 - (a) Location of the Emilia–Romagna region within Italy, and (b) planar extension of the groundwater bodies identified with the trace of the cross-section A–B which corresponds to the simplified schematic hydrostratigraphic cross-section illustrated.

Gravel is gradually replaced by sand deposits in the northern part of the plain and the thickness of fine deposits increases (Regione Emilia Romagna, 2010). These depositional units become mainly silty clayey with local interbedding of coarser material. Four confined hydrogeological units, indicated as A1, A2, A3, and A4 in Fig. 2.1b, are identified within aquifer group A. A free surface layer A0 (with average thickness of about 10 m and discontinuous sand deposits) overlays these units (Fig. 2.1b). An upper confined portion including A1 and A2 and a lower confined portion including A3, A4, aquifer group B and aquifer group C have been distinguished within the aquifer system in a series of studies aimed to delineate ground water bodies for the implementation of Directive 2000/60/CE (Regione Emilia Romagna, 2010). This subdivision was performed upon considering (a) the different strengths of the anthropogenic impacts acting on the system, and (b) the fact that units A1 and A2 are associated with paleo-geographical signatures different from those related to units A3 and A4.

A total of 144 groundwater bodies were identified within the Emilia Romagna region (Regione Emilia Romagna, 2010). This study analyzed chemical data collected within three of these groundwater bodies, i.e., (i) the Alluvial Po plain, (ii) the Appenine alluvial plain, and (iii) the alluvial plain. These are hereinafter identified by the codes 0630-PPCS, 0610-PACS, and 2700-PACI, respectively.

As illustrated in Fig. 2.1b, the two bodies 0630-PPCS and 0610-PACS are located in the upper confined portion of the aquifer system, while the third one (2700-PACI) is a deep confined system. Fig. 2.2 depicts the location and planar extent of the groundwater bodies within the entire aquifer system. Table 1 lists the average depth, the average thickness and the area of the three water bodies analyzed.

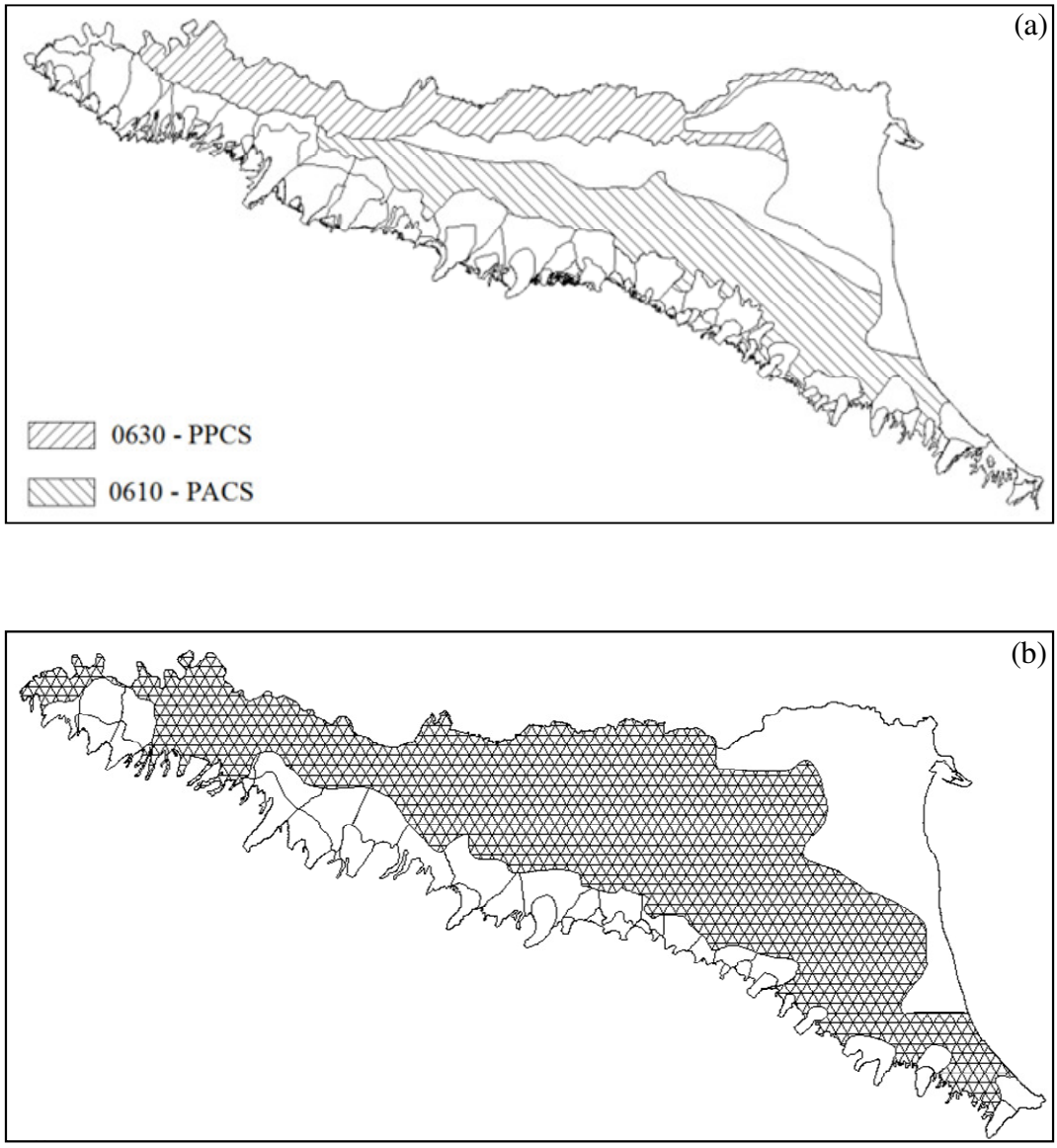

Fig. 2.2 - Groundwater bodies (a) 0630-PPCS and 0610-PACS, and (b) 2700-PACI identified within the Emilia–Romagna region.

Table 2.1
Extension and characteristic scales of the three groundwater bodies analyzed.

groundwater body	**average depth** (m)	**average thickness** (m)	**area** (km^2)
0610 – PACS	75	130	2928
0630 – PPCS	65	110	1995
2700 – PACI	200	180	6934

The groundwater bodies analyzed comprise deep aquifer systems which are kept under confined conditions by aquitards characterized by significant thickness. Oxidation reduction potential (ORP) in these systems is sufficiently stable around reducing conditions. This is consistent with the occurrence of organic matter, i.e., paleo-peats (Amorosi et al., 1996; Cremonini et al., 2008) at the investigated depths and the observation that the reduced form of nitrogen (i.e., NH_4) is detected in available samples. Continuous monitoring of ORP in the three selected aquifer bodies is available between 1987 and 1998. The three systems analyzed are characterized by comparable general redox behavior. Monitored median ORP values for each water body (+36 mV in 0630-PPCS; +10 mV in 0610-PACS; and +3 mV in 2700-PACI) indicate the occurrence of reducing environments with slightly enhanced reducing conditions in the deepest water body (2700-PACI).

Due to their location within the aquifer system, these groundwater bodies are subject to different levels of anthropogenic stress, because of the different exploitation regime, in terms of water consumption and withdrawals. Moreover, the deepest water bodies tend to receive diluted contaminant concentrations from recharge areas, as a consequence of natural attenuation phenomena.

The response of each water system to man-induced stresses is then different due to the different volumes of water stored, which is typically largest for the deepest groundwater bodies. This is then associated with a different system response to a given contaminant mass injected. In general, it is expected that human influence is less acute for the deepest water body, because of (a) the effect of natural attenuation processes and (b) the reduced level of exploitation when compared against the remaining two aquifers.

The choice of these systems has been motivated by their significant planar extent, with representative scale of the order of hundreds of kilometers, and the abundance of monitoring stations associated with records of about 20 years of observations. These recordings have been performed on a six-month basis between 1987 and 2008 and constitute a unique data-base employed in the context of this investigation.

2.2.2 Available data-set

The analysis is based on time series of concentration data recorded at several monitoring locations included in the extensive network of observation wells managed by the “Agenzia Regionale per la Prevenzione e l’Ambiente dell’Emilia-Romagna” (ARPA –

Regional Agency for Environmental Protection). The chemical species considered in this research (metals and inorganic compounds, as reported in the following) have been subject to a preliminary exploratory statistical analysis. The relative fraction of samples exceeding thresholds values currently set by Italian regulation (D. Lgs. 30/09) was then evaluated for each chemical species. In this application, it was assumed that a chemical species associated with observed concentrations exceeding the reference threshold value for at least 5% of the samples collected can be considered as significant to the characterization of the chemical status of a given groundwater body. Increasing this percentage to 10% does not change the number of species which are then subject to the analysis.

Groundwater body 0630-PPCS is characterized by 75 monitoring stations for a total of 1884 samples. Amongst the substances that contribute to define the good chemical status of a groundwater system, only NH_4 and As were found to be of interest, respectively being associated with a total amount of 62.5% and 6.0% of samples exceeding the regulatory limit value. Groundwater body 0610-PACS includes 88 monitoring stations, for a total of 1428 samples. Here, NH_4, B and As were found to be of interest, respectively being associated with an exceedance of the regulatory limit value in 81.4%, 9.9% and 20.7% of the samples analyzed. A set of 56 monitoring stations (corresponding to a total number of 1391 samples), is located within groundwater body 2700-PACI. Here, only NH_4, B, chlorides and As are considered to be of interest, on the basis of the adopted criteria, and they are found to exceed the current Italian regulation limit for a number of samples respectively equal to 78.6%, 13.9%, 11.4% and 9.3% of the total. Following this preliminary analysis, NBLs are estimated only on NH_4, B, and As, which are detected in all the examined groundwater bodies. Current Italian regulation limits coincide with the European Drinking Water Standards and are set as 0.5 mg/L for NH_4, 1000 µg/L for B and 10 µg/L for As.

2.2.3 Data Analysis

When dealing with large scale aquifer systems requiring characterization in terms of their geochemical signature under data scarcity, it can be convenient to analyze available information collected within a monitoring framework through statistical analysis methods. Here, two methodologies are considered, i.e., the Component Separation (CS) and Pre-Selection (PS) (e.g., Voigt et al., 2005), and estimates of Natural Background Level (NBL) and associated Threshold Values (TV) of selected environmental parameters are

provided. Voigt et al. (2005) suggest employing the CS method in the presence of what they define as good knowledge of hydrochemical characteristics of the water body, as supported by a relatively large data-set. On the other hand, these authors suggest resorting to PS under scarcity of monitored data, resulting in a mediocre state of system knowledge.

Examples of application of CS to assess NBLs for several groundwater parameters (e.g., K, Fe, NO_3, Mg, electrical conductivity) in different aquifer systems in Germany are provided by Wendland et al. (2005). Hinsby et al. (2008) illustrate some examples of application of PS to estimate NBLs and TVs of different elements (e.g., As, chlorides, sulphates) in some European Countries (e.g., Portugal, Denmark, Germany, Italy). Preziosi et al. (2009) report an application of PS to the estimation of NBLs and TVs of As, V, F and Cl in a region in central Italy.

2.2.3.1. Component Separation

The methodology is based upon the idea that the empirical frequency distribution, $f_{obs}(c)$, of the concentration, c, of a given environmental parameter can be modeled as a mixture of two contributions, $f_{nat}(c)$ and $f_{inf}(c)$, respectively representing the natural and influenced component, i.e.,

$$f_{obs}(c) = f_{nat}(c) + f_{inf}(c) \quad (1)$$

The former is typically linked to the hydrogeological settings of the aquifer body and the homogeneous and heterogeneous (geo)chemical processes characterizing the interaction between the host porous matrix and fluid flow and transport of chemical species. The influenced component is related to processes directly or indirectly associated with human activities.

The functional format of the two distribution functions is not known a priori. Natural concentration patterns are typically associated with a skewed distribution (e.g., Ahrens, 1953; Chayes, 1954; Miller and Goldberg, 1955; Limbert et al., 2001; Parkin and Robinson, 1992; Warrick et al., 1996). Models which have been adopted in the literature to interpret environmental data include (a) the Log-Normal (Shimizu and Crow, 1988), (b) the generalized Log-Logistic (Singh et al., 2001), (c) the Gamma (Jakeman and Taylor, 1985), and (d) the truncated Normal (Schmoyer et al., 1996) and the Weibull (Nanag, 1998) distribution. The model choice can be based on its goodness-of-fit against experimental data. In this context, Ott (1990) adopted the concept of Successive Random Dilutions to support experimental observations suggesting that pollutant concentrations often tend to appear log-normally distributed. Wendland et al. (2005) also considered a

Log-Normal model in the context of applications related to implementations of the Water Framework Directive. Here, Wendland et al. (2005) approach is followed considering that the natural and influenced component can be described by a Log-Normal and Normal distribution, respectively. On these bases, $f_{obs}(c)$ is approximated as

$$f_{obs}(\mathrm{c}) = k \cdot \left\{ \frac{A}{\sigma_{nat}\sqrt{2\pi}\ c} \cdot e^{-\frac{(\ln c - \ln \mu_{nat})^2}{2\sigma_{nat}^2}} + \frac{(1-A)\cdot t_N}{\sigma_{inf}\sqrt{2\pi}} \cdot e^{-\frac{(c-\mu_{inf})^2}{2\sigma_{inf}^2}} \right\} \quad (2)$$

Here, k is the average size of the classes adopted for the calculation of the relative frequency, A is the mixture weight, μ_{nat} and μ_{inf} respectively are the median of the natural and influenced distribution, σ_{nat} and σ_{inf} being the associated standard deviations, and t_N = 0.5 is a truncation factor insuring that concentrations are always positive. The model is then characterized by five parameters, which are typically estimated by a calibration of model predictions against experimental data.

Parameter estimation is performed within a Maximum Likelihood framework. The estimated NBL value is then calculated after calibration on the basis of the 10th and 90th percentiles, respectively indicated as NBL_{10} and NBL_{90}, of the natural component of the mixture (e.g., Wendland et al., 2005). The variability of NBL_{10} and NBL_{90} between different water bodies is essentially governed by the calibrated weight of the mixture of components. The latter is exclusively an indication of the relative importance of natural and anthropogenic influence within a given water body and does not allow direct comparison between the strength of anthropogenic influence acting on different bodies.

Following, e.g., Wendland et al. (2005), the empirical frequency distribution (1) is constructed on the basis of the set of median values which has been calculated from each available concentration time series. This is tantamount considering an average depiction of the system behavior. Unlike Wendland et al. (2005) the available data set is divided into a set of observation windows to analyze the dynamic evolution of the NBLs of the selected environmental parameters. Data are aggregated according to different lengths of the observation records, i.e., 7, and 10 years, to provide a depiction of the NBLs dynamics at various levels of temporal resolutions.

2.2.3.2. Pre-Selection

Pre-Selection (PS) has been proposed by Wendland et al. (2005), in the framework of the BRIDGE (2007) project. It is a simplified procedure which should be employed to estimate NBLs and TVs of dissolved chemical species within a groundwater body when

information scarcity does not support adopting a Component Separation technique. It has recently been adopted by Preziosi et al. (2009) to assess NBLs and TVs of some chemical species in a groundwater body in Central Italy. The methodology starts by selecting, within the available data-set, samples that meet certain criteria and can be considered unaffected by human influence. Typically adopted criteria are associated with the following constraints: (a) chloride concentrations < 1000 mg/L; (b) nitrates concentrations < 10 mg/L; and (c) NH_4 concentrations < 0.5 mg/L. Additional exclusion criteria (e.g., redox conditions) could be considered as pointed out by Hinsby and Condesso de Melo (2006) and Hinsby et al. (2008) to minimize the occurrence of grouping different populations. After selection, one then calculates the median of the time record of concentrations of the selected species measured at a given monitoring well. Wendland et al. (2005) propose to estimate NBL_{90} as the 90^{th} percentile of the sample formed by all the calculated medians.

Sample cores collected from the porous confined aquifer bodies provide evidence of natural occurrence of paleo-peats (Amorosi et al., 1996; Cremonini et al., 2008) that are associated with large NH_4 concentrations which increase with depth. On these bases, NH_4 concentrations are not considered as indicator of human influence on the environment.

2.2.3.3. Evaluation of Threshold Values (TV)

Muller et al. (2006) propose to estimate the Threshold Value (TV) of a given chemical species detected in the groundwater body upon comparing the estimated NBL against the reference standard (REF) of the receiving groundwater body. The drinking water standards (DWS) or the environmental quality standards (EQS) are typically considered as appropriate reference values (REF). The authors propose the following scenarios: (a) if NBL < REF, then TV = (REF + NBL) / 2; or (b) if NBL ≥ REF, then TV = NBL. Here, concentrations threshold imposed by Italian regulations (D. Lgs. 30/09) is employed as the reference values for the chemical species examined.

2.3. Application in Emilia Romagna: results and discussion

This section presents the results obtained by applying the CS (2) and PS methodologies to assess NBLs and TVs of NH_4, B and As in the three water bodies under study, according to Section 2.2.1. Note that B concentrations measured in water body 0630-PPCS are associated with values exceeding the Italian regulatory limit in less than

5% of the samples. Normalized frequencies are considered in the parameter estimation procedure. The sensitivity of the results to the choice of binning intervals has been analyzed and the results reported are associated with the lowest values of the objective function selected.

The application of CS considering different temporal aggregation windows of data is illustrated. The two groundwater bodies used for this application are 0630-PPCS and 0610-PACS, which are associated with data-sets that allow this kind of analysis.

Monitoring stations that cannot be attributed with certainty to a target groundwater bodies have been excluded from the analysis. Monitoring stations where a period of observations spanning less than 3 years is available are also excluded. Outliers are identified and removed from the data population. Outliers are here identified as median concentrations that lie outside an interval centered around the sample mean and of width equal to three times the sample standard deviation. As a result, it is identified: (a) one outlier for As and NH_4 in groundwater body 0610-PACS; (b) no outliers in groundwater body 0630-PPCS; and (c) one outlier for As in groundwater body 2700-PACI. Excluding these points from the analyses is consistent with allowing that the global behavior of the large scale systems considered is not completely driven by a single and highly localized information.

Physical evidences supporting the differences evidenced amongst the populations of concentrations associated with the three water bodies analyzed include: (a) the slightly enhanced reducing conditions associated with the deepest aquifer; (b) the different strengths of withdrawals (due to human activity and decreasing with depth) stressing the aquifers; and (c) the occurrence of old and less disturbed waters (which are close to natural, geogenic, undisturbed conditions) in the deep groundwater body, which can be correlated with the largest NBL predicted.

For all analyses have been selected only observation wells monitored within the 15 years period 1994-2008 where data have been regularly collected, ensuring the availability of homogeneous data-series.

2.3.1 Ammonium

Table 2.2 shows the main results obtained applying PS to NH_4 data. The estimated NBLs for water bodies 0630-PPCS and 0610-PACS are comparable. An increase in NBL is noted for 2700-PACI, which is associated with the highest average depth. This is consistent with the idea that NBL values need to be estimated independently for each of the water bodies within an aquifer system, because spatial variability of hydrogeochemical and physical processes can lead to variations of NBL values between different water bodies.

Table 2.2
Estimated NH_4 NBL on the basis of PS for the three water bodies analyzed.
EU Drinking Water Standard for NH_4 is 0.5 mg/L.

groundwater body	**estimated NBL** [mg/L]
0610-PACS	4.6
0630-PPCS	5.2
2700-PACI	12.0

Fig. 2.3 depicts the sample relative frequency distribution, $f_{obs}(c)$, of NH_4 for the three water bodies analyzed. It also reports the distributions $f_{nat}(c)$, $f_{inf}(c)$ and $(f_{nat}(c) + f_{inf}(c))$ calibrated according to the methodology illustrated.

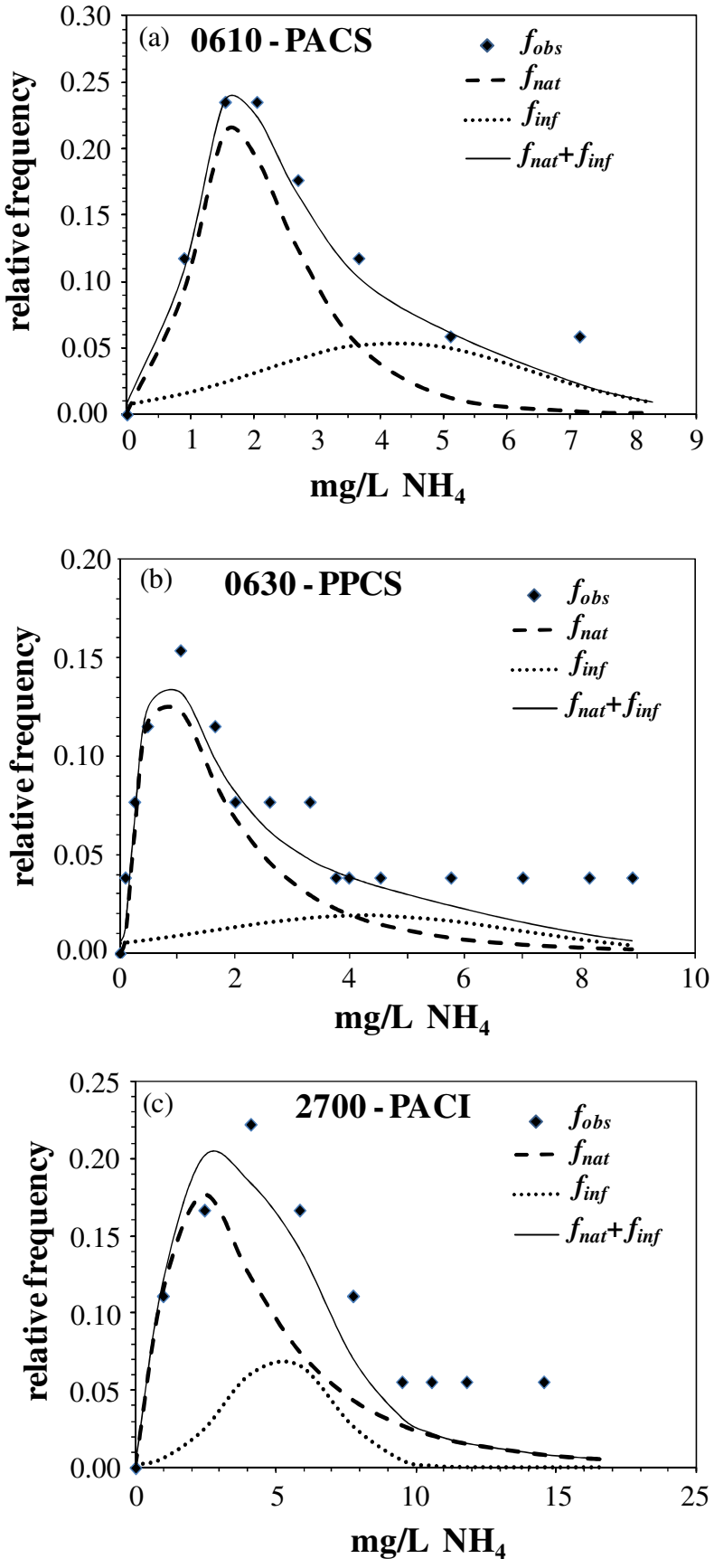

Fig. 2.3 - Empirical frequencies, f_{obs} , of NH_4 together with the natural (f_{nat}) and anthropogenic (f_{inf}) distributions, and their sum ($f_{nat} + f_{inf}$) evaluated on the basis of (2) for groundwater bodies (a) 0610-PACS, (b) 0630-PPCS, and (c) 2700-PACI.

Fig. 2.3a and 2.3b suggest that in the upper water bodies (0610-PACS and 0630-PPCS) (a) the highest empirical frequencies are associated with concentrations ranging between 1 and 3 mg/L and are well interpreted by a Log-Normal distribution, and (b) the contribution of the Normally distributed component becomes relevant to interpret the largest concentrations. In the deepest water body the observed empirical frequency distribution (2700-PACI, Fig. 2.3c) the spread of the anthropogenic component around its mean is less pronounced than in the other aquifer bodies. The long tail characterizing f_{nat} (c) in 2700-PACI results in a large value of NBL_{90}, when compared to the scenario associated with the upper groundwater bodies.

Table 2.3 shows that the estimated NBLs are largest for the deep water body (2700-PACI), consistently with the results of the PS method (Table 2.2).

Table 2.3
Estimated NBLs and TVs obtained after calibration of (2) for NH_4 median-averaged data. EU Drinking Water Standard for NH_4 is 0.5 mg/L.

groundwater body	**0610-PACS**	**0630-PPCS**	**2700-PACI**
NBL_{10} [mg/L]	1.1	0.5	1.4
NBL_{90} [mg/L]	3.7	4.7	10.4
TV [mg/L]	3.7	4.7	10.4

This result is also consistent with the observation that the strength of withdrawals tend to decrease with depth as compared to the extraction rates, e.g., for irrigation purposes, from the upper water bodies. As a result, groundwater in the upper water bodies is renewed more frequently than in the deep systems by anthropogenic effects. Therefore, changes in the NH_4 balance due to, e.g., pumping, are more significant in the two upper systems that for the deep water body where the oldest and less disturbed waters are found. For these reasons, and considering the unlikely event that the NH_4 produced by human activities on the surface can directly reach the deep water body, one can expect an increase in NH_4 NBLs with the depth of a given water body. Note that the estimated TVs are above the current limit set by regulatory standards in Italy (D. Lgs. 30/09).

2.3.2 Boron

Due to the fact that less than 5% of the samples recorded in 0630-PPCS show values of B concentrations exceeding the Italian regulatory limit, B is not considered to be critical for the chemical status of this water body and has been analyzed only for water bodies 0610-PACS and 2700-PACI.

Table 2.4 summarizes the main results of PS, showing a slight increase of NBL with average depth of the groundwater body.

Table 2.4
Estimated NBL for B on the basis of PS for the two water bodies analyzed.
EU Drinking Water Standard for B is 1000 µg/L.

groundwater body	**estimated NBL** [µg/L]
0610-PACS	817
2700-PACI	890

Fig. 2.4 depicts the sample relative frequency distribution of B for the water bodies 0610-PACS and 2700-PACI together with the results of the CS analysis. Note that the weight associated with the anthropogenic component is negligible so that the observed empirical distribution of median concentrations is interpreted entirely in terms of a natural contribution.

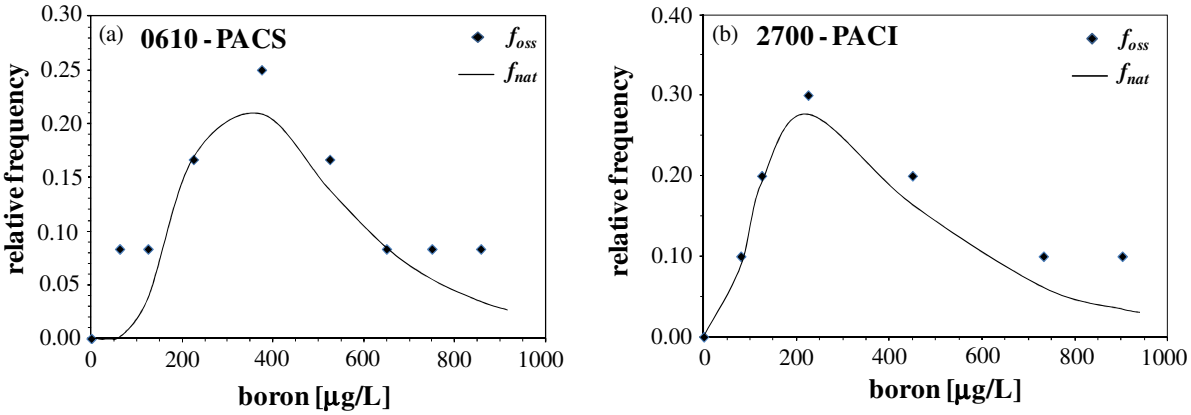

Fig. 2.4 - Observed (f_{obs}) and estimated (f_{nat}) frequencies for B for groundwater bodies (a) 0610-PACS, and (b) 2700-PACI. The observed empirical distribution of median concentrations is interpreted entirely in terms of a natural contribution.

Table 2.5 summarizes the main results obtained via CS, in terms of NBLs and TVs. One can note that these are comparable with those presented in Table 2.4, the NBL_{90} for 0610-PACS being only slightly lower than that for 2700-PACI.

Table 2.5
Estimated NBLs and TV obtained from (2) for B.
EU Drinking Water Standard for B is 1000 µg/L.

groundwater body	**0610-PACS**	**2700-PACI**
NBL_{10} [µg/L]	219	149
NBL_{90} [µg/L]	799	857
TV [µg/L]	899	928

This result appears to be consistent with the observations that (a) in the deep water body (2700-PACI) there is a lower number of production wells than in the upper water bodies, and (b) the impact of the drawdowns on oldest and less disturbed waters tends to decrease with depth. Note that the estimated TVs lie below the current limit set by regulatory standards in Italy (D. Lgs. 30/09) which can be adopted as reference in this case.

2.3.3 Arsenic

Table 2.6 summarizes the main results of PS for As within the three water bodies examined. One can note that while water bodies 0630-PPCS and 2700-PACI are associated with comparable estimates of As NBL, water body 0610-PACS displays the largest NBL value. This is consistent with the analytical evidence that high As content is found in the solid matrix (Zavatti et al., 1995), particularly within the water body 0610-PACS, although not always As in solution is related to As in the aquifer.

Table 2.6
Estimated NBL for As on the basis of PS for the three water bodies analyzed.
EU Drinking Water Standard for As is 10 µg/L.

groundwater body	**estimated NBL** [µg/L]
0610-PACS	33
0630-PPCS	4
2700-PACI	6

Fig. 2.5 depicts the sample relative frequency distribution of As for the three water bodies analyzed. It also reports the distributions f_{nat} (c), f_{inf} (c) and $(f_{nat}$ (c) + f_{inf} $(c))$

calibrated according to the methodology illustrated. Table 2.7 reports the corresponding results in terms of NBLs and TVs.

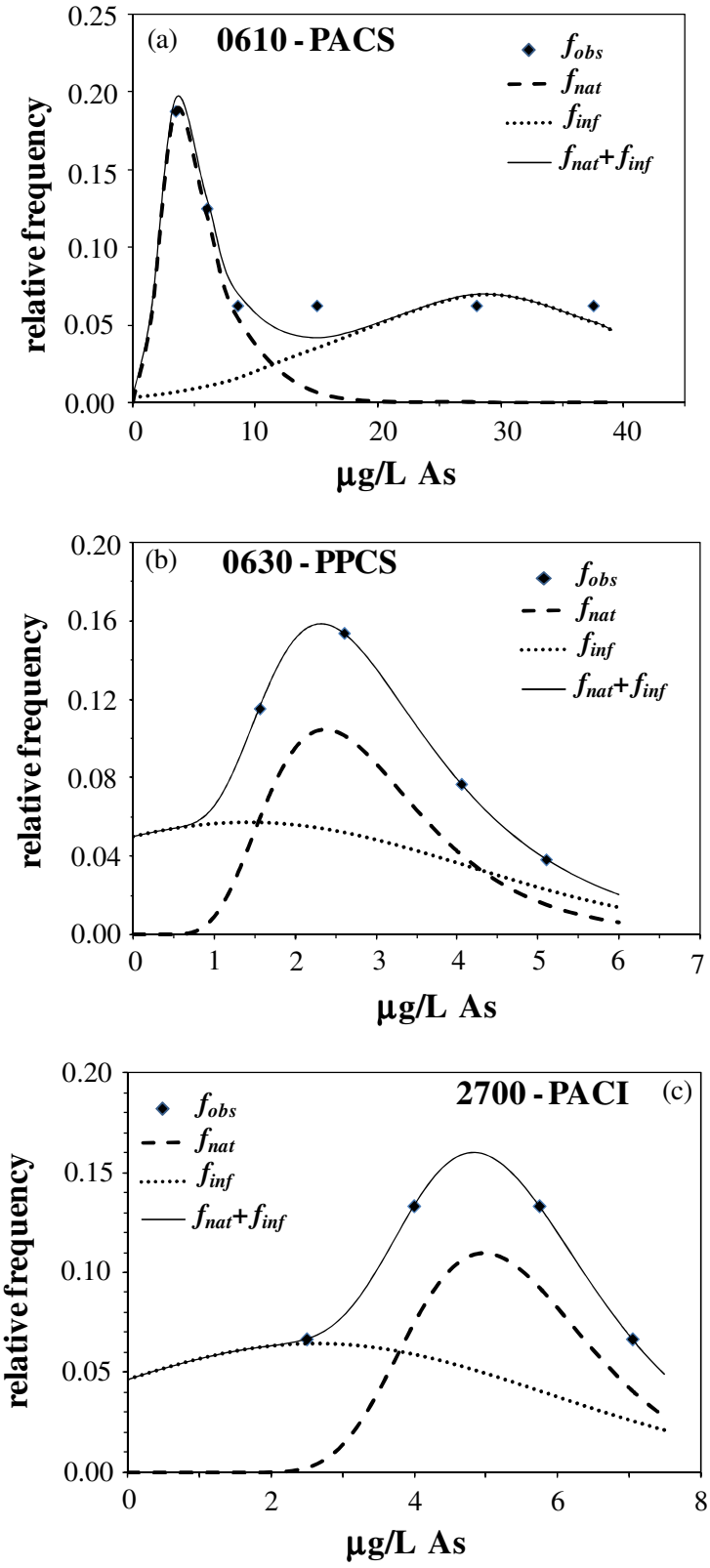

Fig. 2.5 - Empirical frequencies, f_{obs} , of As together with the natural (f_{nat}) and anthropogenic (f_{inf}) distributions and their sum ($f_{nat} + f_{inf}$) evaluated on the basis of (2) for groundwater bodies (a) 0610-PACS, (b) 0630-PPCS, and (c) 2700-PACI.

Table 2.7
Estimated NBLs and TVs of As obtained from (2).
EU Drinking Water Standard for As is 10 µg/L.

groundwater body	**0610-PACS**	**0630-PPCS**	**2700-PACI**
NBL_{10} [µg/L]	2	1	3
NBL_{90} [µg/L]	9	4	7
TV [µg/L]	9	7	8

Analysis of the figures (Fig. 2.5) reveals that the largest sample frequencies are associated with low concentrations (less than 5 µg/L). This result in a Log-Normal distribution more concentrated around low concentrations value and in a Normal distribution with a high variance.

Close inspection of the estimated NBLs listed in Table 2.7 indicates that these are not consistent with observed As occurrence in the solid matrix of the aquifers, effect of natural attenuation processes and the reduction of withdrawals with increasing depth. This is evidenced by the fact that the NBL_{90} associated with the deep water body is lower than that estimated for the upper body 0610-PACS.

This, and the observed differences in the estimated NBL_{90} between the water bodies 0610-PACS and 0630-PPCS support the idea that the complex dynamics of the As system are poorly or only marginally interpreted by global statistical methods such as those applied here. This argument is also supported by considering that the estimated NBL_{90} for As is not consistent with analytical evidences supporting high As content in the solid matrix which, in turn does not necessarily imply the occurrence of large As concentration in solution. As a consequence, a relatively large NBL value is anticipated for this compound in this particular groundwater body. Note that the estimated TV is above the current limit set by regulatory standards in Italy (D. Lgs. 30/09) only in the water body 0610-PACS.

2.3.4 Temporal dynamics of NBLs

The temporal evolution of NBLs is here explored in the framework of CS with reference to data collected in the two water bodies 0610-PACS and 0630-PPCS which are representative of comparable average vertical elevations. The analysis considers NH_4 and B, in light of the observation that the methodology appears to provide NBL estimates

which are inconsistent with the current field evidences related to As (i.e., observed high As levels in the solid matrix are not always linked to large As concentration in solution) and are unable to cope with the complex dynamics driving the evolution of the As geochemical system. Within the record comprising 15 years of observations, temporal windows of 10 and 7 years are employed to assess the impact of the observation time scale on possible trends. The choice of these aggregation windows allows having a sufficiently high number of data to obtain statistically reliable results. The analyses are performed through moving windows with a 2 years overlap.

Fig. 2.6 and 2.7 depict the results for the estimated NBL_{10} and NBL_{90} of NH_4 in the 0610-PACS and 0630-PPCS water bodies, respectively, when the available data-set is subdivided into 10 and 7 years observation windows. The associated NBL_{90} estimated on the basis of the complete 15 years data record (horizontal line) is also reported.

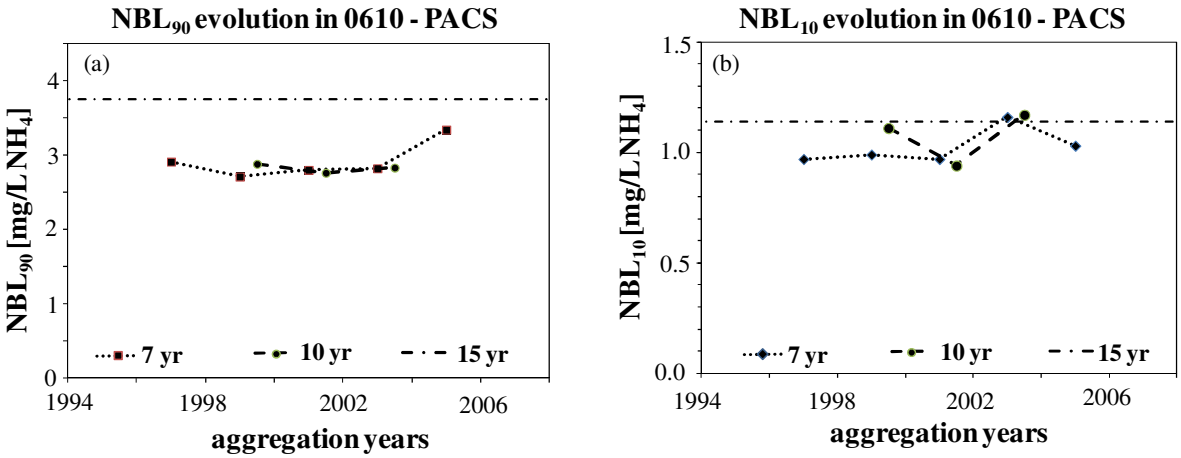

Fig. 2.6 - Temporal evolution of (a) NBL_{90} and (b) NBL_{10} of NH_4 in water body 0610-PACS.

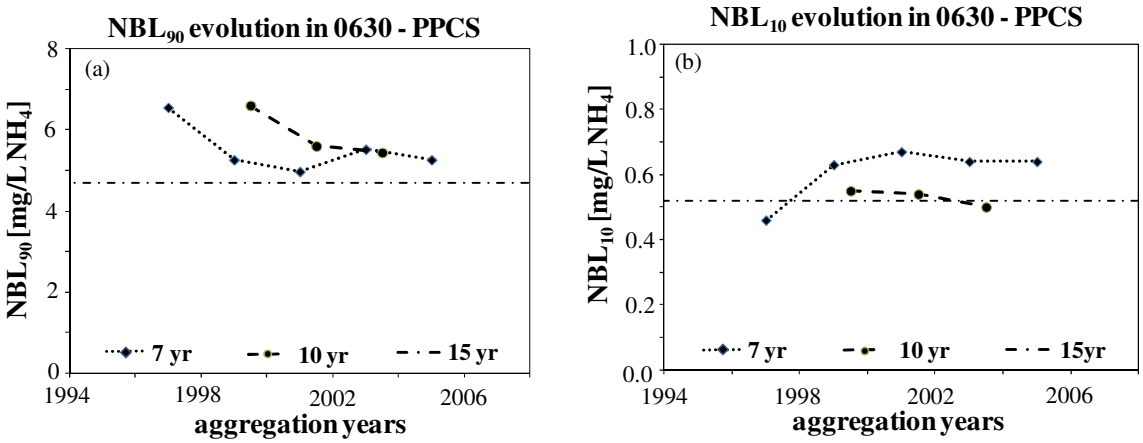

Fig. 2.7 - Temporal evolution of (a) NBL_{90} and (b) NBL_{10} of NH_4 in water body 0630-PPCS.

The corresponding depiction for B is reported in Fig. 2.8. Table 2.8 presents the estimated TVs for NH_4 after disaggregation of the data into temporal windows of 7 and 10 years width.

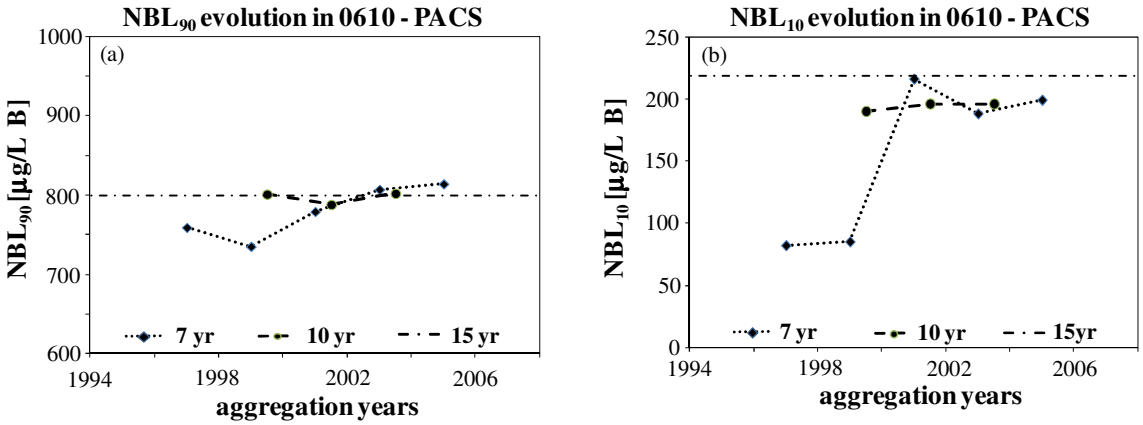

Fig. 2.8 - Temporal evolution of (a) NBL_{90} and (b) NBL_{10} for boron in water body 0610-PACS.

Table 2.8
TVs estimated for NH_4 on the basis of 10 and 7 years aggregation windows.
EU Drinking Water Standard for NH_4 is 0.5 mg/L.

	groundwater body			
	0610-PACS		**0630-PPCS**	
	TV [mg/L]		TV [mg/L]	
Aggregation years	10 year periods	7 year periods	10 year periods	7 year periods
1995-2004	2.8	-	6.6	-
1997-2006	2.7	-	5.6	-
1999-2008	2.8	-	5.4	-
1994-2000	-	2.9	-	6.5
1996-2002	-	2.7	-	5.2
1998-2004	-	2.8	-	4.9
2000-2006	-	2.8	-	5.5
2002-2008	-	3.3	-	5.2

The corresponding results for B are included in Table 2.9 with reference to the water body 0610-PACS (B is not critical for 0630-PPCS, as detailed in see Section 2.3.2).

Table 2.9
TVs estimated for B on the basis of 10 and 7 years aggregation windows.
EU Drinking Water Standard for B is 1000 µg/L.

	groundwater body	
	0610-PACS	
	TV [µg/L]	
Aggregation years	10 year periods	7 year periods
1995-2004	900	-
1997-2006	894	-
1999-2008	901	-
1994-2000	-	879
1996-2002	-	867
1998-2004	-	889
2000-2006	-	903
2002-2008	-	907

Modest variations in the NH_4 NBL_{90} are observed over the time frame of the monitoring campaigns within water body 0610-PACS (Fig. 2.6a). A uniform distribution with a slight upward trend at the end of the observation period is notable in Fig. 2.6a, when data are sub-sampled according to 7 years observation windows. Only mild temporal variations are associated with NBL_{10} (Fig. 2.6b) when data are analyzed on the basis of 7 and 10 years observation windows. The results related to the 7 years aggregation window appear to suggest that the estimated NBL_{10} and NBL_{90} tend to an upper value within the monitoring period.

Decreasing trends are observed for the NBL_{90} of NH_4 associated with water body 0630-PPCS (Fig. 2.7a), independently of the aggregation time adopted. The NH_4 NBL_{90} related to 7 and 10 years observation windows appears to reach asymptotically the value of NBL_{90} obtained from the string of 15 years of observations. NH_4 NBL_{10} values (Fig. 2.7b) are relatively stable, ranging between 0.4 and 0.6 mg/L.

The estimated TVs for NH_4 show small time fluctuations and are always larger than the reference threshold value prescribed by current Italian regulations (D.Lgs. 30/09).

When data are analyzed on the basis of 7 years observation windows, the NBL_{90} (Fig. 2.8a) of B displays an initial decreasing trend. The trend is then reversed with a

relatively uniform increase, with values approaching the results related to the complete 15 years data-base. A qualitatively similar behavior is observed for NBL_{10} (Fig. 2.8b).

Values of NBL_{90} and NBL_{10} evaluated on the basis of the 10 years observation windows display relatively uniform values. B TVs are subject to a slight temporal increase and are always found to be lower than the threshold value prescribed by current Italian regulations which can be adopted as a limit value.

Obtained results indicate that NBLs display some dynamic features. These depend on the evolution and interplay of natural processes and anthropogenic impact developing within a given groundwater body. Small temporal windows highlight the temporal non-homogeneity of the data-set. Use of large observation scales for data aggregation appears to lead to smoothing of the system behavior in the cases examined.

2.4. Conclusions

This study for natural background level evaluation of inorganic compounds leads to the following main conclusions.

1. For the scenarios analyzed over the available observations distributed within a 15 years monitoring period, Component Separation (CS) and Pre-Selection (PS) render estimated values of NBLs which are associated with the same order of magnitude. The ensuing estimated threshold values (TVs) are above (as in the case of NH_4) or below (for B) the threshold limits imposed by the Italian regulations in the water bodies analyzed. The estimated TV for As is above the current limit set by regulatory standards in Italy only in the water body 0610-PACS. The water bodies analyzed are characterized by different responses, in terms of estimated NBLs, to the same chemical species. This supports the need to clearly delineate water bodies within a large scale aquifer system and to assess NBLs and TVs of target species separately for each identified water body.
2. The results are consistent with the expectation that NBLs tend to increase with the average depth of a water body. Within the field cases tested an increase in NBLs with water body depth is found only in the case of NH_4 and to a lesser extent for B. From a physical standpoint, this increase is expected because of (a) the decreasing amount of withdrawals with depth and (b) the effect of natural attenuation processes. In addition to these causes and mechanisms, the occurrence in deep water bodies of dissolved compounds such as As can be the result of release mechanisms from the

(heterogeneous) matrix of the host porous medium which are associated with high concentrations of these sorbed species. When possible, statistical methods should therefore be complemented by (a) robust experimental characterization of the geochemical system and (b) modeling studies performed on the basis of multicomponent reactive transport techniques.

3. The results suggest that methodologies based on global statistics such as Component Separation (CS) are unable to embed the complex dynamics of compounds such as As. As a consequence, these techniques do not allow to obtain estimates consistent with the analyzed hydrogeochemical setting. A notable weakness of the methodologies analyzed is the inability to consider possible correlations between different elements (e.g., high concentrations of As in the presence of high concentrations of Fe) that could be the result of natural processes and might jointly influence the system behavior.
4. Application of CS over different aggregation windows allows identifying temporal dynamics of NBLs and TVs of target compounds within the observation time frame. Identification of these dynamics can provide valuable information in the context of evolving management strategies. This stresses the value of a dynamic monitoring design and analysis of well demarcated groundwater bodies to update the associated NBLs as a function of the temporal dependence of both anthropogenic impacts and natural processes occurring in the subsurface.

References

Ahrens LH. The lognormal distribution of the elements (A fundamental law of geochemistry and its subsidiary). Geochimica et Cosmochimica Acta 1953; 5:49-73.

Amorosi A, Farina M, Severi P, Preti D, Caporale L, Di Dio G. Genetically related alluvial deposits across active fault zones: an example of alluvial fan-terrace correlation from the upper Quaternary of the southern Po Basin, Italy. Sedimentary Geology 1996; 102:275-295.

Bea SA, Carrera J, Ayora C, Batlle F, Saaltink MW. Cheproo: A Fortran 90 object-oriented module to solve chemical processes in earth science models. Computers & Geosciences 2009; 35:1098–112.

BRIDGE - Background cRiteria for the IDentification of Groundwater Thresholds 2007. http://nfp-at.eionet.europa.eu/irc/eionet-circle/bridge/info/data/en/index.htm. (Accessed 15 March 2010).

Buss S, Lloyd J, Streetly M, Foley R, Shanahan I. Development of a Methodology for the Characterisation of Unpolluted Groundwater, Final Report (2002-W-DS/7-M1). Environmental protection agency, Ireland; 2004.

Chayes F. The lognormal distribution of the elements: a discussion. Geochimica et Cosmochimica Acta 1954; 6:119-120.

Cremonini S, Etiope G, Italiano F, Martinelli G. Evidence of possible enhanced peat burning by deep-origin methane in the Po River delta Plain (Italy). The Journal of Geology 2008; 116:401-413.

Decreto Legislativo n. 30 del 16 marzo 2009. Attuazione della direttiva 2006/118/CE, relativa alla protezione delle acque sotterranee dall'inquinamento e dal deterioramento. Pubblicato nella Gazzetta Ufficiale n. 79 del 4 aprile 2009.

Directive 2000/60/EC - Water Framework Directive (WFD). Directive of the European Parliament and of the Council of 23 October 2000 establishing a framework for Community action in the field of water policy, OJ L327, 22 Dec 2000, pp 1-73.

Directive 2006/118/EC, GroundWater Daughter Directive (GWDD). Directive of the European Parliament and of the Council of 12 December 2006 on the protection of groundwater against pollution and deterioration, OJ L372, 27 Dec 2006, pp 19-31.

Edmunds WM and Shand P. Natural Groundwater Chemistry. Oxford: Blackwell Publishing ltd; 2008, 469 pp.

Edmunds WM, Brewerton LJ, Shand P, Smedley PL. The natural (baseline) quality of groundwaters in England and Wales: Part 1: A guide to the natural (baseline) quality study. British Geological Survey Technical Report 1997; WD/97/51.

Edmunds WM, Shand P, Hart P, Ward RS. The natural (baseline) quality of groundwater: a UK pilot study. Sci Total Environ 2003; 310:25-35. doi: 10.1016/S0048-9697(02)00620-4

European Commission. Guidance on groundwater status and trend assessment, guidance document no 18. Technical Report 2009, ISBN 978-92-79-11374-1 European Communities, Luxembourg, 2009.

Griffioen J, Passier HF and Klein J. Comparison of selection methods to deduce natural background levels for groundwater units. Environ. Sci. Technol. 2008; 42:4863–4869.

Hart A, Müller D, Blum A, Hookey J, Kunkel R, Scheidleder A, et al. Preliminary methodology to derive environmental threshold values. D15. Report to the EU project "BRIDGE"; 2006. wfd-bridge.net.

Hinsby K, Condesso de Melo MT, Dahl M. European case studies supporting the derivation of natural background levels and groundwater threshold values for the protection of dependent ecosystems and human health. Sci Tot Environ 2008; 401(1-3):1-20.

Hinsby K, Condesso de Melo MT. Application and evaluation of a proposed methodology for derivation of groundwater threshold values-a case study summary report. In: Report to the EU project ''BRIDGE'' 2006 Deliverable D22. http://www.wfd-bridge.net

Hinsby K, Edmunds WM, Loosli HH, Manzano M, Melo MTC, Barbecot F. The modern water interface: recognition, protection and development - Advance of modern waters in European coastal aquifer systems. In: Edmunds and Milne (Eds.): Palaeowaters in Coastal Europe: evolution of groundwater since the late Pleistocene. Geol. Soc. Spec. Publ., 2001; 189:271-288.

Jakeman A and Taylor J. A hybrid ATDL-gamma distribution model for predicting urban area source acid gas concentration. Atmospheric Environment 1985; 19:1959-1967.

Lichtner PC. Continuum model for simultaneous chemical reactions and mass transport in hydrothermal systems. Geochim Cosmochim Acta 1985; 49:779–800.

Limbert E, Stahel W, Abbt M. Log-normal distribution across the sciences: keys and clues. BioScience 2001; 51(5):341-352.

Miller AW, Rodriguez DR, Honeyman BD. Upscaling sorption/desorption processes in reactive transport models to describe metal/radionuclide transport: A critical review. Environ Sci Technol 2010; 44:7996–8007.

Miller RL and Goldberg ED. The normal distribution in geochemistry. Geochimica et Cosmochimica Acta 1955; 8:53-62.

Muller D, Blum A, Hart A, Hookey J, Kunkel R, Scheidleder A, Tomlin C, Wendland F. Final proposal for a methodology to set up groundwater threshold values in Europe. In: Report to the EU project ‘‘BRIDGE’’ 2006, Deliverable D18. http://www.wfd-bridge.net

Nanag D. Suitability of the normal, Log-normal and Weibull distributions for fitting diameter distributions of neem plantations in Northern Ghana. Forest Ecology and Management 1998; 103:1-7.

Ott WR. A physical explanation of the lognormality of pollutant concentrations. Journal of the Air and Waste Management Association 1990; 40:1378-1383.

Panno SV, Kelly WR, Martinsek AT, Hackley KC. Estimating background and threshold nitrate concentrations using probability graphs. Ground Water 2006; 44(5):697-709.

Parkin T, Robinson J. Analysis of lognormal data. In: Stewart B, editor. Advances in Soil Science. New York: Springer; 1992. p. 194-231.

Preziosi E, Giuliano G, Vivona R. Natural background level and threshold values derivation for naturally As, V and F rich groundwater bodies: a methodological case study in Central Italy. Environ Earth Sci 2009. doi: 10.1007/S12665-009-0404-y

Regione Emilia-Romagna & ENI. Riserve idriche sotterranee della Regione Emilia-Romagna. Firenze: Selca; 1998.

Regione Emilia-Romagna, 2010. Delibera di Giunta n. 350 del 8/02/2010, Approvazione delle attività della Regione Emilia-Romagna riguardanti l'implementazione della Direttiva 2000/60/CE ai fini della redazione ed adozione dei Piani di Gestione dei Distretti idrografici Padano, Appennino settentrionale e Appennino centrale. http://ambiente.regione.emilia-romagna.it/acque/temi/piani%20di%20gestione (Accessed 28 February 2012).

Reimann C and Garret RG. Geochemical background: concept and reality. Sci Tot Environ 2005; 350:12-27.

Ricci Lucchi F, Colalongo ML, Cremonini G, Gasperi G, Iaccarino S, Papani G, Raffi S, Rio D. Evoluzione sedimentaria e paleogeografica del margine appenninico (Sedimentary and

palaeogeographic evolution of the apenninic margin). Guida alla geologia del margine appenninico padano. Guide geologiche regionali, Soc. Geol. Ital. 1982; 17-46.

Ricci Lucchi F. Flysch, molassa, cunei clastici: tradizione e nuovi approcci nell'analisi dei bacini orogenici dell'Appennino settentrionale (Flysh, molassa, clastic deposits: traditional and innovative approaches to the analysis of north Apeninic basins). Cento Anni di Geologia Italiana. Volume Giubilare 1° centenario Soc. Geol. Ital. 1984; 279-295.

Schmoyer R, Beauchamp J, Branndt C, Hoffman F. Difficulties with the lognormal model in mean estimation and testing. Environmental and Ecological Statistics 1996; 3:81-97.

Shimizu K, Crow E. History, genesis, and properties. In: Crow E, Shimizu K, editors. Lognormal Distributions: Theory and Applications. New York: Marcel Dekker; 1988; p. 2-26.

Singh K, Bartolucci A, Bae S. Mathematical modeling of environmental data. Mathematical and Computer Modelling 2001; 33:793-800.

South Australia EPA. Site contamination – Determination of background concentrations. EPA 838/08 guidelines; 2008.

Steefel CI, DePaolo DJ, Lichtner PC. Reactive transport modeling: An essential tool and a new research approach for the Earth sciences. Earth Planet Sci Lett 2005; 240:539-58.

Swedish EPA. Environmental quality criteria for groundwater. Swedish Environmental Protection Agency, Report 5051, Stockholm; 2000.

Voigt HJ, Hannappel S, Kunkel R and Wendland F. Assessment of natural groundwater concentrations of hydrogeological structures in Germany. Geologija – Vilniaus Universitetas 2005; 50:35-47.

Walter T. Determining natural background values with probability plots. EU Groundwater Policy Developments Conference, UNESCO, Paris, France, 13-15 Nov 2008

Warrick W, Musil S, Artiola J. Statistics in pollution science. In: Pepper I, Gerba C, Brusseau M, editors. Pollution Science. London: Academic Press; 1996. p. 95-112.

Wendland F, Blum A, Coetsiers M, Gorova R, Griffioen J, Grima J, et al. European aquifer typology: a practical framework for an overview of major groundwater composition at European scale. Environ Geol 2008; 55(1):77-85.

Wendland F, Hannappel S, Kunkel R, Schenk R, Voigt HJ, Wolter R. A procedure to define natural groundwater conditions of groundwater bodies in Germany. Water Sci Technol 2005; 51(3-4):249-257.

Yeh GT and Tripathi VS. A critical evaluation of recent developments in hydrogeochemical transport models of reactive multichemical components. Water Resour Res 1989; 25:93–108.

Zavatti A, Attramini D, Bonazzi A, Boraldi V, Malagò R, Martinelli G, Naldi S, Patrizi G, Pezzera G, Vandini W, Venturini L, Zuppi GM. Quaderni di Geologia Applicata, Pitagora Editrice Bologna 1995; 2:301-326.

CHAPTER 3

Experimental characterization of arsenic release from different solid matrices

3.1. Introduction

Chapter 2 illustrates the application of global statistical methodologies (i.e., Component Separation and Pre-Selection) to evaluate natural background level (NBL) of inorganic compounds, including arsenic (As), that can display concentration values in groundwater larger than those envisioned by current regulations. This statistical application highlighted that, whenever feasible, statistical methods should be complemented by robust experimental characterization of the geochemical system.

Methodologies based on global statistics appear to be unable to explain the complex dynamics of arsenic, providing NBL values which are inconsistent with the hydrogeochemical setting of the study area. These methodologies do not allow to evaluate possible correlations between different elements (e.g., high concentrations of As in the presence of high concentrations of Fe) that could be the result of natural processes and might jointly influence the system behavior.

Following these conclusions, the main goal of this chapter is to provide additional elements to improve our understanding of geochemical dynamics of As and form the basis for consistent estimates of natural arsenic concentrations in a target groundwater body. This aspect is key to groundwater management strategies, a major challenge for the distinction between anthropogenically and naturally induced arsenic concentration levels.

Confronting this problem typically requires laboratory scale experiments. These are usually performed by means of batch/incubation tests (Reddy and Patrick, 1974 and 1976; Gao and Mucci, 2000; Frohne et al., 2011) or (flow-through) column tests (Lim et al., 2007; Nguyen et al., 2008; Razzak et al., 2009). Batch tests are commonly used to analyze the effect of ORP (oxidation reduction potential) temporal changes, which in turn affect pH (Yu et al., 2007) and could occur in a natural aquifer as a consequence of variations of water table elevations.

A considerable body of evidence from laboratory studies shows that As is released from soils following flooding and the subsequent development of anaerobic conditions (e.g., Deuel and Swoboda, 1972; Hess and Blanchar, 1977; McGeehan, 1996; Frohne et

al., 2011). Guo et al. (1997) measure the rate of As release from spiked sediments under progressive reducing conditions, and attribute such release predominantly to the dissolution and desorption from Fe and Mn oxides. Matis et al. (1997) analyze adsorption of As(V) on synthetic goethite in a batch test and interpret the experimental data by a Langmuir isotherm. Batch tests are also employed to evaluate As adsorption and/or kinetics and/or dissolution of several mineral phases such as, for instance, siderite, green rust (fougerite) and magnetite (Jönsson and Sherman, 2008), calcite (Alexandratos et al., 2007), and scorodite (Harvey et al., 2006). Frohne et al. (2011) use an automated biogeochemical microcosm system to assess the effect of redox potential on the mobility of several metals, including As, by imposing stepwise ORP variations from reducing (approximately −300 mV at pH 5) to oxidizing (+600 mV at pH 5) conditions. These authors find that As concentrations in solution decrease significantly with increasing ORP and conclude that low ORP promotes As mobility.

Several experiments as well as theoretical modeling attempts based on thermodynamic data (e.g., Davis and Ashenberg, 1989; Vink, 1996; Sadiq, 1997) have been performed to characterize As mobility. Batch tests are often performed by employing soil samples which are artificially contaminated (e.g., by mining or pesticides) or enriched with synthetic As solutions (e.g., Manning and Goldberg, 1997; Smith et al., 1999; Nguyen et al., 2008) to identify the mechanisms governing As release. These tests typically employ distilled or deionized water (e.g., Masscheleyn et al., 1991; Burnol et al., 2007) or tap water (e.g., Nguyen et al., 2008). Only a limited set of experiments consider real untreated natural soils (Pfeifer et al., 2004; Frohne et al., 2011) and no tests document the amount of As released from a natural solid matrix subject to redox changes consistent with ORP and pH values measured at field scale. While a few studies analyze the influence of organic matter (i.e., peat or humic/fulvic acids) on As adsorption on mineral phases (e.g., Grafe et al., 2002; Pfeifer et al., 2004; Weng et al., 2009), no studies document As release from deep vegetal matter.

In this context, this Chapter illustrates the results of batch laboratory tests performed on different types of solid matrices which are representative of the natural host porous medium occurring in a deep groundwater system in the Emilia-Romagna Region, Italy. This study aims at reproducing at the laboratory scale real conditions occurring in these deep aquifers. As opposed to the common practice of analyzing surface soil samples collected at depths of 5 - 35 cm (e.g., Masscheleyn et al., 1991; Chatain et al., 2005), experiments are performed on samples collected at a depth larger than 45 m for which no

(or minimal) anthropogenic effects have been observed. Water sampled from the same groundwater body from which the solid matrix was extracted is employed in the experiments as opposed to the common laboratory practice of using distilled or deionized water or of tap water. As detailed in Section 3.2.2, this water is characterized by As concentrations below the detection limit.

The solid matrices samples collected from the aquifer were subject to (*a*) alternated and controlled redox conditions in a batch reactor, mimicking natural field conditions, and (*b*) further geochemical analyses, to improve the characterization of As distribution within the tested solid matrices and discriminate between different arsenic-bearing phases. These information can be obtained by analyzing As partitioning within a specific solid matrix by means of (*a*) fractionation studies by sequential extractions (Manful et al., 1994; Bombach et al., 1994; Voigt et al., 1996; Kavanagh et al., 1997; Matera et al., 2003), or (*b*) speciation analysis by e.g., ICP-MS (e.g., Pantsar-Kallio and Manninen, 1997). The last few decades have witnessed a markedly increased interest in the use of indirect approaches for these types of characterizations, such as selective sequential extractions (SSE). These are essentially based on the application of a series of reagents to a solid matrix sample to sub-divide the total metal content occurring in each extracted phase (Bacon and Davidson, 2008). Sequential extraction methods represent valuable tools to distinguish trace element fractions associated with different solubility according to the mineralogical phases to which they are bounded (Hlavay et al., 2004) and provide useful information to understand natural processes involving the soil-water environment (Bacon and Davidson, 2008). This approach has been used to characterize a wide variety of substrates such as agricultural soils (Moćko et al., 2003), forest soils (Inaba and Takenaka, 2005; Sipos et al., 2005), soils amended by organic wastes (Chaudhuri et al., 2003; Yoo and James, 2003; Bhattacharyya et al., 2005), urban soils (Yang et al., 2006), sewage sludge (Chen et al., 2005; Fuentes et al., 2004), or composts (Zheng et al., 2004) and evaluate metal fractionation, bioavailability and mobilization. SSE is widely used to assess the impact of human activities, such as mining, on environment (Basilio et al., 2005; Galan et al., 2003; Kraft et al., 2006) or to evaluate the effectiveness of clean-up strategies on metals removal from contaminated sediments and soils (Friesl et al., 2003; Rodríguez-Jordá et al., 2010).

Several sequential extraction procedures are available in the literature for elements producing anionic species such as arsenic (e.g., Tessier et al., 1979; Shuman 1985; Gleyzes et al., 2001; Pagnanelli et al., 2004; Claff et al., 2010). Basically, the procedure

enables one to distinguish the metal fractions which are exchangeable, bound to carbonates, iron and manganese oxihydroxides and oxides, or organic matter, and restrained in the residual portion of the matrix. From these basic schemes, new procedures, which differ in terms of the amount and type of reagent used, have been proposed in literature (e.g., Tretner, 2002; Matera et al., 2003) to allow extracting specific fractions and improve characterization of arsenic-bearing phases. Hudson-Edwards et al., (2004) presented a detailed overview of SSE schemes employed to analyze solid-phase partitioning of As in soils and sediments. Most of the studies involving SSE and As have been targeted at assessing the mobility and availability of arsenic in mine wastes (e.g., Ahn et al., 2005; van Elteren et al., 2006), contaminated sediments (e.g., Damris et al., 2005; Jay et al., 2005) and contaminated soils (e.g., Matera et al., 2003). Studies of arsenic natural distribution in particular areas with high natural concentrations involving sediments (e.g., Bhattacharya et al., 2006), peat (González et al., 2006), and coal (Guo et al., 2004) are also available in literature.

This Chapter is devoted to the illustration of the results of SSE applied to four solid matrices representing natural host rocks occurring in a deep groundwater system in the Emilia-Romagna Region, Italy. Partitioning percentages of As within each solid matrix analyzed is detailed on these bases.

3.2. Materials and methods

3.2.1 Study area

Water and solid matrix samples were collected from a confined groundwater body located near the city of Bologna (Emilia-Romagna Region, Italy). As detailed in Section 2.2.1 of Chapter 2, the analyzed groundwater body (i.e., 0610-PACS) is part of the Po Basin. The latter constitutes a syntectonic sedimentary wedge (Ricci Lucchi, 1984) forming the infill of the Pliocene-Pleistocene foredeep. The aquifer system is mainly composed of coarse deposits with subordinate clay, and scarce sand deposits (Regione Emilia–Romagna, 2010).

Continuous monitoring of oxidation/reduction potential (ORP) in the aquifer is available between 1987–1998 and indicates the occurrence of relatively stable and slightly reducing conditions (median monitored ORP value is +10 mV) in the groundwater body analyzed. This is consistent with (*a*) the occurrence of organic matter, i.e., paleo-peats (Amorosi et al., 1996; Cremonini et al., 2008) and vegetal matter which are observed in

the cores sampled at different depths, and (*b*) the detection of the reduced form of nitrogen (i.e., NH_4) in water samples.

The typical As hot-spot behavior (Charlet et al., 2007) was observed in the analyzed groundwater body through the extensive network of monitoring wells managed by ARPA - Regional Agency for Environmental Protection. Arsenic concentrations in this reservoir have been monitored for over 20 years and showed the occurrence of specific localized areas where As concentrations in water reach values which are 10 times larger than the limit value of 10 μg/L. Previous studies (e.g., Zavatti et al., 1995) hypothesized the possible natural origin of As in the overall Po Basin fill of Emilia-Romagna. Additional studies in the Region (Martinelli et al., 2005; Marcaccio et al., 2005) highlighted that possible changes in redox potential, linked to the changes in water table level as a result of withdrawals, could lead to the dissolution of minerals (basically iron oxides/hydroxides) where As is naturally adsorbed (Postma et al., 2007; Berg et al., 2007) or contained in their crystalline structure. This hypothesis is consistent with other studies (e.g., Harvey et al., 2002; Du Laing et al., 2009) according to which the location of the oxic–anoxic interface is subject to change due to fluctuating water table levels caused by pumping activity or seasonal lowering that promote the reduction of As-binding phases and result in high As concentrations in groundwater.

3.2.2 Water and solid matrices sampling

Experiments employed water collected in a borehole located in the analyzed groundwater body, as opposed to distilled, deionized or tap water which is typically used in most reported experiments (e.g., Masscheleyn et al., 1991; Burnol et al., 2007; Nguyen et al., 2008). This enables one to closely reproduce field conditions to which the solid matrix is exposed. Measurements taken at a six-month interval over 20 years at the water sampling location show As concentrations to be always below the detection limit. Other anthropogenic indicator parameters show no significant human influence (chlorides < 30 mg/L, nitrates < 1 mg/L, sulphates < 1 mg/L) on the selected sampling point.

Several samples of the solid matrices were collected and characterized at varying depths along different boreholes spanning the overall thickness and planar extent of the selected multi-layered aquifer. These samples have been collected in 2007 and stored in a facility managed by Geological, Seismic and Soil Survey of Emilia-Romagna Region. On the basis of this preliminary screening, two cores were isolated (i.e., Bentivoglio and

Minerbio) in a particular area of the reservoir where monitored dissolved As concentrations showed large relative values. Table 3.1 reports metal concentrations in solid phase for each core at different sampling depths.

Table 3.1
Metal concentrations in solid phase for the two selected cores at different sampling depths.

Core	Sampling depth (m)	Al mg/kg	As mg/kg	Cd mg/kg	Cr mg/kg	Fe mg/kg	Pb mg/kg	K mg/kg	Mn mg/kg	Ni mg/kg	Cu mg/kg	Na mg/kg	Zn mg/kg	Ca mg/kg	Mg mg/kg
Bentivoglio	41.50	19354	1.9	<0.2	74.9	19450	9.1	6000	801	22.9	13.5	155	39.8	69000	6250
	44.40	13894	7.9	<0.2	42.0	16950	5.5	4400	845	20.9	8.6	125	31.6	85000	5750
	48.25	13476	62.5	<0.2	29.9	61000	5.3	4150	416	13.4	9.0	140	30.1	60000	4750
	48.30	17156	8.6	<0.2	40.1	20800	6.9	5650	710	19.0	10.6	340	37.3	76000	9250
	52.30	14056	4.2	<0.2	35.8	17550	5.7	4750	757	16.7	10.2	130	38.8	72000	5750
	57.90	21040	7.3	<0.2	47.4	24350	7.9	6950	807	24.3	14.8	165	41.1	65000	8000
	70.30	19572	3.6	<0.2	451	17750	10.0	6350	616	18.8	15.0	145	39.9	63000	7000
	72.50	9962	3.8	<0.2	25.4	12200	4.5	3150	709	9.6	6.3	120	25.5	62000	4750
	74.50	45740	66.9	<0.2	76.6	36000	13.3	8000	339	30.5	14.9	370	59.7	19000	5250
Minerbio	31.20	8368	1.4	<0.2	30.6	10600	5.2	3050	394	13.4	5.2	115	22.4	54000	4250
	32.90	5198	1.2	<0.2	24.6	7250	2.9	1900	387	7.0	2.9	100	13.5	50000	2750
	34.10	5882	1.9	<0.2	42.8	8350	3.3	2100	527	14.8	3.2	85	15.0	64000	4250
	105.00	16726	2.9	<0.2	41.7	21800	7.8	6250	559	16.3	6.6	225	31.6	65000	5250
	106.00	14316	1.8	<0.2	32.5	17400	5.3	5050	695	13.8	6.5	155	29.1	70000	4500
	110.70	7742	4.3	<0.2	22.2	10500	4.3	2550	816	10.3	3.2	125	23.2	58000	3750

Large As concentrations are observed in core Bentivoglio at depth 48.25 m (Fig. 3.1a) and 74.50 m (Fig. 3.1b). The solid matrix sampled from this core at these two specific depths has therefore been selected for the tests.

Fig. 3.1a – Core Bentivoglio at depth 44-48 m. Sampled points are marked with red circled

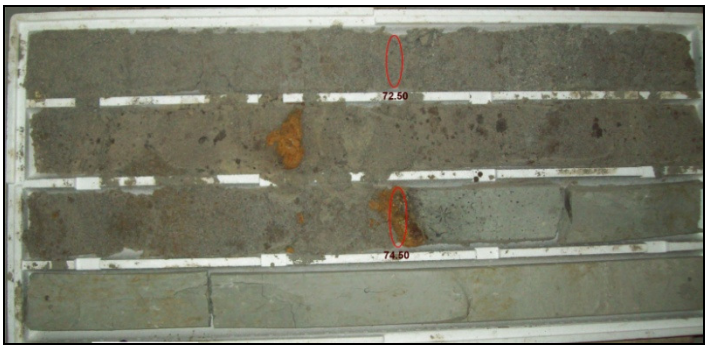

Fig. 3.1b – Core Bentivoglio at depth 72-76 m. Sampled points are marked with red circled.

Samples of organic matter, i.e., fossil vegetal matter, have been collected at the 48.25 m depth. These represent a dimensional fraction larger than 2 mm (Fig. 3.2) and have been obtained by dry sieved analysis which was performed before disintegration of the sample for chemical analysis. The occurrence of organic matter at these depths is likely to be the result of fossil deposition. A characteristic ocher color (Fig. 3.1a) of the surrounding sand was observed at this sampling depth. This could be indicative of the occurrence of iron oxides onto which As could have been adsorbed.

Fig. 3.2 – Fossil vegetal matter collected at the sampling location Bentivoglio

Table 3.2 reports grain size distribution of the solid matrix at different depths along the selected core. Grain size determination were carried out on a few sub-samples by granulometer TDF 3F, with a wet sieved in a range 2000 μm to 2 μm in four size fractions (2000-50, 50-20, 20-2 and <2 μm). Sandy matrix is mainly present (84.2%) at the 48.25 m depth. The sample collected at the 74.5 m depth is mainly composed of sand (45.8%) and silt (32.1%). Occurrence of a sand fraction exceeding 75% is indicative of samples belonging to the target aquifer. The deepest sample (i.e., depth of 74.5 m) represents the bottom of the aquifer, which is in direct contact with the existing aquitard.

Table 3.2
Particle size fractions at various depths along the core Bentivoglio

Sampling depth (m)	Sand 2000-50 µm	Silt 50-20 µm	Silt 20-2 µm	Clay <2 µm
	%	%	%	%
41.5	80.9	7.8	4.3	7.0
44.4	91.2	2.3	2.5	4.0
48.25	84.2	6.0	5.3	4.5
48.3	87.6	3.8	2.8	5.8
52.3	91.2	1.0	2.8	5.0
57.9	78.2	7.5	5.3	9.0
70.3	80.4	6.3	7.3	6.0
72.5	92.9	1.8	1.0	4.3
74.5	45.8	16.8	32.1	5.3

The borehole where solid matrix is extracted was included in 2008 in the extensive ARPA groundwater monitoring network. Groundwater composition in this point is thus available and can be compared with chemical species concentrations detected during the tests.

The matrix sampled at 48.40 m depth was divided into two subsamples according to granulometric fraction. The first subsample is here termed matrix A and comprises mainly sandy material. It is characterized by a granulometric fraction with particle size less than 2 mm which does exceed 89% of the total sample collected at 48.40 m. The second subsample is termed matrix D and is constituted by vegetal matter. It is associated by a granulometric fraction characterized by the occurrence of grain sizes larger than 2 mm over 11% of the total sample.

Samples from two additional solid matrices were respectively collected close to the bottom of the aquifer and in the proximity of the bottom of the aquifer, close to the detected aquitard. These were collected at 73.5 m and 74.5 m depth and respectively termed B and C. Matrix B comprises mainly sand, while matrix C is mostly constituted by silt. Table 3.3 summarizes the type and the depth of the four solid matrices collected for the tests.

Table 3.3
Solid matrices employed for the tests

Matrix	Granulometric fraction type	Sampled depth (m)
A	sand	48.4
B	sand	73.5
C	silt	74.5
D	vegetal matter	48.4

3.2.3 Selective sequential extraction protocol

Amongst the various protocols available in the literature for SSE, the methodology proposed by Torres and Auleda (2013) has been employed in this work to characterize the solid matrix. This sequential extraction procedure allows to distinguish seven fractions: (1) water soluble, (2) exchangeable (i.e., carbonates), (3) low crystalline (i.e., Fe and Mn oxyhydroxides), (4) crystalline (i.e., Fe and Mn oxides), (5) organic matter, (6) sulfides and (7) residual.

Sequential extractions allow to (a) obtain information about arsenic distribution among the different solid phases detected in the selected solid matrix and (b) evaluate the relative contribution of these fractions to the observed field concentrations. These findings, coupled with the experimental evidences presented in the following, could be of potential use in groundwater preservation strategies because they form the basis to understand which fraction prevalently adsorbs As and under which conditions As can be released to groundwater.

3.2.4 Chemical analysis of the solid matrices

Mineralogy of the solid matrices was determined by XRD analysis (Philips, Cu-anode). The sample was homogenized by means of dry physical disintegration at 500 μm for the chemical determination of total content of elements. This was determined according to the methodology of UNI EN 13346 (2002), i.e., 0.5 g of dried homogenized sediment was moistened with 3 mL of HNO_3 65%, 9 mL of HCl 37% in Teflon close beakers. The mixture was treated with a microwawe system Milestone 1200 MEGA according to five steps: (a) 8 minutes at 1500 W - temperature 130°C; (b) 5 minutes at 1500 W – 130°C; (c) 5 minutes at 1500 W – 200°C; (d) 10 minutes at 1500 W – 200°C; and finally (e) 10

minutes for the rapid refrigeration at 20°C. Digests were diluted to 50 mL with deionized water to analyze the soluble fraction after filtration at 0.45 μm hydrophilic syringe filter (Minisart, Goettingen, Germany). The fractions extracted were then analyzed by ICP-MS AGILENT 7500ce for As and Fe content. All analytical reagents employed were characterized by high grade purity. All analytical procedures have been validated using certified and/or internal reference materials.

Table 3.4 reports total chemical element concentration in the different solid matrices tested. Arsenic concentrations in vegetal matter (solid matrix D) are more than one order of magnitude larger than those detected in the other solid matrices. This highlights the significantly different As content that could give rise to different behaviors of these solid matrices during the experiments. Arsenic content in silt (solid matrix C) is larger than that observed for the two sandy matrices (matrices A and B). Differences between As and Fe content measured in the solid matrices employed in the experiments (see Table 3.4) and those observed in the borehole at depths of 48.25 m and 48.30 m and 74.5 m (see Table 3.1) are due to the heterogeneous structure of the solid matrix and possible mixing and subsequent homogenization of different matrices during sampling operations. Comparison of As content in matrices A, B and C along the same borehole shows that the adsorbed concentration in different solid matrices increases with the sampling depth and tends to be largest for the smallest characteristic particle sizes observed at a given sampling depth. Considering that A and B are sands while C is a silt, it can be observed that the largest As content associated with matrix C is consistent with the largest specific area characterizing C matrix particles.

Table 3.4
Concentration of chemical elements in the tested solid matrices

	Solid matrix (depth)			
Element (mg/kg ss)	**A (48.4 m)**	**B (73.5 m)**	**C (74.5 m)**	**D (48.4 m)**
Al	17508.7	8834.7	54493.3	5669.0
As	15.3	36.0	49.4	225.2
B	21.7	<20	59.9	13.7
Cd	< 0.2	< 0.2	0.2	0.2
Cr	38.7	21.4	99.7	28.2
Fe	23406.7	13982.0	39246.7	42590.0
Pb	6.4	4.8	17.6	6.1
K	3533.3	1906.7	15800.0	1896.7
Mn	730.5	849.7	750.3	203.7
Ni	28.5	20.4	86.0	20.0
Cu	10.4	6.9	35.0	18.2
Na	233.3	168.3	676.7	1110.0
Zn	32.8	36.3	130.6	22.8
Ca	69333.3	60666.7	40733.3	63566.7
Mg	5703.3	4216.7	9633.3	2473.7

3.2.5 Reagents employed for the batch test

A common laboratory practice which allows obtaining a closed system under anaerobic conditions involves either the use of an anaerobic chamber or the addition of pure nitrogen (N_2) gas to the sample. Here, pure argon (Ar) was used to replace oxygen because (a) it is chemically inert, and (b) it does not produce additional secondary compounds, contrary to nitrogen. Note that the large atomic weight of Ar (39.948 g/mol) facilitates the replacement of oxygen (atomic weight 15.999 g/mol) by Ar (e.g., Reddy and Patrick, 1974 and 1976) and the efficient lowering of ORP to induce reducing conditions.

Since pure Ar flux does not allow obtaining strongly reducing conditions in a relatively short time, a small amount of sodium ascorbate ($C_6H_7O_6Na$) was supplied to the system to obtain a strongly reducing environment. Sodium ascorbate has been reported to increase the solubilization of As and Fe without significant alteration of the pH (Chatain et al., 2005) and has been used in a column test to obtain a reducing environment (Nguyen et al., 2008). Reverting the system to oxidizing conditions is accomplished by supplying O_2 gas with a very minute amount of H_2O_2 (e.g., Voegelin and Hug, 2003), at 50% in volume and diluted to 15%.

3.2.6 Experimental setup

Fig. 3.3 depicts the details of the experimental setup adopted. The apparatus comprises a conical flask filled with the solid matrix and water where redox and pH variations are continuously monitored by ORP and pH electrodes connected with a PC recorder. An advantage of the adopted system is that redox conditions are well defined, can be modified rapidly, and allow clear reproducibility of the experimental conditions.

A 2L glass vessel hermetically sealed with an air-tight lid is at the core of the setup. It is equipped with a magnetic stirrer, a combined ORP platinum electrode with a silver-silver chloride (Ag/AgCl) reference (Intelligent ORP Electrode HI 3620D, Hanna Instruments), a combined pH electrode with an Ag/AgCl reference (Intelligent pH Electrode HI 1618D, Hanna Instruments) integrated with temperature sensor. These sensors allow measuring ORP, pH and temperature at a very high temporal resolution (i.e., every 30 sec). Data collected by the sensors are recorded on a computer via two data logger (HI 98150N, Hanna Instruments). The system is also equipped with an inlet gas tube to adjust the ORP by adding Ar or O_2, respectively to lower or increase ORP. A cylindrical membrane is placed at the end of the inlet tube with the aim of producing small gas bubbles associated with a high specific surface and improving gas diffusion within the system. A non-return gas exit valve connected to the system by a plastic tube is also set in place. The system is equipped by a sampling tube to collect water samples at different times and analyze As concentrations under the different redox conditions tested. To avoid any external contact, the sampling tube is equipped with an on/off valve opened only during the sampling operations performed through a syringe. A syringe is also employed to inject a specific reagent in the system to increase (using H_2O_2 at 15% in volume) or lower (using sodium ascorbate) the ORP. To obtain a temperature which is similar to what can be found at the reservoir sampling depths the vessel was wrapped with a tygon tube to allow water circulation and linked it to a thermostat set to keep a constant temperature of 15°C during the test.

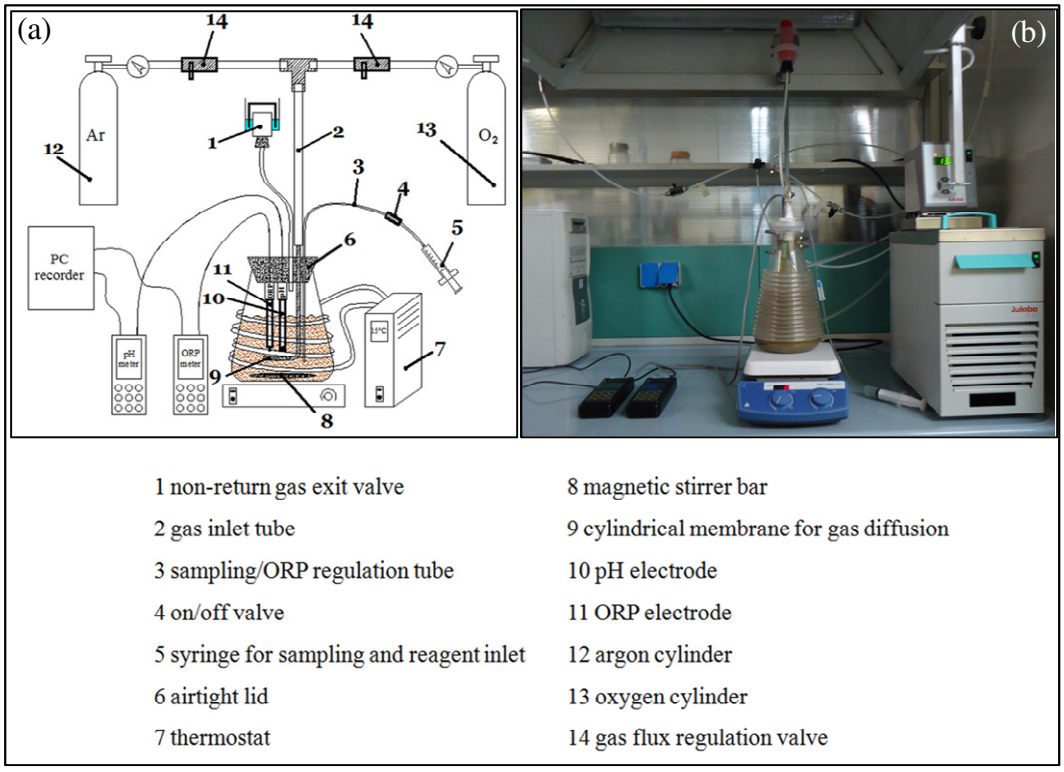

Fig. 3.3 – (a) schematic design and (b) picture of the experimental setup.

3.2.7 Laboratory tests

Experiments are performed under alternating redox conditions according to the following three phases: (1) a reducing stage which is maintained for 48 h (at -150 mV for solid matrix A, B and C and -60 mV for solid matrix D); (2) an oxidizing stage which is sustained for 48 h (at +150 mV for all solid matrices); and (3) a final reducing stage sustained for 72 h. Differences in ORP ranges adopted during the reducing stages are related to different characteristics of the solid matrices. The sandy matrices A and B and the silty matrix C result in a slightly alkaline slurry so that strong reducing conditions are attained without overstressing the system. Vegetal matter D results in an acidic slurry (pH values from 5.2 to 3.9). These low pH values render it difficult to reach strongly reducing conditions, consistent with the Nernst equation (Scott and Morgan, 1990).

Preliminary tests were performed on solid matrix A to design the optimal reagent amount and the duration of each test phase, as summarized in Table 3.5. Tests on solid matrices B and C are associated with an overall duration of 5 days (about 96 hours) while matrices A and D were tested for 7 days (about 168 hours). These differences are linked to the objective of investigating solid matrix behavior when reducing/oxidizing conditions are highly persistent. Duration of the first and second stages for solid matrices B and C and matrices A and D was respectively 24 and 48 hours. The third stage spans 48 and 72

hours, respectively for matrices B and C and matrices A and D. The first water sample was collected after 30 min of stirring and is considered as representative of the initial conditions of the system. Argon flux at 0.9 bar was supplied to remove free dissolved oxygen in water and bring the system to +50 mV. Once this slightly reducing condition is attained, a second sample was taken and 1 mL of sodium ascorbate 1M was then added to lower the ORP and reach the target strongly reducing conditions. Each 10 mL solution sample was passed through a 0.45 µm hydrophilic syringe filter (Minisart, Goettingen, Germany) to analyze the soluble fraction. Samples were collected during the 4 h following sodium ascorbate injection (for all solid matrices) and after 20 additional hours (only for matrices A and D), according to a scheduled sampling interval, as detailed in Table 3.5. The oxidizing step was obtained by supplying O_2 gas and about 1 mL of H_2O_2. Samples were then collected during the subsequent 4 h (for all solid matrices) and during the 24 hours following O_2 supply (only for matrices A and D). During the third reducing stage and for all tested matrices, samples were collected after 0.25, 0.5, 0.75, 1, 1.5, 20, 8.5 hours from the first sodium ascorbate injection. The last sample was taken after 40 hours for the A and D matrices and after 15.5 hours for matrices B and C. Table 3.5 summarizes the sampling protocol adopted.

Table 3.5
Sampling intervals adopted for each stage of the test and time elapsed from the first gas/reactant injection.

<table>
<tr><th>Gas/reactive injection</th><th colspan="2">Elapsed time for sampling</th><th colspan="2">Tested matrices</th><th>Stage</th></tr>
<tr><td>$Ar/C_6H_7O_6Na$</td><td colspan="2">15 min</td><td colspan="2" rowspan="5">All</td><td rowspan="8">reducing</td></tr>
<tr><td rowspan="7"></td><td colspan="2">30 min</td></tr>
<tr><td colspan="2">45 min</td></tr>
<tr><td colspan="2">60 min</td></tr>
<tr><td colspan="2">90 min</td></tr>
<tr><td colspan="2">20 hours</td><td colspan="2" rowspan="3">Only A and D</td></tr>
<tr><td colspan="2">8.5 hours</td></tr>
<tr><td colspan="2">15 hours</td></tr>
<tr><td>O_2/H_2O_2</td><td colspan="2">15 min</td><td colspan="2" rowspan="5">All</td><td rowspan="8">oxidizing</td></tr>
<tr><td rowspan="7"></td><td colspan="2">30 min</td></tr>
<tr><td colspan="2">45 min</td></tr>
<tr><td colspan="2">60 min</td></tr>
<tr><td colspan="2">90 min</td></tr>
<tr><td colspan="2">20 hours</td><td colspan="2" rowspan="3">Only A and D</td></tr>
<tr><td colspan="2">8.5 hours</td></tr>
<tr><td colspan="2">15 hours</td></tr>
<tr><td>$Ar/C_6H_7O_6Na$</td><td colspan="2">15 min</td><td colspan="2" rowspan="6">All</td><td rowspan="8">reducing</td></tr>
<tr><td rowspan="7"></td><td colspan="2">30 min</td></tr>
<tr><td colspan="2">45 min</td></tr>
<tr><td colspan="2">60 min</td></tr>
<tr><td colspan="2">90 min</td></tr>
<tr><td colspan="2">20 hours</td></tr>
<tr><td colspan="2">8.5 hours</td></tr>
<tr><td>40 hours</td><td>15.5 hours</td><td>A
D</td><td>B
C</td></tr>
</table>

The amount of solid matrices and volume of water used for the tests are reported in Table 3.6.

Table 3.6
Amount of solid matrices and volume of water used in each test

Solid matrix	Amount used (g)	Volume of water used (mL)
A, sand	350	1800
B, sand	350	1800
C, silt	260	1550
D, vegetal matter	100	880

Differences of the amount of matrix and water used are related to (a) the small amount of vegetal matter and silt available from the field core and (b) the need to avoid excessive dilution of released As. The solid matrix analyzed in each test was placed in water for about 2 days before the test to allow rehydration. The vessel was then sealed to obtain a closed microcosm and the slurry was stirred to homogenize the mixture solid matrix/water. ORP, pH, and temperature were then automatically recorded and stored for the duration of the tests.

3.2.8 Analytical methods for solution sampling

Each 10 mL solution sample was treated before analysis with 0.3 mL of HNO_3 65%. Element concentrations were determined using atomic absorption spectroscopy with flame (PERKIN ELMER 1100B) for Fe content and inductively coupled plasma mass spectrometry (AGILENT 7500ce) for As content.

All analytical procedures have been validated using certified and/or internal reference materials. Assessment of repeatability and method precision as well as accuracy using quality control samples at different concentration levels were investigated according to UNI CEI ENV 13005 (2000) and ISO ENV 13005 (1999) protocols. The relative standard deviation values for repeatability and intermediate precision were 4% for As and 6% for Fe. All concentrations have been corrected against volume changing due to aliquots of removal samples and reagent injections according to the formulation of Frau et al. (2008).

3.3. Results and Discussion

The complete set results of the tests performed on the sampled solid matrices is here presented. Only ORP was controlled during the tests while pH was left free to evolve naturally to mimic conditions occurring in the field. The mechanism triggering arsenic release/adsorption in all tests was the abrupt and rapid change of redox conditions leading to the largest concentrations of dissolved arsenic detected when reducing conditions were persistent. This was particularly evident for the test performed on solid matrix D, as detailed in the following. Comparison of the amount of As release from solid matrices A and D at the same depth against dissolved As concentrations measured at the field scale in the aquifer system subject to our investigation is also described. The Section is concluded with a presentation of the SSE analyses on As partitioning in the four solid matrices tested.

3.3.1 Solid matrix A (sand)

Fig. 3.4 depicts the XRD results for solid matrix A. These reveal that the sand sample is mainly composed by quartz (46%), calcite (18%), gypsum (11%), plagioclase (10%), feldspar (6%), mica (4%), and chlorite (5%). The peak at 2-Theta = 21° could be consistent with the presence of goethite at trace levels. Goethite and quartz are known to adsorb As (Smedley and Kinniburgh, 2002 and references therein). Therefore, the significant occurrence of quartz in matrix A is consistent with the As concentration measured in the solid matrix (see Table 3.4).

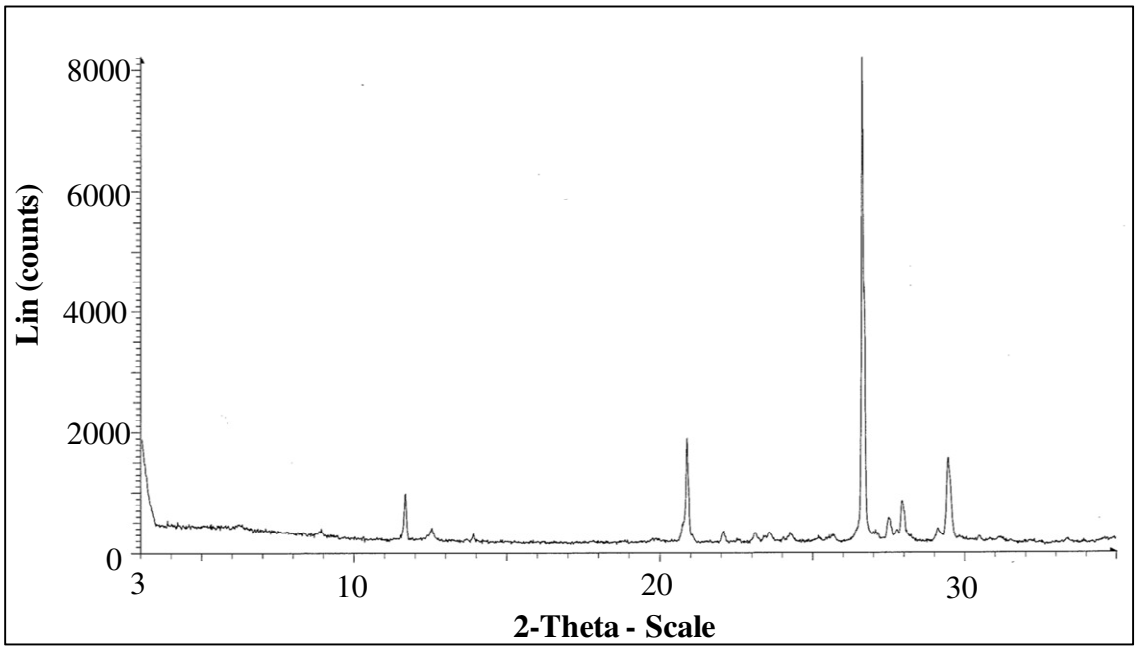

Fig. 3.4 – Results of the XRD analysis performed on solid matrix A (sand).

Fig. 3.5a shows the temporal dynamics of ORP and pH measured during the test. The reducing and oxidizing steps can be clearly identified. The solution displays a small pH variation in the range 6.9 ÷ 7.7. Once the target ORP value is achieved (± 150 mV, positive or negative depending on the stage), the system was left free to evolve naturally and the ensuing ORP and pH trends can be considered as the result of naturally occurring processes.

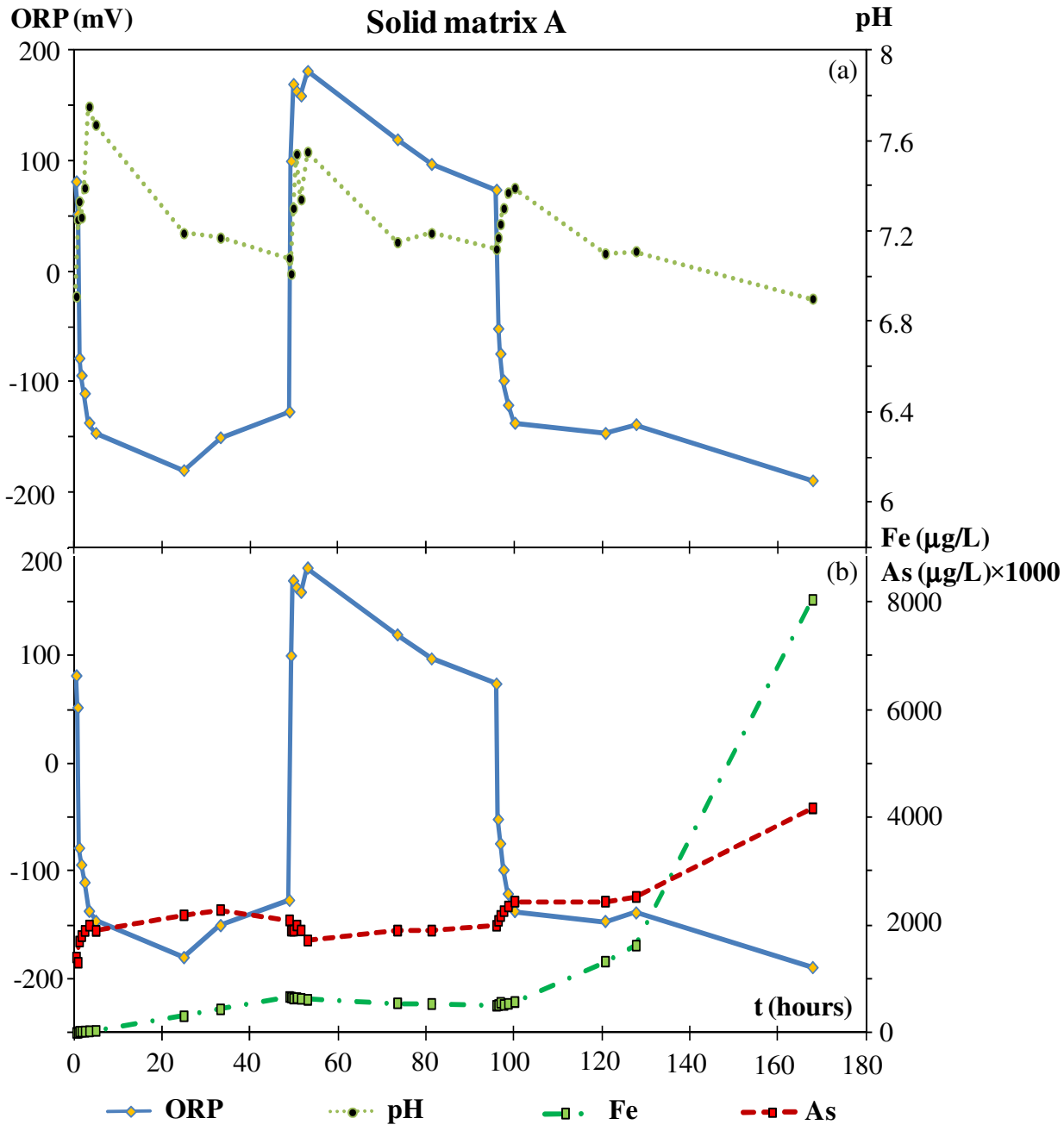

Fig. 3.5 – (a) Temporal variations of ORP and pH during the test on solid matrix A (sand); (b) ORP, Fe and As (× 1000) concentrations. Solid and dashed lines are drawn for visual aid.

The corresponding depiction of the concentrations of dissolved As and Fe observed during the experiment (displayed together with the recorded ORP values for comparison purposes) is reported in Fig. 3.5b. Arsenic release from the crystalline structure of As-bearing minerals is facilitated by sharp changes from oxidizing to reducing conditions and in the presence of a persistent reducing environment (more than 72 hours in our tests). Data reveals a good correlation between As and Fe, consistent with the results of Nickson et al. (2000) and Anawar et al. (2003). This supports the key role of Fe mineral phases on As mobility in both reducing and oxidizing conditions revealing that, despite the occurrence of other minerals which are basically constituted by other geogenic elements, Fe phases appear to display the highest affinity to adsorption of dissolved As and therefore play a prominent role in driving As mobility.

Arsenic release displays a distinct behavior when the solution is brought to reducing conditions: (*a*) As concentration increase at an approximately linear rate and with a steep slope during the initial rapid change from oxidizing to reducing conditions; (*b*) As concentration continues rising, albeit at a lower rate, during both reducing stages when ORP evolves freely; and (*c*) the As in solution increases significantly under persistent and strongly reducing conditions (see the last sampling point in Fig. 3.5b).

The observed behavior of As and pH is consistent with observations by Stumm and Morgan (1996), who showed that arsenate adsorption on iron-oxide surfaces increases when there is a change in iron-oxide net surface charge from positive to negative. This happens when the pH reaches (or exceeds) the zero-charge point, which is about 7.7 for goethite (crystalline iron oxide). Furthermore, the observed decrease in As concentrations is also consistent with the studies of Fuller et al. (1993) who highlight an initial rapid adsorption uptake (in a time frame of less than 5 min) followed by continuous uptake for at least 8 days because of As diffusion to adsorption sites on $Fe(OH)_3$ surfaces. Considering the rate at which As adsorption could occur, 90% of adsorption might have been reached within a few hours (Sadiq, 1997).

Arsenic concentration in water was then expected to decrease during the successive oxidizing phase taking place under free ORP evolution, as a consequence of the high adsorption capacity of iron oxides favored by the induced oxidizing environment. A slight reduction of the ORP occurs during the oxidizing phase due to possible reducing processes which might have occurred in the system, even in the presence of global oxidizing conditions. This is consistent with the slight increase of dissolved arsenic detected during this experimental step (Fig. 3.5b).

One of the main mechanisms of As release is the reductive dissolution of the solid matrix bound to Fe(III) oxy-hydroxides. Significant Fe concentrations should be expected coupled with high As release, consistent with studies documenting a positive correlation between Fe and As (Nickson et al., 2000; Anawar et al., 2003). Fig. 3.5b shows that a sudden, albeit small, release of Fe takes place during the first day of reducing conditions, representing the release of the rapid exchangeable fraction. After this step, and still under reducing conditions, a seemingly linear variation of Fe concentration with time is observed. No significant Fe release is observed during the oxidizing stage, consistent with the Fe adsorption mechanisms already explained. An increase in Fe concentration is observed during the transition to the third experimental phase, switching from oxidizing to reducing conditions, consistent again with iron-oxide dissolution. This dissolution continues when reducing conditions are stable and persistent for long time resulting in increased Fe release.

3.3.2 Solid matrix D (vegetal matter)

Fig. 3.6a displays the ORP and pH temporal variation observed during the test performed with soil matrix D. Similarly to the test carried out on solid matrix A, the two reducing stages (ORP about -60 mV) and the oxidizing step (ORP about +150 mV) can be clearly identified. The test was performed under acidic conditions (pH vary in the range 3.9 ÷ 5.1), consistent with the possible occurrence of humic acids bound to the vegetal matter constituting solid matrix D. Dissolution/precipitation of minerals should not influence significantly the composition of the resulting slurry because the main solid phase in this test is vegetal matter. The system seems to reach redox equilibrium conditions more rapidly than solid matrix A (Fig. 3.6a shows that limited variations of ORP and pH occur within each experimental stage).

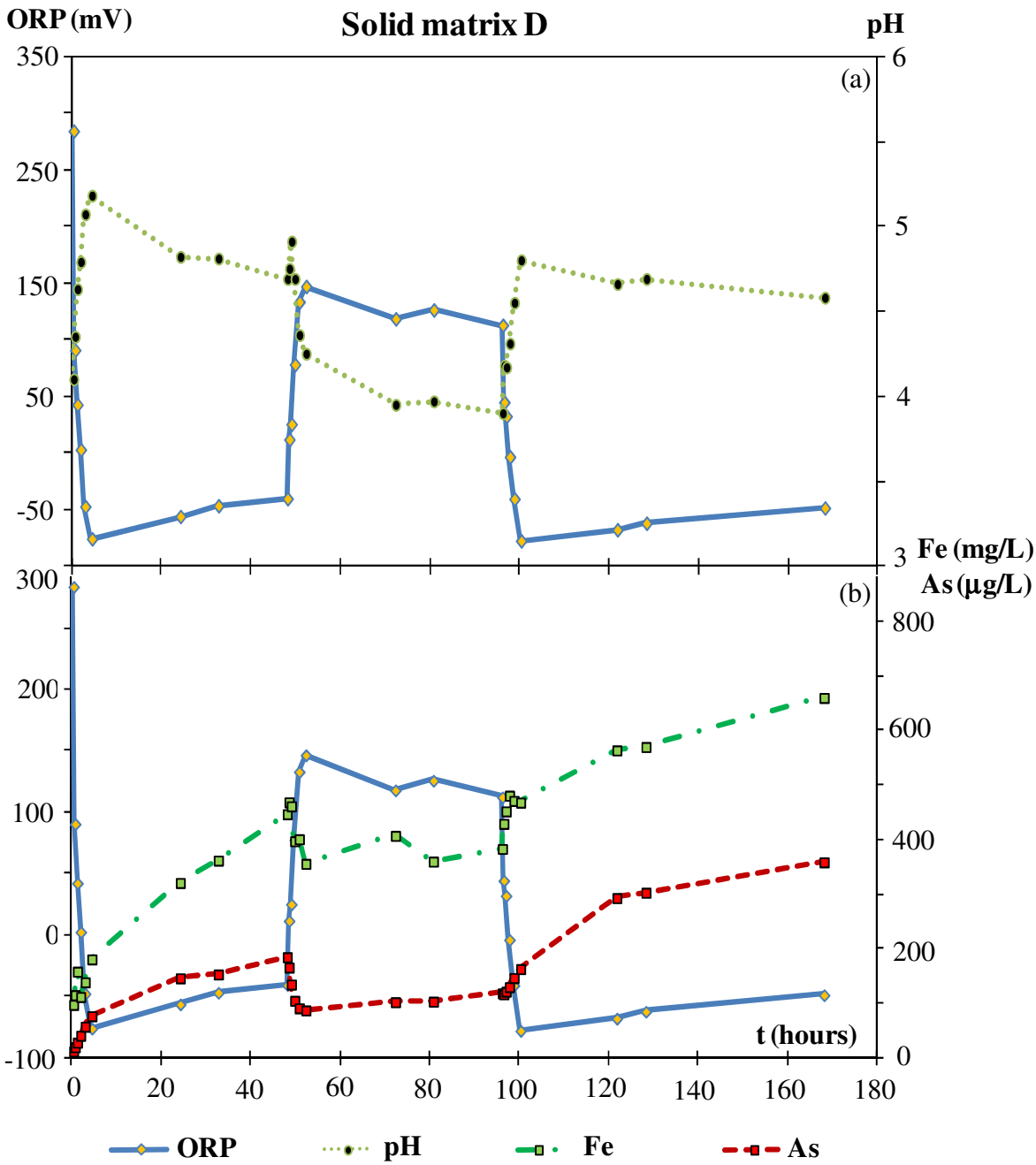

Fig. 3.6 – (a) Temporal variations of ORP and pH during the test on solid matrix D (vegetal matter); (b) ORP, Fe and As concentrations. Solid and dashed lines are drawn for visual aid.

Fig. 3.6b depicts Fe and As concentrations measured in solution as a function of the sampling time. Observed trends were similar to those observed in the experiment performed on matrix A. The actual measured values are consistent with (*a*) the larger As content characterizing solid matrix D (see Table 3.4) and (*b*) the possible catalytic role played by organic matter for both oxidation and reduction reactions (Senesi and Steelink, 1989; Perlinger et al., 1996). Note that Fe concentrations in Fig. 3.6b are expressed in

mg/L because they are larger than values reported in Fig. 3.5b emphasizing the significance of Fe release in this test.

The relatively high concentrations detected at the end of each reducing stage are consistent with organic matter decomposition. The latter is induced by the reduction of dissolved O_2 concentration, and results in increased dissolved CO_2 that enhanced the denitrification. Under reducing conditions Fe and As appear as Fe(II) and As(III), turning adsorbed oxides into soluble forms (Pierce and Moore 1982). The increase in dissolved As concentration appears to be consistent with replacement of As from adsorption sites by competing anions (e.g., HCO_3^-).

Arsenic concentrations in solution during the test were very large, highlighting the significance of As release from the natural organic solid matrix tested. Arsenic concentration in solution decreases rapidly after the fast change from reducing to oxidizing conditions. It subsequently displays a slightly increasing trend during the oxidizing stage. This observation is consistent with As adsorption onto iron (oxy)hydroxides formed as a result of imposed oxidizing environment and the possible formation of aqueous complexes promoted by the binding capacity of organic matter.

Fast release of Fe, representing the rapid exchangeable fraction bound to vegetal matter, is observed during the first day of induced anaerobic conditions. Anaerobic degradation, started after 24 hours of imposed reducing conditions, causes the dissolution of iron minerals phases, which are present in trace amounts, and the breaking of bonds linking iron complexes to vegetal matter. Consistent with these two possible mechanisms, a significant increase in Fe concentration was then observed from about 200 mg/L to about 450 mg/L at the end of first reducing stage.

Rapid decrease of Fe concentration was observed during the transition to oxidizing conditions (Fig. 3.6b, after about 50 h from the beginning of the experiment), consistent with Fe oxidation and binding processes of organic matter. This is then followed by concentration values fluctuating around a value of 380 mg/L during Stage 2. This behavior may be consistent with the possible precipitation, as hydroxide, of the Fe transferred in solution by aerobic oxidation of the organic substance.

Iron concentration increases sharply during the transition to the third (reducing) stage. Finally, it is noted that Fe concentrations continue to increase approximately linearly when reducing conditions are stable and persistent for a long time. This behavior is consistent with different processes, including (*a*) iron oxides redissolution; (*b*) release of aqueous

complexes bound to organic matter during the prior oxidizing stage; and (*c*) release of aqueous complexes from anaerobic degradation of organic matter.

A good correlation between As and Fe concentrations is evidenced, similarly to the case of solid matrix A. This supports the idea that As mobility strongly depends on Fe dynamics also in the presence of organic matter, in agreement with Redman et al. (2002). This behavior could be related to a large availability of adsorption sites that could adsorb large quantities of As under oxidizing conditions. Conversely, the adsorbed As could be remobilized when a reducing environment is created.

Occurrence of dissolved As species at the field scale might then be related to dissolution processes that could have occurred in the aquifer according to different mechanisms, such as dissolution or desorption. Arsenic concentration can then be fixated onto vegetal matter. A further change of the local groundwater redox state to reducing conditions induced by natural causes or anthropogenic activities could remobilize As, increasing resident concentrations.

It should also be noted that As concentrations observed in solution during the third experimental stage are larger than those associated with the first reducing stage despite similar reducing conditions are attained. The evidences stemming from these experiments highlight that this mechanism could depend on the duration and strength of the transition between different redox stages.

3.3.3 Solid matrix B (sand)

Fig. 3.7 depicts the XRD results for solid matrix B, revealing that the sand sample is mainly composed by quartz (53%), calcite (18%), feldspar (10%), plagioclase (8%), gypsum (5%), chlorite (3%) and mica (3%). The peak at 2-Theta = 21° could be consistent with the presence of goethite at trace levels that, together with quartz, could adsorb As (Smedley and Kinniburgh, 2002 and references therein). As for matrix A, the significant occurrence of quartz is consistent with the arsenic concentration measured in the solid matrix (see Table 3.4).

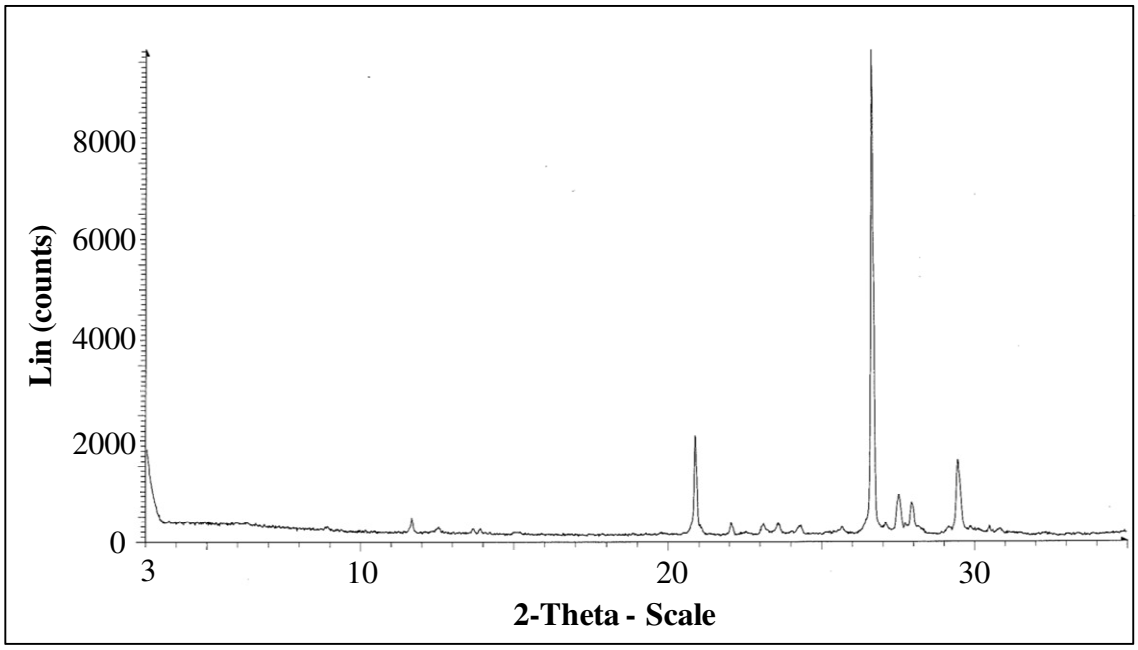

Fig. 3.7 – Results of the XRD analysis performed on solid matrix B (sand).

Fig. 3.8a shows the temporal dynamics of ORP and pH measured during the test. The reducing and oxidizing steps can be clearly identified. The solution displays a limited pH variation in the range 7.0 ÷ 8.2. Once the target ORP value is achieved (± 150 mV, positive or negative depending on the stage), the system was left free to evolve naturally and the ensuing ORP and pH trends can be considered as the result of naturally occurring processes.

The corresponding depiction of dissolved As and Fe concentrations observed during the experiment is reported in Fig. 3.8b, together with the recorded ORP values. As observed for matrix A, arsenic release from the crystalline structure of As-bearing minerals is facilitated by sharp changes from oxidizing to reducing conditions and in the presence of a persistent reducing environment (about 48 hours in this test). The key role of iron on As mobility in both reducing and oxidizing conditions is confirmed also in this test by the good correlation (excluding values during the transition to oxidizing stage at about 25 hours from the beginning of the test) between As and Fe, as observed also for matrix A.

Mechanisms of As and Fe release evidenced for matrix A are also consistent with released concentrations observed in this test, an exception being given by values measured at about 25 hours from the beginning of the test.

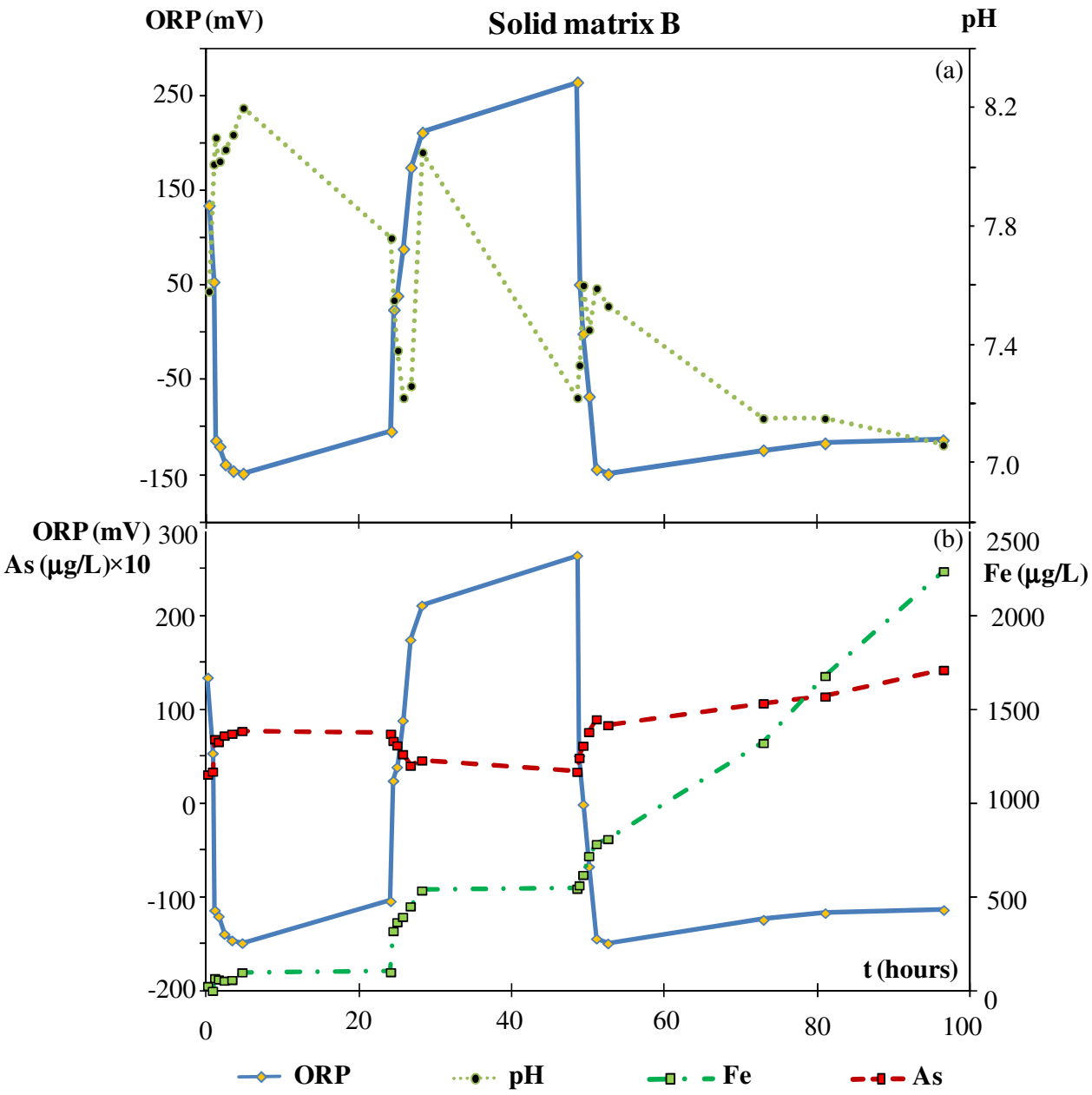

Fig. 3.8 – (a) Temporal variations of ORP and pH during the test on solid matrix B (sand); (b) ORP, Fe and As (× 10) concentrations. Solid and dashed lines are drawn for visual aid.

Matrices A and B are characterized by different behavior with reference to Fe concentrations during the transition to oxidizing stage. Arsenic adsorbs on Fe(III) oxy-hydroxides in an oxidizing environment, switching to the less mobile specie (i.e., As(V)). A reduction of As concentrations in water is therefore observed. A corresponding decrease of Fe concentrations was expected because Fe precipitates as Fe(III) under oxidizing conditions and form complexes that may adsorb As and immobilize Fe, thus reducing Fe concentration in water. The upward trend observed in Fe concentrations during this transition appears to be consistent with the possible release of iron from the oxidizable fraction (i.e., organic matter and sulfides), considering that this test is associated with

redox values which are much larger than those associated with tests performed on solid matrices A and C. Iron release masks the concurrent precipitation of iron in oxides / hydroxides form which results in an increase of dissolved Fe concentrations despite the presence of oxidizing conditions. Arsenic concentrations observed at the end of the test are larger than those measured for matrix A and are consistent with the larger (about twice) As content detected in matrix B (see Table 3.4). Iron concentrations measured in this test are lower than those detected with matrix A, consistent with lower Fe content occurring in matrix B (see Table 3.4) and with the shorter persistence of reducing conditions in this test.

3.3.4 Solid matrix C (silt)

XRD results for solid matrix C are depicted in Fig. 3.9. These reveal that the silty matrix C is chiefly composed by: quartz (35%), gypsum (17%), calcite (10%), mica (10%), plagioclase (10%), chlorite (10%) and feldspar (8%). The occurrence of quartz and the presence of goethite at trace levels, consistent with the peak at 2-Theta = 21°, are in agreement with As concentration measured in the solid matrix (see Table 3.4).

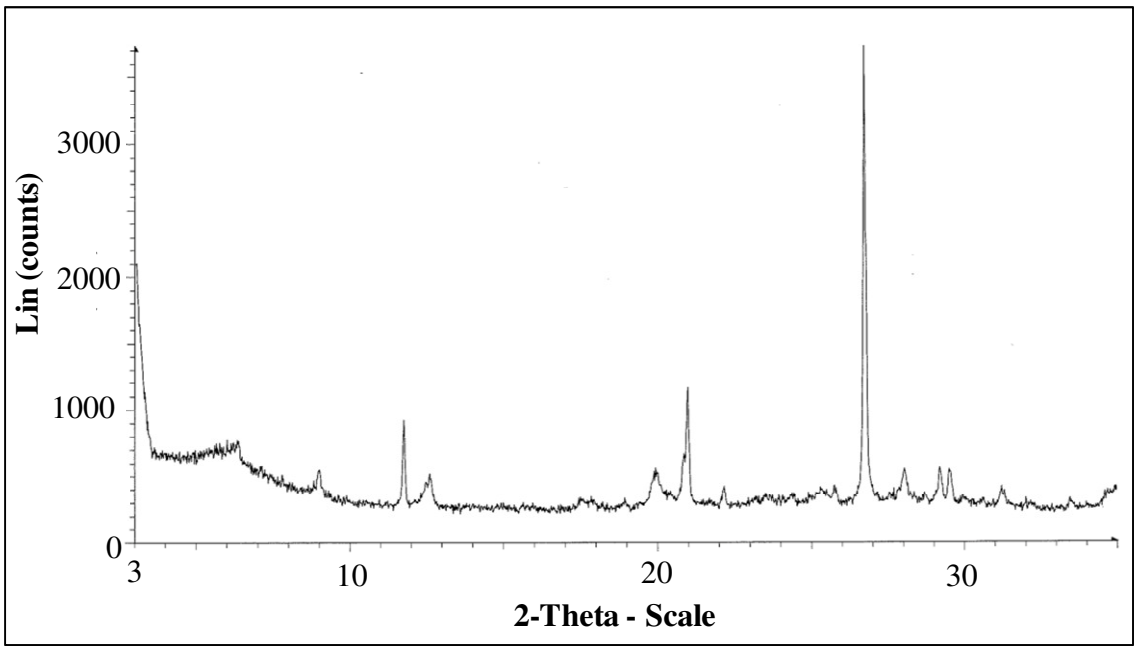

Fig. 3.9 – Results of the XRD analysis performed on solid matrix C (silt).

Fig. 3.10a displays the temporal dynamics of ORP and pH measured during the test. The reducing and oxidizing steps can be clearly identified. The solution displays a small

pH variation in the range 7.0 ÷ 8.4. Once the target ORP value is achieved (± 150 mV, positive or negative depending on the stage), the system was left free to evolve naturally and the ensuing ORP and pH trends can be considered as the result of naturally occurring processes.

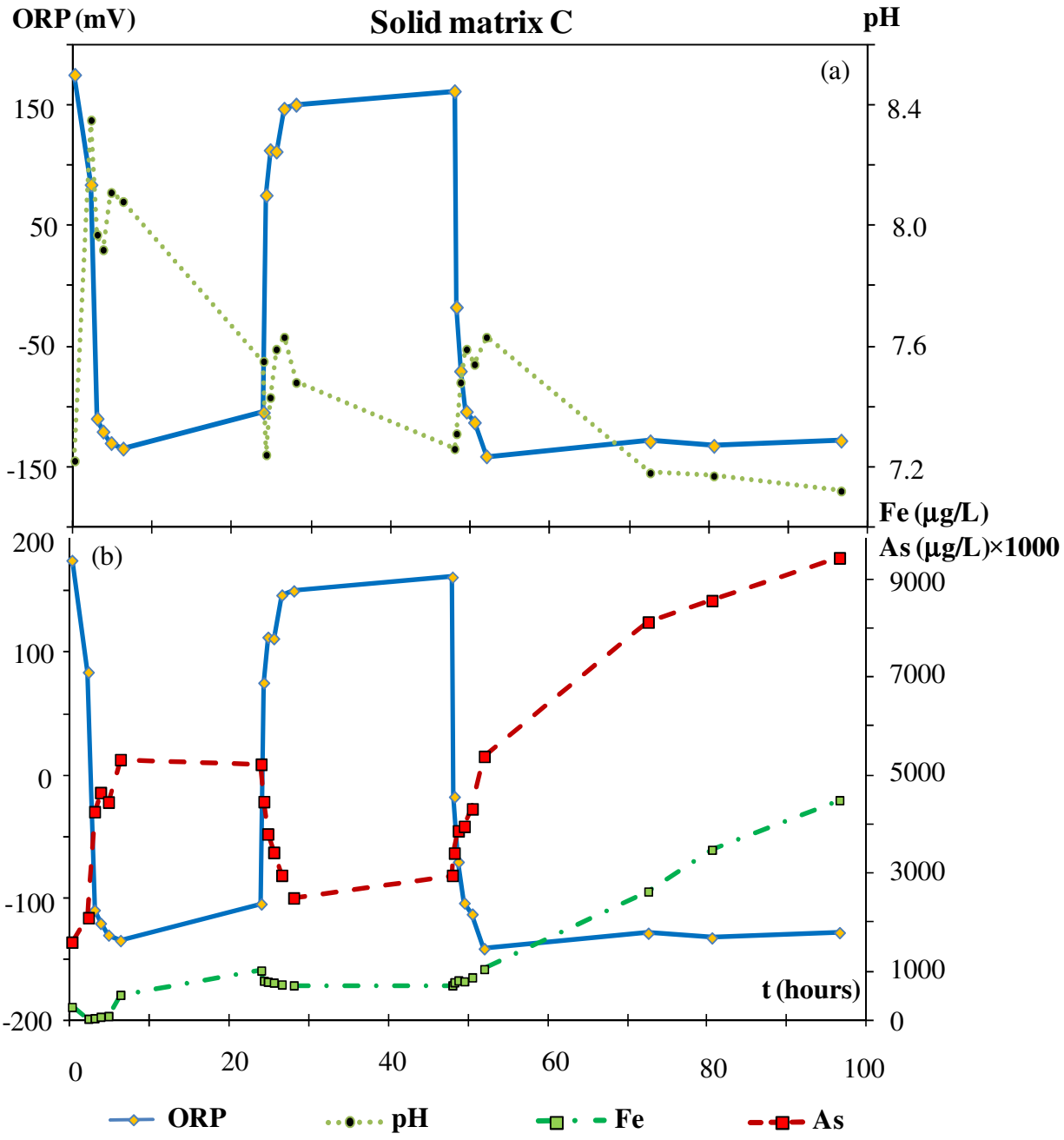

Fig. 3.10 – (a) Temporal variations of ORP and pH during the test on solid matrix C (silt); (b) ORP, Fe and As (× 1000) concentrations. Solid and dashed lines are drawn for visual aid.

Fig. 3.10b depicts Fe and As concentrations measured in solution as a function of the sampling time together with the corresponding ORP. Arsenic and iron trends during this

test are similar to those observed in the other experiments presented, consistent with the previously described mechanisms governing As and Fe trends.

Despite the different features (e.g., particle size) characterizing matrices A and B (i.e., sands) and matrix C (i.e., silt), which result in different adsorption/desorption capacities, the key mechanism triggering arsenic release/adsorption in this test is confirmed to be the abrupt and rapid change of redox conditions. As in the tests previously discussed, this leads to increased arsenic concentrations when reducing conditions are persistent.

Values of As concentrations released from solid matrix C are close to those released from solid matrix B (note that an amount of solid matrix C which is lower than that associated with matrix B is used in the test). This is consistent with the larger As content occurring in solid matrix C (see Table 3.4) and highlights the potential of As adsorption/desorption capacity characterizing this solid matrix. This process is mainly linked to the observation that silt matrices (i.e., matrix C) are associated with a higher specific surface than sand (i.e., matrices A and B) due to differences in particle sizes.

The amount of As released at the end of the test is very close to the limiting value indicated by Italian regulation (10 μg/L), even as (*a*) a reduced amount of solid matrix is being employed (as compared to the other tests performed), and (*b*) the duration of the reducing stage was shorter than that considered for matrix A. This highlights the significant role that the occurrence of the fine solid matrix C could play in the determination of local arsenic concentrations in groundwater.

3.3.5 Comparative analysis between the matrices tested

Comparison of figures 3.5 and 3.6 reveals that the amounts of As released from solid matrices A and D is very different despite they were sampled at the same depth. This is consistent with the observation that the As content in solid matrix D is 15 times larger than that detected in solid matrix A (see Table 3.4). These differences highlight the significant role of vegetal matter in the large As concentrations observed in the groundwater in the study area (Molinari et al., 2012 and references therein). Vegetal matter appears to show high As binding capacity during the transition to the oxidizing stage when As concentrations in water decreases by about 100 μg/L (Fig. 3.6).

Fig. 3.11 juxtaposes the dynamics of As released concentrations monitored during the tests on matrices A and D. The matrices sampled at the same depth display qualitatively similar dissolved As trends during the various stages of the test. Note that solid matrix A

contains a small amount of vegetal matter, associated with the particle size fraction smaller than 2 mm. This could result in an amplification of the mechanisms that govern As mobility in sandy aquifers systems. Considering that most aquifers comprise sand with a little amount of organic matter (peat or vegetal matter), these findings are of potential use in the framework of groundwater quality management because the detection of a significant amount of vegetal matter in a given aquifer area could be consistent with high As concentrations detected in groundwater. From the perspective of a field scale scenario, induced non-uniform flows caused by pumping could also contribute to redox variations with time and subsequent increase of dissolved As concentrations.

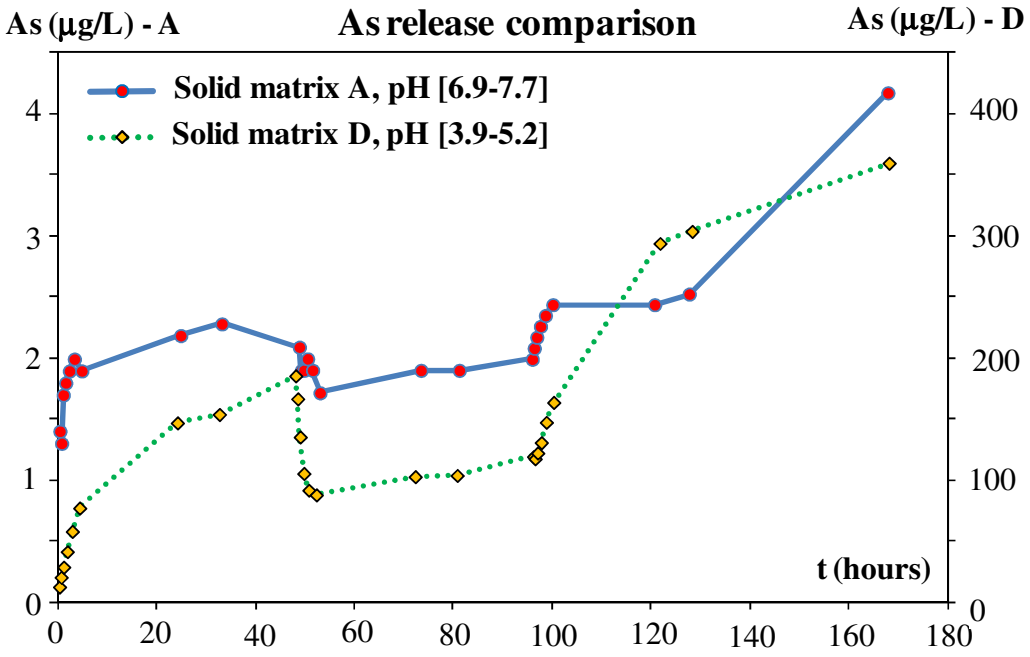

Fig. 3.11 – Comparison between As release observed during the tests on solid matrices A and D (note the different vertical axes).

As mentioned in Section 3.2.2, solid matrices A and D have been collected from a monitoring well which was included in 2008 in the ARPA groundwater monitoring network. Record of As concentrations are available in this monitoring well from 2008 to 2011 and can be compared with the aqueous concentrations measured during the tests. Dissolved As concentrations detected in the borehole vary from 2 to 74 µg/L while range between 1.3 and 4.2 µg/L and between 12.6 and 360 µg/L during the test performed respectively on solid matrices A and D. Measured dissolved concentrations depend on solid-liquid ratio adopted during the tests which is different from that observed in the field. Other processes occurring in the presence of advective-dispersive field-scale

processes do not allow to directly transfer the observed laboratory scale concentration levels to field scale. However, these findings suggest that field-scale concentrations could be considered as some weighted contributions from the two solid matrices A and D. The relative weights associated with the two matrix components are proportional to the local volumetric fraction of each matrix in the porous medium. This conceptual picture is also consistent with the hypothesis that the occurrence of vegetal matter can amplify As concentrations released from a sandy matrix.

Values of pH measured in the field range between 7.3 and 8.3. The observed pH variations during the experiment range between (*a*) 6.9 and 7.7 or (*b*) 3.9 and 5.2, respectively for solid matrix A and D. Measured pH values during the test can be considered as representative of natural pH conditions occurring in the field under the assumption that the aquifer is mainly constituted by the analyzed solid matrix. In this sense, solid matrix D plays only a limited role to lower the total observed pH due to its intrinsic acidic features. This mechanism is consistent with the observation that, while there might be additional reactions which can affect pH, the pH range observed in the field under redox conditions similar to those associated with performed laboratory experiments is very close to that of solid matrix A where only a little amount of vegetal matter is found.

Even as the duration of the stages considered for the test performed on the different matrices are different, comparison of the observed As dynamics (Fig. 3.5, 3.6, 3.8 and 3.10) highlighted that all solid matrices tested are characterized by the same general behavior and different order of magnitude of the observed dissolved concentrations. The latter evidence is consistent with the different As content of the matrices considered.

Close comparison between matrices C (silt) and D (vegetal matter) seems to highlight the same pseudo-logarithmic trend of As concentration during the third reducing stage. This observation evidences that fine and vegetal matrices, which are respectively characterized by large specific surface and large number of available adsorption sites, can release As with similar mechanisms in the presence of persistent reducing conditions. Released As concentrations appear to display similar trends under aerobic and anaerobic conditions for matrices A and B (i.e., which are characterized by the same composition, i.e., both of them are sands).

3.3.6 Selective sequential extractions results for the tested solid matrices

Fig. 3.12 reports the results of SSE for the solid matrices analyzed. It is clear that As content in solid matrix D is larger than that observed in the other matrices. Matrix A, which was sampled at the same depth of solid matrix D (i.e., 48.4 m), is characterized by a total As concentration which is about 9 times lower than that observed for vegetal matrix D. This underlines the high As binding capacity of organic matter.

Solid matrices A and B, which are both sands and are respectively sampled at 48.4 m and 73.5 m depth, display a different behavior with reference to As partitioning in extracted fractions and total As content. The latter is more than two times larger for matrix B than for matrix A. This highlights that the same type of solid matrix can result in different As content and fractioning along a given core. Note that matrix B has been collected close to the bottom of the aquifer.

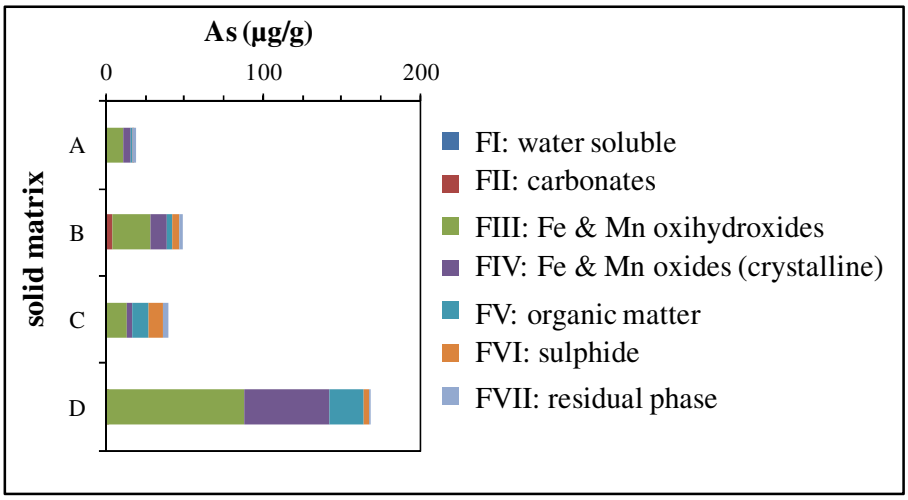

Fig. 3.12 – Arsenic partitioning in solid matrices A, B, C and D.

Table 3.7 reports the relative proportion of As content in each extracted fraction and for all solid matrices analyzed. These results highlight that amorphous and crystalline phases constitute the most important fractions governing As partitioning in all samples. The key role of amorphous phases on As adsorption is clearly evidenced from the percentages of fraction FIII which represent the largest contribution in all solid matrices (these exhibit values larger than 50% for matrices A, B and D and larger than 30% for matrix C). The amount of As associated with Fe and Mn oxides and representing the crystalline fraction is also significant for all solid matrices, with the exception of the silty matrix C, where notable contents of this fraction are not evidenced.

Negligible As was found in fraction FI, which represents the rapidly exchangeable fraction in water. This supports the idea that that solid-water interaction is not sufficient to trigger As release. Arsenic association with carbonates is very poor for solid matrices A, C and D, while being only slightly significant for matrix B. Considering matrices A, B and C, one can note that increasing As concentrations were found in fractions FV (organic matter) and FVI (sulphide), consistent with the existence of predominant anaerobic conditions which take place at increasing depths along the sampling borehole.

Even as A and D matrices are characterized by similar percentages of As occurrence in the FIII and FIV fractions, consistent with the observation that both samples were collected at the same depth (i.e., 48.4 m), the percentage of As found in the FV fraction of matrix D is 10 times larger than that observed in matrix A. This suggests that organic matter is characterized by As binding capacity which is larger than that related to sand. This is a particularly important observation when considering scenarios where these two matrices are in contact with paleo-waters which can be rich in dissolved As.

Table 3.7
Percentage of As content in each extracted fraction for the solid matrices analyzed.

Solid matrix				
A	**B**	**C**	**D**	**Fractions**
0.1%	0.4%	0.05%	0.2%	FI: water soluble
0.1%	7.1%	0.1%	0.02%	FII: carbonates
56.1%	51.0%	33.7%	52.0%	FIII: Fe & Mn oxihydroxides
29.9%	21.4%	7.4%	32.1%	FIV: Fe & Mn oxides (crystalline)
1.4%	7.5%	26.0%	13.1%	FV: organic matter
2.7%	8.1%	23.0%	1.7%	FVI: sulphide
9.7%	4.5%	9.8%	0.8%	FVII: residual phase

Table 3.7 highlights the different behavior of silty matrix C when compared against the other matrices tested and quantified in terms of (a) As partitioning (resulting in significant As association with low crystallinity phases as well as with organic substrates and sulphide fractions), and (b) fine granulometric composition. Comparison between matrices A and D seems to reveal that the significant differences observed for As adsorption be due to the capacity of matrix D to bind As in the FV fraction. This enhances dissolved As enrichment when the matrix is in contact with water.

3.4. Conclusions

Key aims of the experimental characterization of the sampled matrices were (*a*) the investigation of the high As concentrations detected at some sites within Emilia-Romagna aquifers, and (*b*) the assessment of the possibility to relate these to real field redox conditions dynamics acting on in situ solid matrices. For this purpose, arsenic partitioning in different solid fractions occurring in the tested matrices were also analyzed and the trend and magnitude of As release from four specific natural solid matrices was explored by a set of batch experiments performed under alternating redox conditions. The experiments lead to the following major conclusions:

- Laboratory scale experiments show a distinct correlation between temporal dynamics of aerobic/anaerobic conditions and As release into the solution. Iron is associated with release trends from the tested solid matrices which are quite similar to those of As. These observed trends are driven by sudden changes of redox scenarios and as well as by temporally sustained redox conditions.
- The high As content observed in the vegetal matter tested, as compared to values characterizing sand A at the same depth, highlights the large binding capacity of organic matter. As a consequence, the occurrence of vegetal matter in an aquifer can enhance the release of As in groundwater. This evidence suggests the need to quantify the actual contribution of organic matter on real concentrations detected in groundwater bodies for the characterization of areas with potential high As concentration content.
- Arsenic is released faster from organic matter than from As-bearing minerals. This suggests that a significant occurrence of organic matter in groundwater could lead to different behaviors of aquifers in terms of temporal dynamics of dissolved species concentrations in the presence of time-varying redox conditions.
- Arsenic concentrations released from silty matrix C highlight the potential role that the presence of this solid matrix could play in the occurrence of high local As concentrations in groundwater, consistent with the large specific surface which characterize this fine solid matrix (note that the test performed on matrix C was associated with a smaller amount of solid matrix than that characterizing the experiments performed on matrices A and B).
- Total observed As concentration at the field scale in the target aquifer system could be mainly driven by (a) the amount of adsorbed As on the different solid matrices and (b) the relative fraction of each matrix occurring in the system.

- To obtain results close to natural concentrations measured in a given groundwater body, experiments should be performed employing solid matrices and water collected at depths which are consistent with those of the target water body and relying on observation boreholes which are not influenced by anthropogenic activity.
- High As concentrations detected in Emilia-Romagna could be consistent with the high natural content of this metalloid which is prevalently adsorbed on vegetal matter and mobilized by variations in redox conditions.

Selective sequential extractions highlighted the existence of different As fractions within the tested solid matrices. The fractioning study leads to the following key conclusions:

- Low crystallinity and crystalline phases are the most important fractions governing As partitioning within a given solid matrix.
- Organic matter (i.e., vegetal matter) displays the largest binding capacity, when compared against sandy and silty matrices. This can lead to large As content when matrices characterized by considerable vegetal matter content are in contact with paleo-waters which are rich in dissolved As.

References

Ahn JS, Park YS, Kim JY, Kim KW. Mineralogical and geochemical characterization of arsenic in an abandoned mine tailings of Korea. Environ Geochem Health. 2005;27(2):147-57.

Alexandratos VG, Elzinga EJ, Reeder RJ. Arsenate uptake by calcite: Macroscopic and spectroscopic characterization of adsorption and incorporation mechanisms. Geochimica et Cosmochimica Acta. 2007;71:4172-4187.

Amorosi A, Farina M, Severi P, Preti D, Caporale L, Di Dio G. Genetically related alluvial deposits across active fault zones: an example of alluvial fan–terrace correlation from the upper Quaternary of the southern Po Basin, Italy. Sediment Geol. 1996;102:275-295.

Anawar HM, Akaib J, Komakic K, Teraod H, Yoshiokae T, Ishizukaf T, et al. Geochemical occurrence of arsenic in ground water of Bangladesh: sources and mobilization processes. Journal of Geochemical Exploration. 2003;77:109-131.

Bacon JR and Davidson CM. Is there a future for sequential chemical extraction?. Analyst. 2008;133:25–46.

Basilio MSV, Friese K, de Lena JC, Nalini HA, Roeser HMP. Adsorption of As, Cu, Pb and Cr for the assessment of metal retention by two different residues from iron ore mines. Química Nova. 2005;28(5):822-828.

Berg M, Stengel C, Trang PTK, Hung Viet P, Sampson ML, Leng M, et al. Magnitude of arsenic pollution in the Mekong and Red River Deltass Cambodia and Vietnam. Sci. Total Environ. 2007;372 (2-3):413-425.

Bhattacharyya P, Chakraborty A, Chakrabarti K, Tripathy S, Powell MA. Chromium uptake by rice and accumulation in soil amended with municipal solid waste compost. Chemosphere. 2005;60(10):1481–1486.

Bombach G, Pierra A, Klemm W. Arsenic in contaminated soil and river sediment. Fresenius J. Anal. Chem. 1994;350:49–53.

Burnol A, Garrido F, Baranger P, Joulian C, Dictor MC, Bodénan F, et al. Decoupling of arsenic and iron release from ferrihydrite suspension under reducing conditions: a biogeochemical model. Geochemical Transactions. 2007;8:12. doi:10.1186/1467-4866-8-12.

Chaudhuri D, Tripathy S, Veeresh H, Powell MA, Hart BR. Mobility and bioavailability of selected heavy metals in coal ash-and sewage sludge-amended acid soil. Environ. Geol. 2003;44:419-432.

Charlet L, Chakraborty S, Appelo CAJ, Roman-Ross G, Nath B, Ansari AA, et al. Chemodynamics of an arsenic ‘‘hotspot’’ in a West Bengal aquifer: A field and reactive transport modeling study. Applied Geochemistry. 2007;22:1273-1292.

Chatain V, Sanchez F, Bayard R, Moszkowicz P, Gourdon R. Effect of experimentally induced reducing conditions on the mobility of arsenic from mining soil. Journal of Hazadous Materials. 2005;B122:119-128.

Chen YX, Hua YM, Zhang SH, Tian GM. Transformation of heavy metal forms during sewage sludge bioleaching. J Hazard Mater. 2005;123(1-3):196-202.

Claff SR, Sullivan LA, Burton ED, Bush RT. A sequential extraction procedure for acid sulfate soils: Partitioning of iron. Geoderma. 2010;155:224-230.

Cremonini S, Etiope G, Italiano F, Martinelli G. Evidence of possible enhanced peat burning by deep-origin methane in the Po River delta Plain (Italy). J Geol. 2008;116:401-413.

Damris M, O'Brien GA, Price WE, Chenhall BE. Fractionation of sedimentary arsenic from Port Kembla Harbour, NSW, Australia. J Environ Monit. 2005;7(6):621-30.

Davis A and Ashenberg D. The aqueous geochemistry of the Berkeley Pit, Butte, Montana, USA. Appl. Geochem. 1989;4:23-36.

Deuel LE and Swoboda AR. Arsenic solubility in a reduced environment. Soil Sci. Soc. Am. Proc. 1972;36:276-278.

Du Laing G, Rinklebe J, Vandecasteele B, Tack FMG. Trace metal behavior in estuarine and riverine floodplain soils and sediments: a review. Sci. Total Environ. 2009;407:3972-3985.

Frau F, Biddau R, Fanfani L. Effect of major anions on arsenate desorption from ferrihydrite-bearing natural samples. Applied Geochemistry. 2008;23:1451-1466.

Friesl W, Lombi E, Horak O, Wenzel WW. Immobilization of heavy metals in soils using inorganic amendments in a greenhouse study. J. Plant Nutr. Soil Sci. 2003;166-191.

Frohne T, Rinklebe J, Diaz-Bone RA, Du Laing G. Controlled variation of redox conditions in a floodplain soil: Impact on metal mobilization and biomethylation of arsenic and antimony. Geoderma. 2011;160:414–424. doi:10.1016/j.geoderma.2010.10.012

Fuentes A, Lloréns M, Sáez J, Soler A, Aguilar MI, Ortuño JF, Meseguer VF. Simple and sequential extractions of heavy metals from different sewage sludges. Chemosphere. 2004;54(8):1039-1047.

Fuller CC, Davis JA, Waychunas GA. Surface chemistry of ferrihydrite: Part 2. Kinetics of arsenate adsorption and coprecipitation. Geochim. Cosmochim. Acta. 1993;57:2271-2282.

Galan E, Gomez-Ariza JL, Gonzalez I, Fernandez-Caliani JC, Morales E, Giraldez I. Heavy metal partitioning in river sediments severely polluted by acid mine drainage in the Iberian Pyrite Belt. Applied Geochemistry. 2003;18(3):409-421.

Gao Y and Mucci A. Acid base reactions, phosphate and arsenate complexation, and their competitive adsorption at the surface of goethite in 0.7 M NaCl solution. Geochimica et Cosmochimica Acta. 2000;65(14):2361-2378.

Gleyzes C, Tellier S, Sabrier R, Astruc M. Arsenic characterisation in industrial soils by chemical extractions. Environ. Technol. 2001;22:27–38.

Grafe M, Eick MJ, Grossl PR, Saunders AM. Adsorption of arsenate and arsenite on ferrihydrite in the presence and absence of dissolved organic carbon. J. Environ. Qual. 2002;31:1115-1123.

González ZI, Krachler M, Cheburkin AK, Shotyk W. Spatial distribution of natural enrichments of arsenic, selenium, and uranium in a minerotrophic peatland, Gola di Lago, Canton Ticino, Switzerland. Environ Sci Technol. 2006;40(21):6568-74.

Guo TZ, DeLaune RD, Patrick WH. The influence of sediment redox chemistry on chemically active forms of arsenic, cadmium, chromium, and zinc in estuarine sediment. Environ. Internat. 1997;23:305-316.

Guo R, Yang J, Liu Z. Thermal and chemical stabilities of arsenic in three Chinese coals. Fuel Processing Technology. 2004;85:903– 912.

Harvey CF, Swartz CH, Badruzzaman AB, Keon-Blute N, Yu W, Ali MA, et al. Arsenic Mobility and Groundwater Extraction in Bangladesh. Science. 2002;298:1602-1606.

Harvey MC, Schreiber ME, Rimstidt JD, Griffith MM. Scorodite Dissolution Kinetics: Implications for Arsenic Release. Environ. Sci. Technol. 2006;40:6709-6714.

Hess RE and Blanchar RW. Dissolution of arsenic from waterlogged and aerated soil. Soil Sci. Soc. Am. J. 1977;41:861-865.

Hlavay J, Prohaska T, Weisz M, Wenzel WW, Stingeder GJ. Determination of trace elements bound to soils and sediment fractions (IUPAC technical report). Pure Appl. Chem. 2004;76(2):415–442.

Hudson-Edwards KA, Houghton SL, Osborn A. Extraction and analysis of arsenic in soils and sediments. Trends in Analytical Chemistry. 2004;23:10–11.

Inaba S and Takenaka C. Changes in Chemical Species of Copper Added to Brown Forest Soil in Japan. Water, Air, and Soil Pollution. 2005;162(1-4):285-293.

ISO ENV 13005. Guide to the expression of uncertainty in measurement (GUM); 1999.

Jay JA, Blute NK, Lin K, Senn D, Hemond HF, Durant JL. Controls on arsenic speciation and solid-phase partitioning in the sediments of a two-basin lake. Environ Sci Technol. 2005;39(23):9174-81.

Jönsson J and Sherman DM. Sorption of As(III) and As(V) to siderite, green rust (fougerite) and magnetite: Implications for arsenic release in anoxic groundwaters. Chemical Geology. 2008;255:173-181.

Kavanagh PJ, Farago ME, Thornton I, Braman RS. Biovailability of arsenic in soil and mine wastes of the Tamar valley, SW England. Chem. Spec. Bioavail. 1997;9 (3):77–81.

Kraft C, von Tumpling jr. W, Zachmanna DW. The effects of mining in Northern Romania on the heavy metal distribution in sediments of the rivers Szamos and Tisza (Hungary). Acta hydrochim. hydrobiol. 2006;34:257–264.

Lim MS, Yeo IW, Clement TP, Roh Y, Lee KK. Mathematical model for predicting microbial reduction and transport of arsenic in groundwater systems. Water research. 2007;41:2079-2088.

Manful G, Verloo M, Remmerie B. The ecochemistry of arsenic in a contaminated soil: a case study. In: Proceedings of Soil Remediation, Paris, Faculté des Sciences Agronomiques. 1994;34–40.

Manning BA and Goldberg S. Arsenic (III) and arsenic (V) adsorption on three California soils. Soil Sci. 1997;162(12):886-895.

Marcaccio M, Martinelli G, Messori R, Vicari L. Processi di rilascio dell'arsenico nelle acque sotterranee dell'Emilia-Romagna. In: Presenza e diffusione dell'arsenico nel sottosuolo e nelle risorse idriche italiane, nuovi strumenti di valutazione delle dinamiche di mobilizzazione. Linea editoriale di Arpa, Agenzia Regionale Prevenzione e Ambiente dell'Emilia-Romagna; 2005. p.199-208. ISBN 88-87854-17-3.

Martinelli G, Marcaccio M, Farina M, Canepa P, Cantagalli L, Billi L. L'arsenico nei sedimenti profondi della pianura emiliano-romagnola: prime evidenze. In: Presenza e diffusione dell'arsenico nel sottosuolo e nelle risorse idriche italiane, nuovi strumenti di valutazione delle dinamiche di mobilizzazione. Linea editoriale di Arpa, Agenzia Regionale Prevenzione e Ambiente dell'Emilia-Romagna; 2005. p.215-224. ISBN 88-87854-17-3.

Masscheleyn PH, DeLaune RD, Patrick Jr WH. Effect of redox potential and pH on arsenic speciation and solubility in a contaminated soil. Environ. Sci. Technol. 1991;25:1414-1419.

Matera V, Le Hécho I, Laboudigue A, Thomas P, Tellier S, Astruc M. A methodological approach for the identification of arsenic bearing phases in polluted soils. Environ. Pollut. 2003;126:51–64.

Matis KA, Zouboulis AI, Malamas FB, Afonso MDR, Hudson MJ. Flotation removal of As(V) onto goethite. Environ. Pollut. 1997;97:239-245.

McGeehan SL. Arsenic sorption and redox reactions: Relevance to transport and remediation. J. Environ. Sci. Health Part A-Environ. Sci. Engineer. Toxic Hazard. Subst. Control. 1996;31:2319-2336.

Moćko A, Wacławek W. Three-step extraction procedure for determination of heavy metals availability to vegetables. Anal Bioanal Chem. 2004;380(5-6):813-817.

Molinari A, Guadagnini L, Marcaccio M, Guadagnini A. Natural background levels and threshold values of chemical species in three large-scale groundwater bodies in Northern Italy. Sci. Total Environ. 2012;425:9-19, doi:10.1016/j.scitotenv.2012.03.015.

Nguyen KP, Itoi R, Yamashiro R. Influence of Redox Potential on Arsenic Release from Soil. Memoirs of the Faculty of Engineering. Kyushu University. 2008;68(2):129-140.

Nickson RT, McArthur JM, Ravenscroft P, Burgess WG, Ahmed KM. Mechanism of arsenic release to groundwater, Bangladesh and West Bengal. Appl Geochem. 2000;15:403-413.

Pagnanelli F, Moscardini E, Giuliano V, Toro L. Sequential extraction of heavy metals in river sediments of an abandoned pyrite mining area: pollution detection and affinity series. Environmental Pollution. 2004;132:189–201.

Pantsar-Kallio M and Manninen PKG. Speciation of mobile arsenic in soil samples as a function of pH. Sci. Total Environ. 1997;204:193–200.

Perlinger J, Angst W, Schwarzenbach RP. Kinetics of reduction of hexachloroethane by juglone in solutions containing hydrogen sulfide. Environ Sci Technol. 1996;30:3408-3417.

Pfeifer HR, Gueye-Girardet A, Reymond D, Schlegel C, Temgoua E, Hesterberg DL, et al. Dispersion of natural arsenic in the Malcantone watershed, southern Switzerland: field evidence for repeated sorption–desorption and oxidation–reduction processes. Geoderma. 2004;122:205-234.

Pierce ML and Moore CB. Adsorption of arsenite and arsenate on amorphous iron hydroxide. Water Res. 1982;16:1247-1253.

Postma D, Larsen F, Minh Hue NT, Duc MT, Viet PH, Nhan PQ, et al. Arsenic in groundwater of the Red River flS. Arsen, Vietnam: Controlling geochemical processes and reactive transport modeling. Geochim. Cosmochim. Acta. 2007;71 (21):5054-5071.

Razzak A, Jinno K, Hiroshiro Y, Halim MA, Oda K. Mathematical modeling of biologically mediated redox processes of iron and arsenic release in groundwater. Environ Geol. 2009;58:459-469.

Reddy KR and Patrick WH Jr. Effect of alternate aerobic and anaerobic conditions on redox potential, organic matter decomposition and nitrogen loss in a flooded soil. Soil Biol. Biochem. 1974;7:87-94.

Reddy KR and Patrick WH Jr. Effect of frequent changes in aerobic and anaerobic conditions on redox potential and nitrogen loss in a flooded soil. Soil Biol. Biochem. 1976;8:491-495.

Redman AD, Macalady D, Ahmann D. Natural organic matter affects arsenic speciation and sorption onto hematite. Environ Sci Technol. 2002;36:2889-2896.

Regione Emilia–Romagna. Delibera di Giunta n. 350 del 8/02/2010, Approvazione delle attività della Regione Emilia–Romagna riguardanti l'implementazione della Direttiva 2000/60/CE ai fini della redazione ed adozione dei Piani di Gestione dei Distretti idrografici Padano, Appennino settentrionale e Appennino centrale; 2010http://ambiente.regione.emilia-romagna.it/acque/temi/piani%20di%20gestione. Accessed 28 February 2012.

Ricci Lucchi F. Flysch, molassa, cunei clastici: tradizione e nuovi approcci nell'analisi dei bacini orogenici dell'Appennino settentrionale (FLYSH, molassa, clastic deposits: traditional and innovative approaches to the analysis of north Apennine basins). Cento Anni di Geologia Italiana Volume Giubilare 1 centenario Soc. Geol. Ital.;1984. p. 279-95.

Rodríguez-Jordá MP, Garrido F, García-González MT. Assessment of the use of industrial by-products for induced reduction of As, and Se potential leachability in an acid soil. Journal of Hazardous Materials. 2010;175(1–3):328–335.

Sadiq M. Arsenic chemistry in soils: an overview of thermodynamic predictions and field observations. Water Air Soil Pollut. 1997;93:117-136.

Scott MJ and Morgan JJ. Energetics and conservative properties of redox systems. ACS Symp. Ser. 1990;416:779-781.

Senesi N and Steelink C. Application of ESR spectroscopy to the study of humic substances. In: Hayes MHB et al. Humic Substances II. In Search for the Structure. Chichester: Wiley. 1989. p. 373-408.

Shuman LM. Fractionation method for soil microelements. Soil Sci. 1985;140(1):11–22.

Sipos P, Németh T, Mohai I. Distribution and possible immobilization of lead in a forest soil (Luvisol) profile. Environ Geochem Health. 2005;27(1):1-10.

Smedley PL and Kinniburgh DG. A review of the source, behaviour and distribution of arsenic in natural waters. Appl. Geochem. 2002;17:517–568.

Smith E, Naidu R, Alston AM. Chemistry of arsenic in soils: I. Sorption of arsenate and arsenite by four Australian soils. J. Environ. Qual. 1999;28:1719–1726.

Stumm W and Morgan JJ. Aquatic Chemistry. 3rd ed. New York: Wiley; 1996.

Tessier A, Campbell PGC, Bisson M. Sequential extraction procedure for speciation of particulate trace metals. Anal. Chem. 1979;51(7):844–851.

Tretner A. Sorptions und Redoxprozesse von Arsen an oxidischen Oberflächen - Experimentelle Untersuchungen, University of Heidelberg. 2002.

Torres E and Auleda M. A sequential extraction procedure for sediments affected by acid mine drainage. Journal of Geochemical Exploration. 2013

Yang Y, Campbell CD, Clark L, Cameron CM, Paterson E. Microbial indicators of heavy metal contamination in urban and rural soils. Chemosphere. 2006;63(11):1942-1952.

Yoo MS, James BR. Zinc Extractability and Plant Uptake in Flooded, Organic Waste-Amended Soils. 2003;168(10):686-698.

Yu K, Böhme F, Rinklebe J, Neue HU, DeLaune RD. Major biogeochemical processes in soils - a microcosm incubation from reducing to oxidizing conditions. Soil Sci. Soc. Am. J. 2007;71:1406-1417.

UNI CEI ENV 13005. Guida all'espressione dell'incertezza di misura; 2000.

UNI EN 13346. Caratterizzazione dei fanghi. Determinazione di elementi in tracce e del fosforo - Metodi di estrazione con acqua regia, 1/9/2002; 2002.

van Elteren JT, Slejkovec Z, Arcon I, Glass HJ. An interdisciplinary physical-chemical approach for characterization of arsenic in a calciner residue dump in Cornwall (UK). Environ Pollut. 2006;139(3):477-88.

Vink BW. Stability relations of antimony and arsenic compounds in the light of revised and extended Eh –pH diagrams. Chem. Geol. 1996;130:21– 30.

Voegelin A and Hug SJ. Catalyzed Oxidation of Arsenic(III) by Hydrogen Peroxide on the Surface of Ferrihydrite: An in Situ ATR-FTIR Study. Environ. Sci. Technol. 2003;37:972-978.

Voigt DE, Brantle SL, Hennet RJC. Chemical fixation of arsenic in contaminated soils. Appl. Geochem. 1996;11:633–643.

Weng L, Van Riemsdiik WH, Hiemstra T. Effects of fulvic and humic acids on arsenate adsorption to goethite: experiments and modeling. Environ Sci Technol. 2009;43(19):7198-7402.

Zavatti A, Attramini D, Bonazzi A, Boraldi V, Malagò R, Martinelli G, et al. La presenza di arsenico nelle acque sotterranee della pianura padana: evidenze ambientali e ipotesi geochimiche. In: Quaderni di Geologia Applicata. Bologna: Pitagora Editrice; 1995. p. 301-326.

Zheng GD, Chen TB, Gao D, Luo W. Dynamic of lead speciation in sewage sludge composting. Water Sci Technol. 2004;50(9):75-82.

CHAPTER 4

Geochemical modeling of Arsenic release and partitioning in natural soils

4.1. Introduction

The results obtained from the batch tests described in Chapter 3 enable one to understand the overall mechanisms governing arsenic release from different solid matrices when redox conditions change over time across a range of values consistent with real field evidences. Batch tests do not allow to (*a*) evaluate the details of the relative contribution of minerals and/or organic fractions, which constitute the solid matrix of the host porous medium, to As mobilization, and (*b*) clearly identify the role played by the main solid phases that occur in aquifer systems in addition to iron related phases, on pH and redox dynamics which ultimately trigger As release. Mathematical modeling of experimentally observed trends can assist to improve the knowledge of these processes and define a conceptual picture enabling one to improve the description of the key physico-chemical processes that could take place in the natural environment investigated.

Geochemical modeling of processes involving As bearing solid matrices is employed for several applications, including the determination of factors controlling As distribution in the soil-water environment (e.g., Davis et al., 1994; Lumsdon et al., 2001), the impact of competitive adsorption on As release (Gao and Mucci, 2001), the estimation of geogenic elements concentrations in uncontaminated cores to define remediation strategies in contaminated areas of the same aquifer (Stollenwerk and Coleman, 2003), the evaluation of the chemical composition of water in monitoring wells (Armienta et al., 2001), the assessment of potential sources/sinks for As release/retention (e.g., Welch and Lico, 1998). Geochemical models are typically supported by experimental information stemming from different sources, depending on the processes investigated and the available instrumentations. For example, modeling can be supported by sequential extractions (e.g., Parkhurst, 1995; Stollenwerk and Coleman, 2003), batch experiments (Gao and Mucci, 2001), electron microprobe analysis (EMPA) (Davis et al., 1994), X-ray absorption spectroscopy (XAS) (Schreiber et al., 2000), scanning electron microscopy (SEM)/energy dispersive spectroscopy (EDS) (Carrillo-Chavez et al., 2000) to obtain robust and physically based results.

Modeling of reactions that could occur in a gas/water/rock system basically relies on two approaches, respectively considering (*a*) chemical equilibrium or (*b*) kinetic behavior. Approaches based on system equilibrium assume that reactions are very fast (instantaneous) as compared to groundwater residence time but do not provide information about the time required to reach equilibrium or the way the system changes along the reaction path. Kinetic approaches consider the time evolution of reaction rates that involve mineral phase residing in the groundwater system and explicitly embed the possible reactions that could occur along chemical pathways (Langmuir, 1997; Sracek et al., 2004). The thermodynamic equilibrium approach is frequently employed in geochemical modeling because, in the absence of significant anthropogenic alteration, concentration of dissolved species tends to remain approximately constant over time scales of hundreds of years for most deep confined groundwater bodies and for some deep unconfined systems (Langmuir, 1997). The kinetic approach has been applied to natural systems to a lesser extent because reaction rates between minerals and groundwater are difficult to predict due to (*a*) their dependence on the surface characteristics of mineral grains, (*b*) occurrence of adsorbed trace substances on mineral surfaces, and (*c*) possible activities of biological organisms (Berner, 1978) which are seldom quantifiable in a reliable and robust way. The limited ability to accurately measure the wetted surface areas of reacting minerals in soil-aquifer systems (White and Peterson, 1990), or to account for complex mineral-surface effects, such as catalysis, hampers the rigorous application of kinetic concepts to reactive processes developing in groundwater bodies (Langmuir, 1997). At the same time, it is noted that reactions involving minerals, organic substances and other reactants often do not reach equilibrium within the time frame of a laboratory scale experiment. Therefore, mathematical modeling of, e.g., dissolution/precipitation processes involving target solid phases through laboratory experiments often relies on a kinetic approach (Parkhurst and Appelo, 1999).

Mathematical modeling of geochemical dynamics of a given system can involve the calculation of saturation indices (SI) of a water sample with respect to different minerals. When $SI > 0$, water is supersaturated with respect to the mineral and the mineral phase could precipitate; when $SI < 0$, water is undersaturated with respect to the mineral and this mineral could dissolve. When $SI=0$ water is at thermodynamic equilibrium with respect to the mineral (Langmuir, 1997).

Examples of computer codes usually employed for geochemical modeling include MINTEQA2 (Allison et al., 1991), PHREEQC (Parkhurst, 1995) and PHREEQC-2

(Parkhurst and Appelo, 1999), NETPATH (Plummer et al., 1994), GEOSURF (Sahai and Sverjensky, 1998), FITEQL 4.0 (Herbelin and Westall, 1996; 1999), ECOSAT (Keizer and Van Riemsdijk, 1996). Differences between these codes are chiefly due to some aspects such as the thermodynamic databases employed for aqueous speciation calculation, the complexation models used for sorption simulation and chemical equilibrium constants, the type of solver employed for the computations (Sracek et al., 2004).

Recent studies (e.g., Sharif et al., 2008; Nath et al., 2009) evaluate the role of lithology and mineral species on As distribution in sub-surface environments to understand the mobility and distribution of chemical species (e.g., As, Fe and Mn) in groundwater. Redox conditions (i.e., aerobic/anaerobic) is the most influential factor on speciation and, therefore, mobility of metals and metalloids such as As (Frohne et al., 2011). Redox conditions can vary as a consequence of changes in wetting conditions of minerals in soil-aquifer system. Laboratory studies showed that As is released from sediments following flooding and subsequent development of anaerobic conditions (e.g., Deuel and Swoboda, 1972; Hess and Blanchar, 1977; McGeehan, 1996). Considerable studies (e.g., Harvey et al., 2006; Alexandratos et al., 2007; Jönsson and Sherman, 2008) evaluate adsorption and/or kinetics of elements such as As on various mineral phases. On the other hand, no studies appear to report analyses of dissolution/precipitation rates of minerals typically occurring in natural systems (e.g., scorodite, arsenopyrite, ferrihydrite, magnetite) and amenable to influence As dynamics in the presence of different and alternating redox conditions consistent with values measured at field scale. In this context, this study analyzes As dynamics and the behavior of ferrihydrite, rhodochrosite, pyrolussite, calcite and organic matter occurring in a natural aquifer which is subject to changes in aerobic/anaerobic conditions. The solid phases considered in this study typically occur in the groundwater system of Emilia-Romagna, as evidenced by the results of selective sequential extractions presented in Section 4.3.1. The geochemical model here presented provides valuable information for future groundwater modeling researches aimed at investigating geochemical behavior in natural environment subject to redox changes due to anthropogenic activities and/or natural processes. The relevance of this work is that rate parameters are calibrated on the basis of experimental concentrations obtained from a batch test employing natural solid matrix of a given aquifer and is part of a comprehensive effort aimed at investigating the natural background levels of As concentrations detected in a groundwater body located in the Emilia-Romagna Region, Italy.

This Chapter illustrates the development and application of a mathematical geochemical model which can interpret the trends observed during the batch experiments involving solid matrix A and described in Chapter 3. Modeling is supported by the results of selective sequential extractions (SSE) performed on the soil matrix considered. The model allows reproducing the main experimental trends observed for As, Fe, Mn, redox and pH during the batch test and enable one to (*a*) discriminate the role of the different solid phases analyzed on the overall geochemical dynamics observed during the test, and (*b*) obtain a robust characterization of the geochemical system under investigation.

4.2. Materials and methods

4.2.1 Modeling software

Modeling of the geochemical processes under investigation has been performed in the framework of PHREEQC-2 (version 2.18.3-5570) (Parkhurst and Appelo, 1999) platform to simulate the geochemical reactions taking place in the experimental microcosm described in Chapter 3 and evaluate the role of different solid phases on redox and pH changes which might trigger As release.

PHREEQC is a geochemical program which can be applied to interpret several hydrogeochemical environments. It is based on equilibrium chemistry of aqueous solutions interacting with minerals and gases and has the capability to model kinetic reactions with rate equations that can be specifically defined for particular cases. The computational framework offered by PHREEQC is useful to calculate the distribution of aqueous species when one or more solid phases are brought into contact with water. In this work, modeling was performed on the basis of the Minteq.v4 database (Allison et al., 1991), which was modified when required. The most significant modifications to this database include (*a*) the implementation of a specific solid phase enriched in As which is built on the basis of ferrihydrite dissolution reaction available in the Minteq.v4 database, and (*b*) the introduction of reactions describing the decomposition of organic matter and hydrogen peroxide in water (i.e., reactions R4 and R5 reported in Table 4.1).

4.2.2 Selective sequential extraction

As described in Section 3.2.3 of Chapter 3, the methodology proposed by Torres and Auleda (2013) has been employed to characterize the solid matrix tested. The analysis of

As partitioning within the seven fractions identifiable by this protocol enables one to (a) obtain information about the distribution of target chemical species among the different solid phases associated with the selected solid matrix, (b) highlight the occurrence of solid phases which provide key restraints to the analyzed species, and (c) evaluate the relative contribution of each fraction, during the release processes, to the concentration values observed in the batch test. These findings are critical in the framework of geochemical modeling because they allow to understand dominant roles of the fractions prone to adsorb or to release As and the conditions under which these processes can take place in groundwater.

4.3. Results and Discussion

This Section illustrates the geochemical model and the results associated with its application to simulate the reactions taking place in the experimental microcosm described in Chapter 3 when the implemented solid phases are brought in contact with water. Mineral phases employed in the model have been identified on the basis of main metals partitioning occurring in matrix A, on the grounds of the SSE study described in Chapter 3 and in Section 4.3.1 of this Chapter.

4.3.1 As, Fe and Mn partitioning for PHREEQC simulation

Fig. 4.1 reports partitioning of As, Fe, Mn and Ca onto solid matrix A. Association between As and Fe & Mn phases, for both low crystallinity (i.e., FIII) and crystalline (i.e., FIV) hydroxides, is clearly evidenced from As fractioning in Fig. 4.1. The SSE results highlight that more than 80% of As occurring in solid matrix A is bound to these two fractions (FIII and FIV) and that low crystallinity hydroxides bear more As than crystalline oxides. Therefore, large As concentrations are expected in solution when these two phases are subject to dissolution. Arsenic in the analyzed solid matrix is not associated with carbonates and its occurrence in organic matter and sulphide fractions is negligible.

SSE results reveal that Fe basically occurs in low crystallinity hydroxides, crystalline oxides and sulphide fractions where the crystalline fraction is the largest one. It is also noted that about 80% of the total Mn occurring in the solid matrix is present as carbonates with minor proportion of low crystallinity and crystalline oxides. Similarly to Mn, Ca is

mostly present as carbonate. The large occurrence of carbonates binding Mn and Ca in the analyzed solid matrix A suggests the need to include the effect of these minerals in the model, because they can have an important pH buffering role and their occurrence is consistent with the non significant pH variations observed along the experiment.

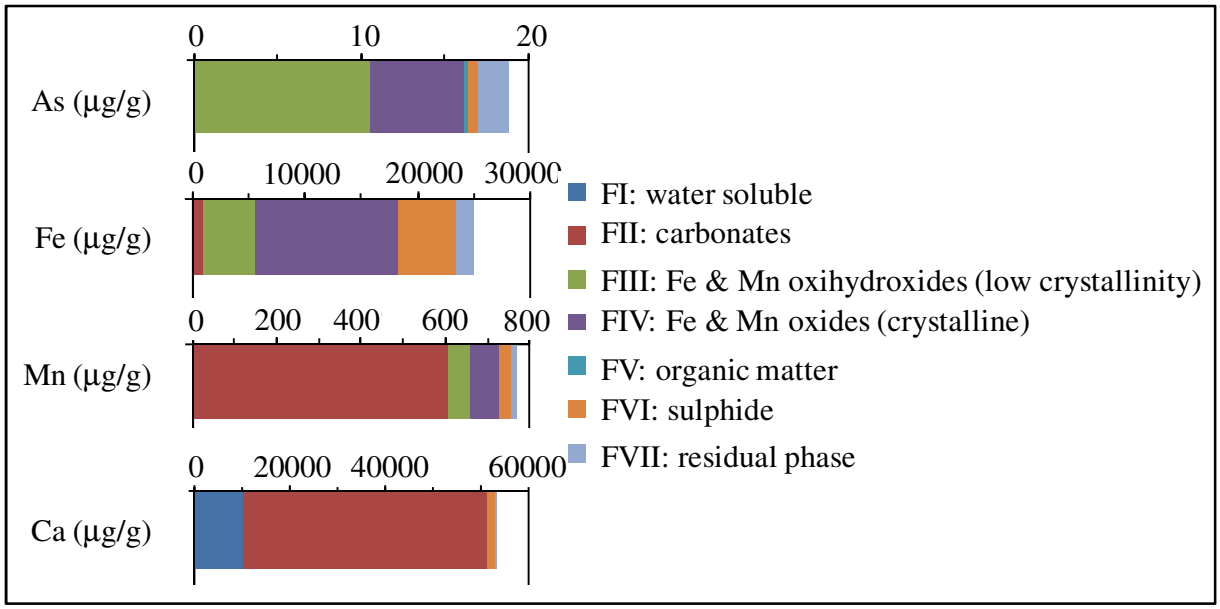

Fig. 4.1 – Partitioning of As, Fe, Mn and Ca in solid matrix A as a result of sequential extractions.

4.3.2 Modeling settings

Four mineral phases, one aqueous phase and the occurrence of organic matter have been implemented in the geochemical model to reproduce the main trends observed during each stage of the batch test.

Consistent with the observation that As mainly occurs in Fraction FIII of the SSE, As enriched ferrihydrite ($Fe(OH)_3$), which is a low crystallinity mineral phase, was considered to model As and Fe concentrations detected along the test.

Organic matter, simulated as CH_2O, rhodochrosite ($MnCO_3$), calcite ($CaCO_3$) and hydrogen peroxide (H_2O_2) (the latter being used only for the oxidizing stage) were included in the model to mimic pH and ORP (oxidation reduction potential) changes during the three stages of the test. Moreover, Mn concentrations were simulated upon considering also dissolution/precipitation of pyrolusite (MnO_2), consistent with the results of sequential extractions (Fig. 4.1) and the occurrence of a fraction of Mn associated with oxides.

Redox and dissolution/precipitation processes involving the implemented solid phases through the experimental stages were simulated with a kinetic approach to take into

account the observation that minerals, organic substances, and other reactants often do not react to equilibrium in the time frame of an experiment (Parkhurst and Appelo, 1999). Table 4.1 reports reactions stoichiometries of the solid and liquid phases implemented in the model.

Table 4.1
Reactions stoichiometries employed in the model.

	Reaction stoichiometry	Reactant phase
R1	$Fe(OH)_3(HAsO_4) + 3H^+ + e^- = Fe^{2+} + 3H_2O + HAsO_4^{2-}$	ferrihydrite enriched in As
R2	$MnCO_3 = Mn^{2+} + CO_3^{2-}$	rhodochrosite
R3	$MnO_2 + 4H^+ + 2e^- = Mn^{2+} + 2H_2O$	pyrolusite
R4	$CaCO_3 = Ca^{2+} + CO_3^{2-}$	calcite
R5	$CH_2O + 2H_2O = HCO_3^- + 5H^+ + 4e^-$	organic matter
R6	$H_2O_2 = O_2 + 2H^+ + 2e^-$	hydrogen peroxide

Considering the protocol of the batch test described in Chapter 3, two sub-stages can be distinguished within each stage due to different stirring conditions: (*a*) continuous stirring during the 5 hours following the reactant (i.e., sodium ascorbate and hydrogen peroxide) injection, and (*b*) discontinuous stirring for the three samples, respectively collected after 24.0, 32.5, 47.5 hours for phases (1) and (2) and after 24.0, 32.5, 72.5 hours for phase (3). This resulted in different reaction kinetics within the same stage, consistent with As and Fe trends observed in the experiment.

The last sample of the test, which was collected after 168 hours from the beginning of the experiment (i.e., following about 40 hours of non-homogenized conditions), exhibits the largest As, Fe and Mn concentrations. This is consistent with the occurrence of strong and persistent reducing conditions leading to oxihydroxides dissolution which evidences the existence of three different kinetic rates within the third stage. This can also be seen from Fig. 4.2b and Fig. 4.2c where experimental As and Fe concentrations detected in the third reducing stage exhibit three different linear trends with three different slopes supporting the occurrence of three different kinetic rates within this stage of the test.

Experimental values observed at each sampling time were fitted by calibrating the reaction rates of the implemented reactions and the As/Fe ratio by means of the non-linear least squares parameter estimation software PEST (Doherty, 2004) in conjunction with PHREEQC.

Values for initial ORP and pH and initial water composition were set equal to the observations associated with the first experimental sample collected after about 48 hours

of water/solid matrix contact and before injection of gas and/or reactant. The initial amount of solid phases was deduced from the results of sequential extractions on the basis of the fraction of the main element constituting the bulk structure of a given solid phase.

4.3.3 Modeling results

Fig. 4.2 reports the comparison of experimental (solid lines) and simulated (dotted lines) values of ORP and pH, As, Fe and Mn concentrations in the three stages of the test. Estimated rate constants of minerals and liquid phases and the corresponding estimation of confidence intervals are respectively listed in Table 4.2 and Table 4.3. Fig. 4.3 reports the simulated mineral variations and corresponding saturation index of rhodochrosite, ferrihydrite, calcite and pyrolusite. Organic matter variation along the simulation is reported in Fig. 4.4.

Even though the model was able to reproduce the key dynamics observed during the test, it can be noted that simulated ORP values (Fig. 4.2a) are always lower than their experimental counterparts in both reducing stages. This is related to the assumption that modeled ORP values are only the result of organic matter decomposition and mineral dissolution while O_2 pressure within the experiment was adjusted by argon and oxygen injection to guarantee attaining the target ORP value (about -150 mV) during the reducing stages. The calibration of hydrogen peroxide rate constant allowed an improved ORP simulation in the oxidizing stage, in terms of relative differences between simulated and experimental ORP values in the two reducing stages. This behavior is also related to the observation that the model does not consider the injection of sodium ascorbate because (*a*) the amount added is negligible with respect to the amount of slurry in the batch system (i.e., about 2 mL of reactant in about 1.8L of slurry), and (*b*) it is assumed that the effect of sodium ascorbate (which is an organic molecule) injection can also be simulated by tuning the effective dissolution rate parameter of organic matter.

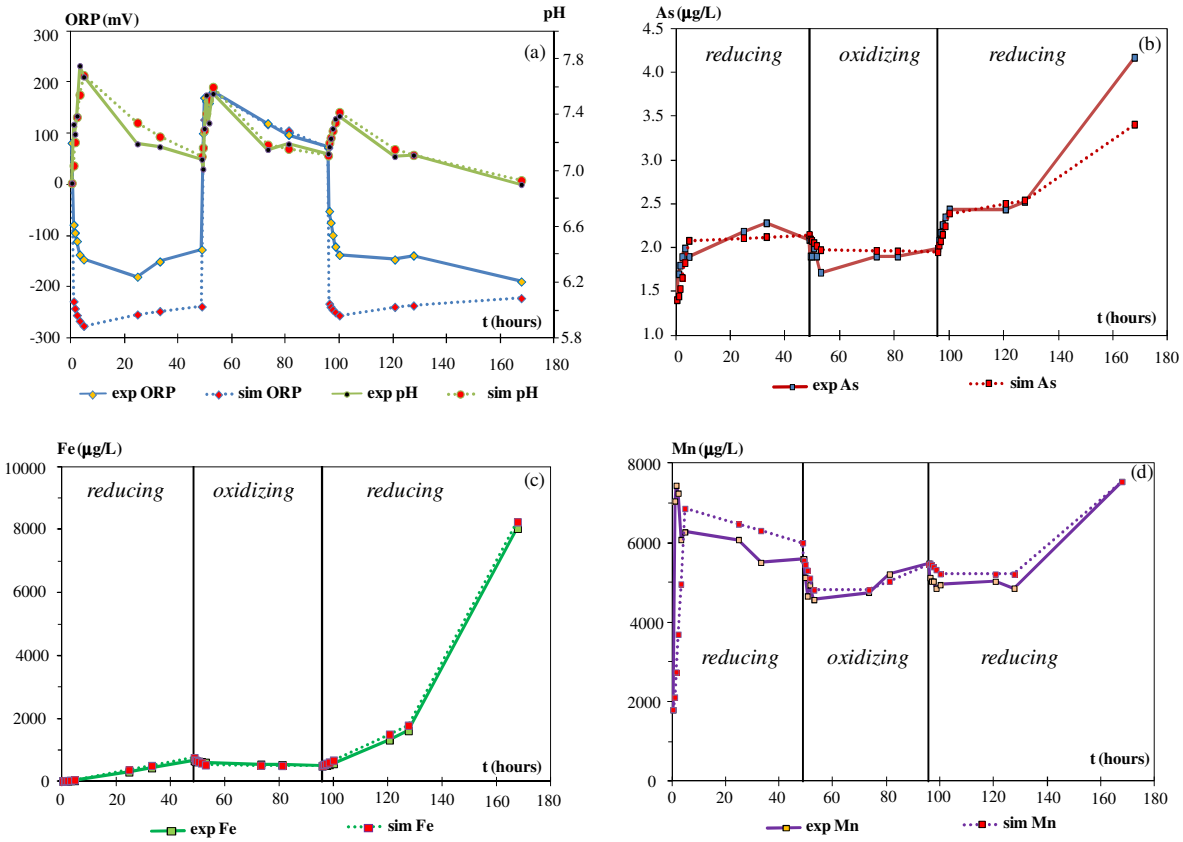

Fig. 4.2 – Comparison between experimental and simulated values of (a) ORP and pH, (b) As, (c) Fe and (d) Mn concentrations during the three stages of the test.

As a result of the initial reducing conditions, rhodochrosite and calcite dissolve within the first 5 hours of the test. This dissolution process is consistent with the observed raising of pH and Mn concentrations (Fig. 4.2a, d). After this time frame, calcite and pyrolusite dissolution resulted in a slightly supersaturation of rhodochrosite. The latter then precipitates (Fig. 4.3a) leading to pH and Mn decrease which is associated with ORP raising (last three points of the first reducing stage in Fig. 4.2a).

On the other hand, a rapid As release (Fig. 4.2b) coincides with a poor increase in dissolved Fe (Fig. 4.2c) in the first 5 hours of the test. After this phase (at about 25 hours from the beginning of the experiment), dissolved Fe concentration increases significantly and dissolved As concentrations display a reduced rate of increase. These findings suggest that only the As adsorbed on the Fe-hydroxide surface is initially mobilized and the As associated with the bulk mineral structure is mobilized only at a later stage.

When the system is reverted to oxidizing conditions, the solution becomes supersaturated in ferrihydrite. The latter then precipitates and adsorbs As. This leads to a decrease in dissolved As and Fe concentrations during the first 5 hours of the oxidizing stage (Fig. 4.2b, c). The decreasing trend of dissolved Mn concentrations (Fig. 4.2d)

observed during this time frame is modeled by assuming occurrence of rhodochrosite precipitation. This follows from the observation that (*a*) the saturation index of rhodochrosite is close to zero at the beginning of the oxidizing conditions (Fig. 4.3a), and (*b*) pyrolusite dissolves during the oxidizing stage supplying Mn to the slurry and triggering rhodochrosite precipitation which, in turn, leads to the Mn decreasing trend observed at the beginning of the oxidizing stage (at about 50 hours from the beginning of the experiment). After this decrease, Mn concentrations in solution begin to rise again (last three points of the oxidizing phase in Fig. 4.2d). This is consistent with subsaturation conditions (and therefore dissolution) of pyrolusite (Fig. 4.3d) after the first 5 hours of the oxidizing stage.

The fast As decrease observed during the rapid induced change to oxidizing conditions is consistent with As adsorption on iron phases which become supersaturated and precipitate under oxidizing conditions. This fast As decrease is followed by a constant trend for the remaining part of the oxidizing stage (Fig. 4.2b) consistent with (*a*) the stationary trend of Fe concentration in solution (Fig. 4.2c), and (*b*) the relatively constant saturation index of ferrihydrite (Fig. 4.3b), the latter being always under supersaturation conditions during this stage of the test.

While pH is expected to decrease following ferrihydrite precipitation and organic matter oxidation (Fig. 4.4), it is noted that experimental values increase during the first 5 hours of the oxidizing stage (Fig. 4.2a). This trend is consistent with (*a*) the significant calcite dissolution (Fig. 4.3c) at the beginning of the oxidizing conditions, and (*b*) the slow dissolution rate of pyrolusite (Fig. 4.3d) within this stage. At about 58 hours from the beginning of the test, pH decreases to a nearly constant value of 7.2 (last three points associated with the oxidizing conditions in Fig. 4.2a), consistent with the constant saturation index of all mineral phases (Fig. 4.3) in this specific time interval and the buffering role played by pyrolusite dissolution which avoids a significant pH decrease due to organic matter oxidation.

In the third stage of the test the newly induced reducing conditions lead to remobilization of Mn, Fe and As, which had been previously precipitated and adsorbed on oxihydroxides during the oxidizing stage. These reducing conditions result in ferrihydrite and pyrolusite dissolution, which lead to the increase of dissolved As, Fe and Mn concentrations which are observed starting at about 95 hours from the beginning of the test and consistently continuing until the end of the experiment. Close inspection of the experimental and modeled results reveals that Mn aqueous concentrations initially

decrease to then display a significant increase at the end of the experiment. This type of trend is consistent with the different behavior displayed by rhodochrosite (Fig. 4.3a) and pyrolusite (Fig. 4.3d) at the beginning of the second reducing stage and at the end of the test. More specifically, pyrolusite dissolves when the system is reverted to anaerobic conditions and supplies Mn to the slurry triggering rhodochrosite precipitation; on the other hand, the persistence of strongly reducing conditions enhances pyrolusite dissolution at the end of the test. This dissolution process is associated with larger rate than that observed in the preceding anaerobic stages. These Mn dynamics are also consistent with calcite and hydroxides dissolution which increase pH up to slightly alkaline conditions (pH ≈ 7.5) and cause rhodochrosite precipitation.

It is observed that under reducing conditions which persist for long time (about 40 hours during the third experimental stage) the calibrated constant rate of organic matter oxidation (Table 4.2, Stage 3.3) is larger than the dissolution rate of the remaining mineral phases. Therefore, this causes pH to decrease (last three points of the reducing stage in Fig. 4.2a). Even if pH decreases Mn and Fe concentrations observed a simultaneous increase in solution for the first time in the experimental values recorded at the end of the test. This is consistent with the dissolution of Fe-Mn-oxides, which occurs only at the end of the test after long persistence of reducing conditions.

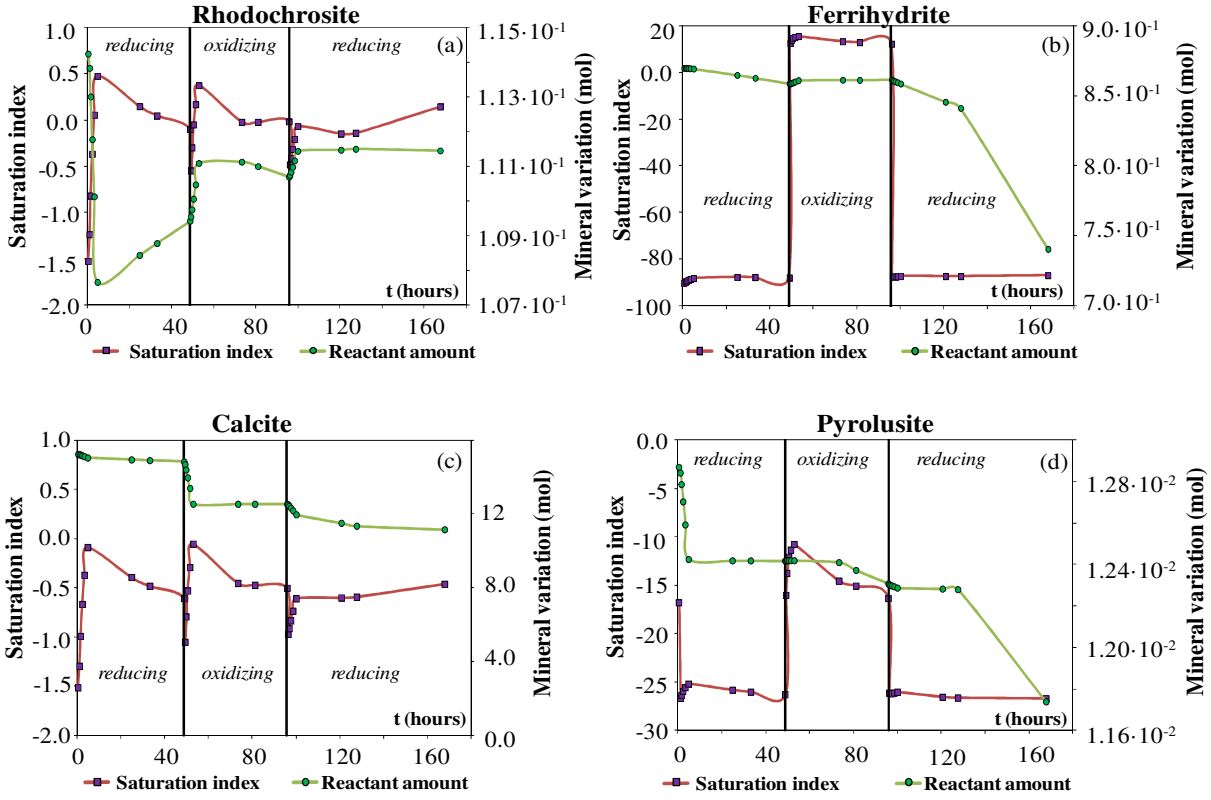

Fig. 4.3 – Simulated mineral variations and corresponding saturation indexes of (a) rhodochrosite, (b) ferrihydrite, (c) calcite and (d) pyrolusite.

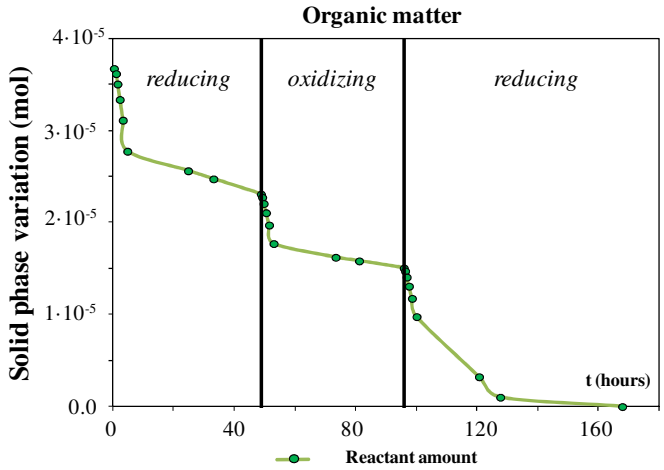

Fig. 4.4 – Simulated organic matter variations during the test.

Table 4.2 reports estimated rate constants for each mineral and/or liquid phase implemented in the geochemical model, together with As/Fe ratios considered within each sub-stage while the corresponding confidence intervals are reported in Table 4.3. The differences in As/Fe ratio and ferrihydrite rate constant observed in the two reducing stages are consistent with the observation that Fe and As released in the last stage are the result of the dissolution of the ferrihydrite which has precipitated in the preceding oxidizing stage. The calibrated values of ferrihydrite effective rates show that (*a*) Fe release due to ferrihydrite dissolution is faster in the third stage than in the first reducing period, and (*b*) Fe dynamics during the rapid changes of redox conditions are associated with the same rate, which displays opposite sign during precipitation (stage 2.1) and dissolution (stage 3.1), as seen in Fig. 4.2c. Organic matter is associated with a relatively large effective rate during the rapid change from oxidizing to reducing conditions (i.e., stage 1.1 and 3.1). At the end of the test, when reducing conditions persist for long time (i.e., about 40 hours), organic matter is then characterized by an effective rate which is about four order of magnitude larger than those observed during the other stages. Carbonates (i.e., rhodochrosite and calcite) play a complementary buffering role to avoid excessive pH lowering by organic matter decomposition, as evidenced in Table 4.2. Hydrogen peroxide is characterized by a constant rate, which is of the same order of magnitude of the rate associated with organic matter. This highlights the relevance of considering this aqueous phase for a proper simulation of the behavior of the experimental microcosm during the oxidizing stage.

Table 4.2
Estimated rate constants and As/Fe ratios per each sub-stage

	STAGE 1 - reducing		STAGE 2 - oxidizing		STAGE 3 - reducing		
sub-stage	1.1	1.2	2.1	2.2	3.1	3.2	3.3
As/Fe	0.0157	0.00007	0.0006	0.0005	0.0018	0.0001	0.0001
$k_{Ferrihydrite}$ ($mol \cdot kgw^{-1}\ s^{-1}$)	$4.0 \cdot 10^{-11}$	$8.0 \cdot 10^{-11}$	$-2.0 \cdot 10^{-10}$	$-5.0 \cdot 10^{-12}$	$2.0 \cdot 10^{-10}$	$2.0 \cdot 10^{-10}$	$8.0 \cdot 10^{-10}$
$k_{Rhodochrosite}$ ($mol \cdot kgw^{-1}\ s^{-1}$)	$4.0 \cdot 10^{-9}$	$-1.0 \cdot 10^{-10}$	$-1.0 \cdot 10^{-9}$	$5.0 \cdot 10^{-11}$	$-4.5 \cdot 10^{-10}$	$-1.0 \cdot 10^{-11}$	$3.0 \cdot 10^{-12}$
k_{CH2O} ($mol \cdot kgw^{-1}\ s^{-1}$)	$1.7 \cdot 10^{-8}$	$8.0 \cdot 10^{-10}$	$1.0 \cdot 10^{-8}$	$4.0 \cdot 10^{-10}$	$1.0 \cdot 10^{-8}$	$2.4 \cdot 10^{-9}$	$1.0 \cdot 10^{-4}$
k_{H2O2} ($mol \cdot kgw^{-1}\ s^{-1}$)	---	---	$2.0 \cdot 10^{-8}$	$7.1 \cdot 10^{-10}$	---	---	---
$k_{Calcite}$ ($mol \cdot kgw^{-1}\ s^{-1}$)	$1.0 \cdot 10^{-9}$	$1.0 \cdot 10^{-10}$	$1.2 \cdot 10^{-8}$	$1.0 \cdot 10^{-12}$	$3.0 \cdot 10^{-9}$	$4.7 \cdot 10^{-10}$	$1.0 \cdot 10^{-10}$
$k_{Pyrolusite}$ ($mol \cdot kgw^{-1}\ s^{-1}$)	$2.4 \cdot 10^{-9}$	$1.0 \cdot 10^{-12}$	$1.0 \cdot 10^{-12}$	$9.5 \cdot 10^{-11}$	$9.0 \cdot 10^{-11}$	$9.0 \cdot 10^{-12}$	$2.9 \cdot 10^{-10}$
Note: negative k denotes precipitation							

Table 4.3
Confidence intervals of the estimated rate constants per each sub-stage

	STAGE I - reducing				STAGE II - oxidizing				STAGE III - reducing					
sub-stage	1.1		1.2		2.1		2.2		3.1		3.2		3.3	
confidence limit	lower limit	upper limit	lower limit	upper limit	lower limit	upper limit	lower limit	upper limit	lower limit	upper limit	lower limit	upper limit	lower limit	upper limit
$k_{Ferrihydrite}$ ($mol \cdot kgw^{-1} \cdot s^{-1}$)	$-2.35 \cdot 10^{-9}$	$2.43 \cdot 10^{-9}$	$-8.70 \cdot 10^{-10}$	$1.03 \cdot 10^{-9}$	$-3.25 \cdot 10^{-11}$	$4.30 \cdot 10^{-10}$	$-2.54 \cdot 10^{-10}$	$2.64 \cdot 10^{-10}$	$-1.74 \cdot 10^{-10}$	$5.72 \cdot 10^{-10}$	$1.12 \cdot 10^{-10}$	$2.86 \cdot 10^{-10}$	$-6.14 \cdot 10^{-9}$	$7.74 \cdot 10^{-9}$
$k_{Rhodochrosite}$ ($mol \cdot kgw^{-1} \cdot s^{-1}$)	$-1.71 \cdot 10^{-2}$	$1.71 \cdot 10^{-2}$	$-8.29 \cdot 10^{-3}$	$8.29 \cdot 10^{-3}$	$-1.57 \cdot 10^{-5}$	$1.57 \cdot 10^{-5}$	$-6.11 \cdot 10^{-3}$	$6.11 \cdot 10^{-3}$	$-5.66 \cdot 10^{-4}$	$5.66 \cdot 10^{-4}$	$-9.79 \cdot 10^{-5}$	$9.79 \cdot 10^{-5}$	$-5.21 \cdot 10^{-3}$	$5.21 \cdot 10^{-3}$
k_{CH2O} ($mol \cdot kgw^{-1} \cdot s^{-1}$)	$-2.57 \cdot 10^{-2}$	$2.57 \cdot 10^{-2}$	$-1.24 \cdot 10^{-2}$	$1.24 \cdot 10^{-2}$	$-1.58 \cdot 10^{-6}$	$1.60 \cdot 10^{-6}$	$-3.31 \cdot 10^{-4}$	$3.31 \cdot 10^{-4}$	$-3.77 \cdot 10^{-5}$	$3.77 \cdot 10^{-5}$	$-1.48 \cdot 10^{-4}$	$1.48 \cdot 10^{-4}$	$-1.19 \cdot 10^{-2}$	$1.21 \cdot 10^{-2}$
k_{H2O2} ($mol \cdot kgw^{-1} \cdot s^{-1}$)	---	---	---	---	$-1.80 \cdot 10^{-5}$	$1.81 \cdot 10^{-5}$	$-8.33 \cdot 10^{-3}$	$8.33 \cdot 10^{-3}$	---	---	---	---	---	---
$k_{Calcite}$ ($mol \cdot kgw^{-1} \cdot s^{-1}$)	$-8.64 \cdot 10^{-5}$	$8.64 \cdot 10^{-5}$	$-2.92 \cdot 10^{-5}$	$2.92 \cdot 10^{-5}$	$-1.33 \cdot 10^{-5}$	$1.33 \cdot 10^{-5}$	$-6.03 \cdot 10^{-3}$	$6.03 \cdot 10^{-3}$	$-4.38 \cdot 10^{-6}$	$4.38 \cdot 10^{-6}$	$-3.76 \cdot 10^{-6}$	$3.76 \cdot 10^{-6}$	$-2.60 \cdot 10^{-6}$	$2.60 \cdot 10^{-6}$
$k_{Pyrolusite}$ ($mol \cdot kgw^{-1} \cdot s^{-1}$)	$-1.71 \cdot 10^{-2}$	$1.71 \cdot 10^{-2}$	$-8.29 \cdot 10^{-3}$	$8.29 \cdot 10^{-3}$	$-1.57 \cdot 10^{-5}$	$1.57 \cdot 10^{-5}$	$-6.11 \cdot 10^{-3}$	$6.11 \cdot 10^{-3}$	$-5.66 \cdot 10^{-4}$	$5.66 \cdot 10^{-4}$	$-9.79 \cdot 10^{-5}$	$9.79 \cdot 10^{-5}$	$-5.21 \cdot 10^{-3}$	$5.21 \cdot 10^{-3}$

4.3.4 Modeling implications

Modeling results highlight that two forms of As are released during the second reducing stage (Fig. 4.2b): (1) As adsorbed on outer surface of oxihydroxides minerals, and (2) As included in the bulk structure of low crystallinity phases. Thus, As concentrations are observed to raise faster when the system is switched to reducing conditions, suggesting that the As adsorbed on external surface of oxihydroxides minerals was completely released. Then, at the end of the test, after long persisting reducing conditions, high Fe and Mn concentrations and As were detected in water, suggesting release of As included in the bulk structure of low crystallinity phases.

Simulated As concentration are generally in good agreement with experimental concentrations with the exception of As dissolved concentration simulated at the end of the test (Fig. 4.2b), which is lower than its experimental counterpart. The observed difference in final As concentration could be due to (*a*) the modeling assumption that the As/Fe ratio for ferrihydrite is the same in sub-stages 3.2 and 3.3 (see Table 4.2) while, after about 40 hours of reducing conditions without stirring, a different value for this ratio may have occurred and (*b*) the occurrence of a possible contribution of other oxides to As release, e.g., contributions stemming from Mn phases binding As, that could occur in solution but are not considered in the proposed model. The latter point is supported by the results of SSE on Mn partitioning in solid matrix A (see Section 4.3.1). It is also consistent with the observation that Mn and Fe display similar trends in the last part of the test (while displaying opposing trends during the preceding phases) with a significant increase in dissolved concentration values, suggesting that this raise could be due to the occurrence of the same type of mineral, such as hydroxides restraining As, which are not contemplated in the model. This observation suggests that the role of Mn oxides on As release could be significant for long time scales of interaction between water and solid matrix in a strongly reducing environment.

4.4. Conclusions

The simplified geochemical model presented, supported by evidences from selective sequential extractions analyses, is shown to be capable of reproducing (both qualitatively and quantitatively) the main experimental features characterizing the As, Fe, Mn and redox/pH trends observed during the batch test performed on solid matrix A and described in Chapter 3. Interpretation of modeling outputs provides key information for improved

understanding of the mechanisms and geochemical processes governing the system under investigation. Effective rate parameters calibrated in this study are of potential use for future researches involving modeling of As dynamics within large scale aquifer systems. The work leads to the following major conclusions:

1. Arsenic is significantly associated with low crystallinity and crystalline Fe-Mn-oxyhydroxides. These phases represent about 80% of the total As occurring in the tested solid matrix. Therefore, large As release is expected when the low crystallinity phases are subjected to dissolution.
2. Arsenic dynamics appear to be governed to a large extent by Fe than Mn even as the role of Mn oxides could be significant for long time scales of interaction between water and solid matrix in strongly reducing environments.
3. Arsenic is released firstly from the outer surface of Fe-oxihydroxides minerals, displaying a rapid rate when redox conditions change rapidly. It exhibits large concentrations in water when persistent reducing conditions trigger the crystalline structure dissolution of the binding mineral.
4. Iron dynamics during rapid changes in redox conditions follow the same (but with opposite sign) rate.
5. The presence of organic matter strongly affects pH and redox conditions, thus influencing As speciation and mobility.

References

Alexandratos VG, Elzinga EJ, Reeder RJ. Arsenate uptake by calcite: Macroscopic and spectroscopic characterization of adsorption and incorporation mechanisms. Geochimica et Cosmochimica Acta. 2007;71:4172-4187.

Armienta MA, Villasenor G, Rodriguez R, Ongley LK, Mango H. The role of arsenic-bearing rocks in groundwater pollution at Zimapán Valley, México. Environ. Geol. 2001;40:571–581.

Allison JDD, Brown S, Novo-Gradac KJ. MINTEQA2/PRODEFA2, A geochemical assessment model for environmental systems: version 3.0 user's manual. Athens, GA, U.S. EPA. 1991.

Berner RA. Rate control of mineral dissolution under earth surface conditions. Am. J. Sci. 1978;278:1235-1252.

Carrillo-Chávez A, Drever JI, Martinez M. Arsenic content and groundwater geochemistry of San Antonio-El Triunfo, Carrizal and Los Planes aquifers in southernmost Baja California, Mexico. Environ. Geol. 2000;39:1295–1303.

Damris M, O'Brien GA, Price WE, Chenhall BE. Fractionation of sedimentary arsenic from Port Kembla Harbour, NSW, Australia. J Environ Monit. 2005;7(6):621-30.

Davis A, Kempton JH, Nicholson A, Yare B. Groundwater transport of arsenic and chromium at a historical tannery, Woburn, Massachusetts. Appl. Geochem. 1994;9:569–582.

Doherty J. PEST Model-Independent Parameter Estimation. User Manual (5th ed). 2004. Watermark Numerical Computing, Australia.

Deuel LE and Swoboda AR. Arsenic solubility in a reduced environment. Soil Sci. Soc. Am. Proc. 1972;36:276-278.

Frohne T, Rinklebe J, Diaz-Bone RA, Du Laing G. Controlled variation of redox conditions in a floodplain soil: Impact on metal mobilization and biomethylation of arsenic and antimony. Geoderma. 2011;160:414–424. doi:10.1016/j.geoderma.2010.10.012

Gao Y and Mucci A. Acid base reactions, phosphate and arsenate complexation, and their competitive adsorption at the surface of goethite in 0.7 M NaCl solution. Geochim. Cosmochim. Acta. 2001;65:2361–2378.

Harvey MC, Schreiber ME, Rimstidt JD, Griffith MM. Scorodite Dissolution Kinetics: Implications for Arsenic Release. Environ. Sci. Technol. 2006;40:6709-6714.

Herbelin AL and Westall JC. FITEQL: a computer program for determination of chemical equilibrium constants from experimental data. Report 96-01, Department of Chemistry, Oregon State University, Corvallis, OR. 1996.

Herbelin AL and Westall JC. FITEQL 4.0: a Computer Program for Determination of Chemical Equilibrium Constants from Experimental Data. Report 99-01, Department of Chemistry, Oregon State University, Corvallis. 1999.

Hess RE and Blanchar RW. Dissolution of arsenic from waterlogged and aerated soil. Soil Sci. Soc. Am. J. 1977;41:861-865.

Jönsson J and Sherman DM. Sorption of As(III) and As(V) to siderite, green rust (fougerite) and magnetite: Implications for arsenic release in anoxic groundwaters. Chemical Geology. 2008;255:173-181.

Keizer MG and Van Riemsdijk WH. ECOSAT, A Computer Program for Calculation of Speciation and Transport in Soil–Water Systems. Version 4.3, Dept. Soil Science and Plant Nutrition, Wageningen Agriculture University, Wageningen, Netherlands. 1996.

Langmuir D. Aqueous Environmental Geochemistry. Prentice Hall, NJ. 1997.

Lumsdon DG, Meeussen JCL, Paterson E, Garden LM, Anderson P. Use of solid phase characterization and chemical modelling for assessing the behaviour of arsenic in contaminated soils. Appl. Geochem. 2001;16:571–581.

McGeehan SL. Arsenic sorption and redox reactions: Relevance to transport and remediation. J. Environ. Sci. Health Part A-Environ. Sci. Engineer. Toxic Hazard. Subst. Control 1996;31:2319-2336.

Nath B, Chakraborty S, Burnol A, Stüben D, Chatterjee D, Charlet L. Mobility of arsenic in the sub-surface environment: An integrated hydrogeochemical study and sorption model of the sandy aquifer materials. Journal of Hydrology. 2009;364:236–248.

Pantsar-Kallio M and Manninen PKG. Speciation of mobile arsenic in soil samples as a function of pH. Sci. Total Environ. 1997;204:193–200.

Parkhurst DL. Users Guide to PHREEQC, A Computer Program for Speciation, Reaction-path, Advective-Transport, and Inverse Geochemical Calculations. U.S. Geol. Surv. Water Resour. Invest. Rep. 95-4227. 1995.

Parkhurst DL and Appelo CAJ. PHREEQC-2, A Hydrogeochemical Computer Program. US Geol. Surv., Water Resour. Invest. 1999.

Parkhurst DL and Appelo CAJ. User's guide to PHREEQC (version 2) – A computer program for speciation, batch-reaction, one-dimensional transport, and inverse geochemical calculations. US Geol. Surv., Water-Resour. Invest. Rep. 99–4259. 1999.

Plummer LN, Prestemon EC, Parkhurst DL. An Interactive Code (NETPATH) for Modeling Net Geochemical Reactions along a Flow Path, Version 2.0. US Geol. Surv., Water Resour. Invest. Rep. 94-4169. 1994.

Rodríguez-Jordá MP, Garrido F, García-González MT. Assessment of the use of industrial by-products for induced reduction of As, and Se potential leachability in an acid soil. Journal of Hazardous Materials. 2010;175(1–3):328–335.

Sahai N and Sverjensky DA. GEOSURF: A Computer Program for Modeling Adsorption on Mineral Surfaces from Aqueous Solution. Computers and Geosciences. 1998;24:853-873.

Schreiber ME, Simo JA, Freiberg PG. Stratigraphic and geochemical controls on naturally occuring arsenic in groundwater, eastern Wisconsin, USA. Hydrogeol. J. 2000;8:161–176.

Sharif MU, Davis RK, Steele KF, Kim B, Hays PD, Kresse TM, Fazio JA. Distribution and variability of redox zones controlling spatial variability of arsenic in the Mississippi River Valley alluvial aquifer, southeastern Arkansas. Journal of Contaminant Hydrology. 2008;99:49–67.

Sracek O, Bhattacharya P, Jacks G, Gustafsson JP, Brömssen M. Behavior of arsenic and geochemical modeling of arsenic enrichment in aqueous environments. Applied Geochemistry. 2004;19:169–180.

Stollenwerk KG and Coleman JA. Natural remediation potential of arsenic-contaminated ground water. In: Welch AH and Stollenwerk KG. (Eds.), Arsenic in Ground Water: Geochemistry and Occurrence. Kluwer Academic Publishers, Boston, MA, pp. 351–379. 2003.

Torres E and Auleda M. A sequential extraction procedure for sediments affected by acid mine drainage. Journal of Geochemical Exploration. 2013

Welch AH and Lico MS. Factors controlling As and U in shallow groundwater, southern Carson Desert, Nevada. Appl. Geochem. 1998;13:521–539.

White AF and Peterson ML. Role of reactive-surface-area characterization in geochemical kinetic models. In Chemical modeling of aqueous systems 11, ed. D. C. Melchior and R. L. Bassett. ACS Symposium Series 416, pp. 461-75. Washington, DC: Am. Chem. Soc. 1990.

CHAPTER 5

Conclusions

A major aim of this research was the investigation of arsenic partitioning and dynamics on the assessment of groundwater background levels of this metalloid in target aquifers of the Emilia-Romagna Region, Italy. This analysis is critical to provide a proper classification of the chemical status of the selected aquifers. The research goals were achieved through the implementation and application of mathematical and experimental approaches. These have allowed to acquire improve understanding of the mechanisms governing the complex geochemical dynamics of arsenic which led to the large hot-spot concentrations detected in some of the target groundwater bodies.

Global statistical methodologies highlighted that the analyzed groundwater bodies are characterized by different responses, in terms of estimated NBLs, with respect to a given chemical species. This supports the need to assess NBLs of target species separately for each identified water body.

Consistent with (*a*) the decreasing amount of withdrawals with depth and (*b*) the effect of natural attenuation processes, up to about 40 m depth estimated NBLs were found to increase with the average depth of the investigated water bodies for all chemical species analyzed. Estimates associated with different temporal aggregation windows evidenced that NBLs can display different temporal dynamics within the observation time frame. This result stresses the need for continuous monitoring of water bodies to update the associated NBLs as a function of the temporal dependence of both anthropogenic impacts and natural processes occurring in the subsurface. A notable weakness of the global statistical methodologies employed is the inability to embed the physico-chemical dynamics of species which could be the result of natural processes and might influence NBLs.

Experimental characterization of arsenic dynamics (i.e., partitioning and mobility) has been performed on the natural solid matrices investigated. The experiments showed a distinct correlation between temporal dynamics of aerobic/anaerobic conditions and arsenic release into the solution. Even as iron minerals phases (low crystallinity and crystalline) were found to strongly influence arsenic dynamics, the largest arsenic release were observed from vegetal matter. The latter releases the metalloid faster and with larger

concentrations detected in Emilia-Romagna aquifers could be consistent with the localized occurrence of vegetal matter which releases arsenic as a consequence of redox changes.

Modeling study evidenced that large dissolved arsenic concentrations should be expected when the low crystallinity phases (associated with Fe and/or Mn) are subject to dissolution. It was noted that Fe minerals appear to govern arsenic dynamics for short time scales while Mn phases can contribute significantly to arsenic release over long time scales.

This work evidenced the importance of grounding NBL estimates on the actual geochemical dynamics governing the behavior of target chemical species to provide a proper assessment of the chemical status of a given aquifer. This observation is supported, e.g., by the results obtained with reference to ammonium. The latter is characterized by background values which are about 10 times larger than the limiting value imposed by current Regulations in the deepest water body analyzed due to the large natural occurrence of decomposed peats. In the case of arsenic, the localized occurrence of vegetal matter, which was found to strongly influence the geochemical dynamics of the system, suggested that the large arsenic concentrations detected in the analyzed water bodies can be considered strongly related to particular local natural conditions.

The complex geochemical dynamics and partitioning characterizing arsenic behavior in the tested solid matrices evidenced that arsenic natural background levels depend on the local processes occurring at the micro-scale which are clearly not embedded within an estimation process based only on global statistical methods. It is concluded that estimates of NBLs of chemical species such as arsenic need to be performed by considering real field conditions to assure consistency with the hydro-geo-chemical behavior of the tested aquifer.

ANNEX 1
SUMMARY OF RESEARCH PRODUCTS

Papers

In press – Volume relativo al monitoraggio delle acque sotterranee in Emilia-Romagna, Pitagora Editrice.
Applicazione metodologica per la stima delle concentrazioni naturali di sostanze pericolose in corpi idrici sotterranei della pianura alluvionale padana e appenninica.
L. Guadagnini, **A. Molinari**, M. Marcaccio, A. Palumbo, A. Guadagnini

02/2013 - Science of the Total Environment (ISI-listed, IF 2011: 3.286).
Arsenic release from deep natural solid matrices under experimentally controlled redox conditions, volume 444, pages 231–240
A. Molinari, L. Guadagnini, M. Marcaccio, S. Straface, X. Sanchez-Vila, A. Guadagnini
http://dx.doi.org/10.1016/j.scitotenv.2012.11.093

12/2012 – Ecoscienza
Metalli e sostanze inorganiche, la stima dei valori di fondo, number 6, pages 63-65. ISSN 2039-0432.
M. Marcaccio, **A. Molinari**, L. Guadagnini, A. Guadagnini.
http://www.arpa.emr.it/cms3/documenti/_cerca_doc/ecoscienza/ecoscienza2012_6/marcaccio_et_al_es6_12.pdf

11/2012 – Ecomondo, meeting 2012, Rimini, Italy
Valori di fondo naturale e valori soglia di specie chimiche potenzialmente contaminanti per l'individuazione dello stato chimico delle acque sotterranee dell'Emilia-Romagna, Morselli Ed., Maggioli Editore, pages 977-982.
M. Marcaccio, **A. Molinari**, L. Guadagnini, A. Guadagnini, A. Palumbo, I. Pellegrino

04/2012 – Science of the Total Environment (ISI-listed, IF 2011: 3.286).
Natural background levels and threshold values of chemical species in three large-scale groundwater bodies in Northern Italy, volume 425, pages 9–19
A. Molinari, L. Guadagnini, M. Marcaccio, A. Guadagnini
http://dx.doi.org/10.1016/j.scitotenv.2012.03.015

08/2010 – Biogeosciences Journal (ISI-listed, IF 2010: 3.587).
Characterization of broom fibers for PRB in the remediation of aquifers contaminated by heavy metals, volume 7, pages 2545-2556
C. Fallico, S. Troisi, **A. Molinari**, and M. F. Rivera.
http://dx.doi.org/10.5194/bg-7-2545-2010

Posters

06/2012 – 7th EUropean congress on REgional GEOscientific cartography and Information systems 2012, Bologna, Italy.
Mapping the spatial distribution of arsenic, boron and ammonium in the deep groundwater bodies of Emilia-Romagna (Italy) and natural background levels assessment.
M. Marcaccio, A. Guadagnini, **A. Molinari**, L. Guadagnini, A. Palumbo, I. Pellegrino.

04/2012 – European Geosciences Union (EGU) General Assembly 2012 Vienna, Austria.
Hydraulic characterization of "Furcraea andina" fibers as alternative medium for bioremediation of contaminated porous media (aquifers) by means of PRB.
M.F. Rivera-Velasquez, C. Fallico, **A. Molinari**, P. Santillan and M. Salazar.
http://meetingorganizer.copernicus.org/EGU2012/EGU2012-4686.pdf

09/2011 – ModelCare conference 2011 Leipzig, Germany.
Estimate of natural background levels of arsenic, boron and ammonium for three groundwater bodies in Emilia-Romagna, Italy
A. Molinari, L. Guadagnini, M. Marcaccio, A. Guadagnini
http://www.modelcare2011.org/MODELCARE_2011/Start_files/MC_Abstractband_web.pdf

04/2011 – European Geosciences Union (EGU) General Assembly 2011 Vienna, Austria.
Preliminary methodological application for estimating the natural concentrations of hazardous species in two groundwater bodies in Italy
A. Molinari, L. Guadagnini, M. Marcaccio, A. Guadagnini
http://meetingorganizer.copernicus.org/EGU2011/EGU2011-2456-1.pdf

Oral presentations

07/2011 – GII (Gruppo Italiano di Idraulica) meeting 2011. Università degli Studi di Roma 3; Roma, Italy.
Stima delle concentrazioni naturali di sostanze pericolose in corpi idrici sotterranei.
A. Molinari, L. Guadagnini, M. Marcaccio, A. Guadagnini.

ACKNOWLEDGMENTS

First and foremost, I would like to express my heartfelt gratitude and thanks to *Prof. Alberto Guadagnini*, my tutor and doctoral supervisor, for his excellent guidance and technical expertise that set high standards for my Ph.D work. His constant words of encouragement, endless patience, and steadfast faith in my work motivated and propelled me to achieve my personal and professional goals which I set for myself before embarking on this journey rich of many satisfactions.

Sincere and affectionate thanks are for *Dr. Laura Guadagnini* for her valuable advices and for having supported all my research activities at each step even in the different locations where my research work took me.

A warm thank is for *Dr. Marco Marcaccio* (ARPA Emilia-Romagna, Bologna, Italy) for his precious and innumerable discussion sessions regarding my research work which contributed to improve the quality and the relevance of the results achieved during my Ph.D work. I also want to thank him and all ARPA Emilia-Romagna for funding my scholarship at Politecnico di Milano.

I am also thankful to *Prof. Salvatore Straface* (Università della Calabria, Cosenza, Italy) who supported and encouraged me in starting this important experience of my life and for his constant interest on the development of all my research activities.

I would also like to express my thanks to *Prof. Xavier-Sanchez Vila* (Universitat Politecnica de Catalunya, Barcelona, Spain) who hosted me in his department for three months giving me the possibility to acquire precious skills both in professional and personal field.

I am thankful to *Prof. Carlos Ayora* (Institute of Environmental Assessment and Water Research, Barcelona, Spain) for his valuable and extremely helpful advices during some research activities.

I would like to specially thank my family for their constant moral support and words of encouragement during the entire period of this important adventure of personal and professional grow of my life.